CRANFIELD UNIVERSITY

ARUN PRABHAKAR

FUNDAMENTAL INVESTIGATION UNDERSTANDING CASTING OF LEAD SHEET

SCHOOL OF AEROSPACE, TRANSPORT AND MANUFACTURING

PhD in Manufacturing

Doctor of Philosophy
Academic Year: 2015–2019

Supervisor: Professor Mark R Jolly
Associate Supervisor: Professor Konstantinos Salonitis

April 2020

CRANFIELD UNIVERSITY

SCHOOL OF AEROSPACE, TRANSPORT AND MANUFACTURING
PhD in Manufacturing

Doctor of Philosophy

Academic Year: 2015–2019

ARUN PRABHAKAR

FUNDAMENTAL INVESTIGATION UNDERSTANDING CASTING OF LEAD SHEET

Supervisor: Professor Mark R Jolly
Associate Supervisor: Professor Konstantinos Salonitis
April 2020

This thesis is submitted in partial fulfilment of the requirements for the degree of Doctor of Philosophy.

Abstract

Lead sheet is widely used in the construction industry for roofing and flashing applications. The roots of this process can be tracked back to the Roman times when sandcast lead sheets were used for a wide variety of applications. Sandcast lead sheets are characterised by their superior aesthetic performance and mottled appearance. These days such sheets are used for premium roofing and flashing applications in the heritage construction industry. Lead sheet is also manufactured using a type of continuous casting process also called as the 'Direct Method (DM)'. This thesis focuses on a fundamental investigation of both these processes used for manufacture of cast lead. Just like any casting process, sand casting of lead sheet suffers from the presence of surface defects. In this study, a surface defect type, hereby referred to as 'grooves', has been investigated. The focus has been laid on the identification of the main factors affecting defect formation in this process. Based on a set of screening experiments performed using Scanning Electron Microscopy (SEM) as well as the existing literature, a number of factors affecting the formation of such defects was identified and their corresponding significance was estimated.

Two-dimensional Computational Fluid Dynamics (CFD) simulations have been performed to simulate the melt flow and solidification stages of the lead sandcasting process. The effects of process parameters such as pouring temperature, screed velocity and clearance between the screed and the sandbed on the final quality of the lead sheet are investigated. Sheet quality is quantified by measuring the variance and the average of the final sheet thickness over the sandbed length. The CFD model has been validated against experimental results by comparing the evolution of the lead-sandbed interface temperature against data collected by thermocouples during the evolution of the process.

The direct method of casting lead is a much more energy efficient compared to the conventional rolling process which requires a casting process before rolling to achieve the required thickness. This work also looks into the energy consumption in different stages of the DM process and suggests

pointers for improvement. An energy audit of the process is conducted, and the consumption is analysed at different stages and compared with rolled lead. A two-dimensional numerical model of the DM process was developed and different process parameters affecting the thickness of the final cast sheet is studied. Effects of parameters like volume flow rate, heat transfer coefficient, speed of rotation of the casting drum and its immersion are investigated. The studies were conducted in collaboration with ML Operations, a cast lead sheet manufacturer based in Derbyshire and the findings of the study were implemented successfully.

Contents

List of Figures

List of Tables

List of Abbreviations

SATM	School of Aerospace, Technology and Manufacturing
SEEA	School of Energy, Environment and Agrifoods
DM	Direct Method
SEM	Scanning Electron Microscopy
CFD	Computational Fluid Dynamics
RNG	Renormalized Group
DoE	Design of Experiments
ANN	Artificial Neural Networks
ANOVA	Analysis of Variance
OME	Operational material efficiency
FAVOR	Fractional Area-Volume Obstacle Representation
VOF	Volume of Fluid Method

Acknowledgement

First and foremost, I would like to sincerely thank my supervisors, Professor Mark Jolly and Professor Konstantinos Salonitis for giving me this opportunity, for their continuous support and motivation. I would like to thank ML Operations and Innovate UK for funding the project and all the staff members at ML Operations who supported me in the past few years with my experiments and helping me with their experiences and ideas. I am extremely grateful to Mr Boudewijn Tuinenburg, Managing Director of ML Operations for constantly supporting and encouraging me to pursue the necessary experiments even during busy production times. I would like to specially thank Dr Michail Papanikolaou for helping me with simulations and providing technical expertise whenever needed and to Mr Steve Pope and Dr Tracey Roberts for helping me with metallography and SEM analyses. I would also like to thank Flow 3D staff members for their constant support.

I am very thankful to all my friends especially Surya for helping me with my experiments, providing me with a place to stay during my visits to Cranfield, Vinayak, Diwakar and Anirudh who helped me with a number of technical concepts and for the time they spent in helping me fine-tune my ideas.

I am extremely grateful to my high school mathematics teacher and author Mr A Prabhakaran, for always motivating me to pursue higher education and research.

Lastly, I would like to thank my parents and family for their unconditional love and continuously supporting me throughout, especially my younger brothers Adarsh and Adithya for helping me proofread the thesis and being there whenever I needed them.

गुरुर्ब्रह्मा गुरुर्विष्णु र्गुरुर्देवो महेश्वरः
गुरु साक्षात परब्रह्मा तस्मै श्रीगुरवे नमः

GururBrahma GururVishnu GururDevo Maheshwaraha
Guru Saakshaat ParaBrahma Tasmai Sri Gurave Namaha

The Teacher is Lord Brahma because he creates the knowledge inside us. The Teacher is Lord Vishnu because he preserves and operates the knowledge in our mind on to the right path. The Teacher is Lord Shiva because he destroys the wrong thoughts and transforms us with the right kind of knowledge. Thus, The Teacher or The Guru is the live supreme God and I salute and bow to my teacher

To all my teachers.

Chapter 1

Introduction

1.1 Lead

Lead has been one of the earliest metals to be used among other metals including gold, silver, copper, iron and tin and its use dates back to around 3000 BC [1], [2]. Lead coins were used by the Chinese around 2000 BC. Probably the most prominent use of lead in history was during the Roman civilisation. The Romans used lead for a wide variety of applications. The well-known Roman water pipes Figure 1.1 were made by rolling sheet lead into tubes and welding them together at the joint using molten lead [1]. They also used sheet lead for many other applications like roofing, lining baths and manufacture of sarcophagi Figure 1.2 [1], [3]–[5].

The use of lead for construction purposes declined substantially with the decline of the Roman Empire. In the UK, the York Minster Cathedral built in 650 AD was one of the first buildings known to have had a lead roof [7]. The use of lead became more common in the 11th and 12th century primarily for roofing applications while the use was limited mostly to prestige buildings like churches, cathedrals and some important houses, due to its high cost. Such sheets were mostly made at the

Figure 1.1: A roman water pipe made from sand cast lead sheet [6]

Figure 1.2: Remains of a Roman coffin made from sand cast lead sheet [6]

construction site using an open sand casting process [8]. The Industrial Revolution resulted in creation of a lot of wealth and lead to construction of a number of buildings of civic importance in the UK. This combined with the Victorian love of the Gothic style and considerable production of lead, resulted in its extensive use as a roofing material during this time. Since then, the popularity of lead as a roofing material has stayed to this day and newer methods of manufacture of sheet lead were invented [8].

1.1.1 Production and Uses

More than 100,000 tonnes of lead sheet is (11340 kgm^{-3}) used every year worldwide with a high demand from countries like Belgium, France, Spain, Germany, UK, Ireland and Holland [9]. Lead based products are easy to identify and economical to collect and recycle mainly due to its physical-chemical properties and product design. Lead is recycled more than any other metal and has one of the highest end-of-life recycling rates amongst commonly used metals [10].

The type of lead production has changed through the years. Previously lead was mainly obtained though primary lead production where its ore, Galena is subjected to a roasting process [1]. However, by 2011 the secondary sources accounted for more than 77% of lead production in Europe. Scrap from lead roofing, flashings and lead-acid batteries are re-melted and refined and are the main sources of raw materials for secondary lead manufacturing [11]. These days almost 50% of the lead that is produced worldwide is from secondary sources with high rates of production in Europe and America while China has a high primary rate of production [12].

Lead is used mostly for batteries and with the increase in production of electronic devices which are powered by battery, the demand for lead batteries is likely to increase.

These days lead in its sheet form is widely used for radiation protection and in the construction industry for roofing and flashing applications. The malleability and ductility of lead combined with its high resistance to corrosion makes it appropriate for roofing applications and architectural cladding. Around 85% of the demand for lead sheet arises from the construction sector [10]. Lead is also very dense (11340 kgm^{-3}) and possesses a high attenuation coefficient (5.549 $cm2g^{-1}$ at 100 KeV) especially for high energy X-rays which makes it an ideal material for radiation protection [14]. Moreover lead sheets are fully recyclable, durable, long lasting,

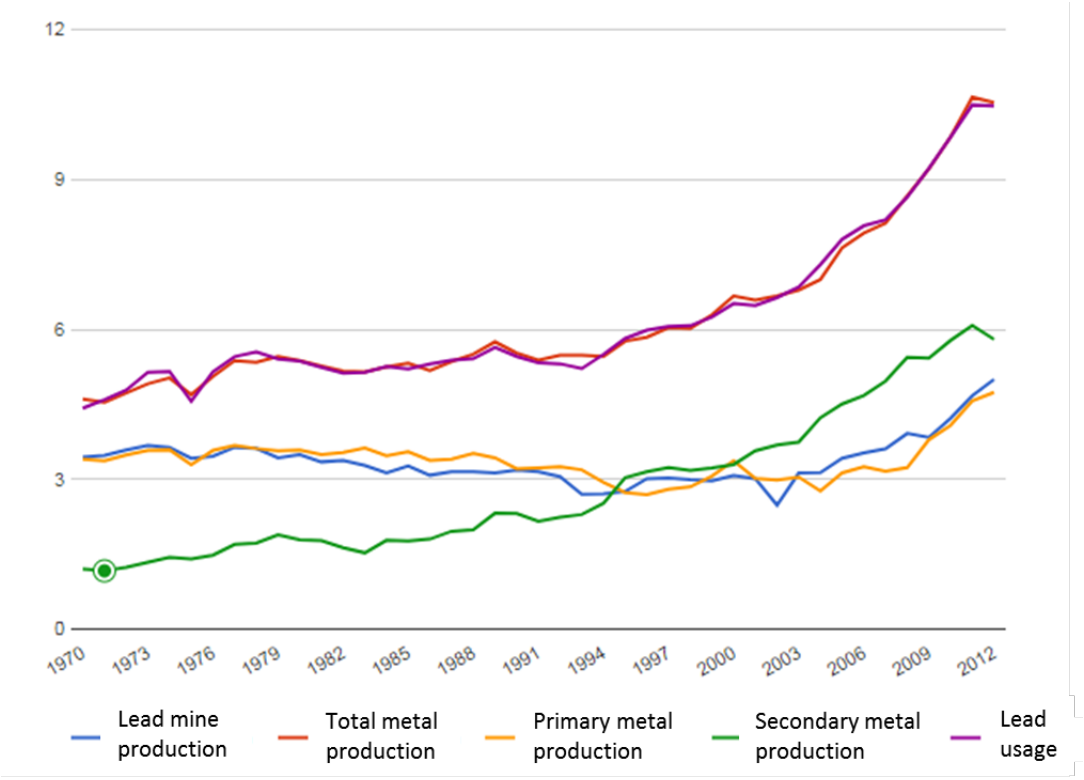

Figure 1.3: Global lead production and usage (Million tonnes). [13]

needs low maintenance and has a low environmental impact [15].

Lead sheet used for construction purposes is mostly produced from recycled lead via three main techniques. The majority of sheet lead is produced by 'rolling', which involves casting lead slabs and then rolling them in a mill until the desired thickness has been obtained [16]. In another direct method, sheet of specific thickness is continuously cast upon a rotating water-cooled drum in a bath of molten lead [17]. The most traditional method of manufacture of lead sheet employs the sand casting technique [3]. Sandcast lead sheets are mainly used for roofing purposes in the heritage industry, mostly for renovating old churches, cathedrals, state homes etc., due to their attractive sheen and superior appearance compared to rolled sheet.

1.1.1.1 Continuously cast lead sheet or DM (Direct Method) sheet

The Direct Method of casting of lead sheet was initially invented in 1956 for the production of lead sheet potentially based on a process invented by Sir Henry Bessemer for the production of sheets of iron [18]. In this process, a rotating drum which is water cooled, internally, is partly immersed into a pool of molten lead, resulting in continuous casting of thin sheet over the drum as shown in the schematic in Figure 1.4.

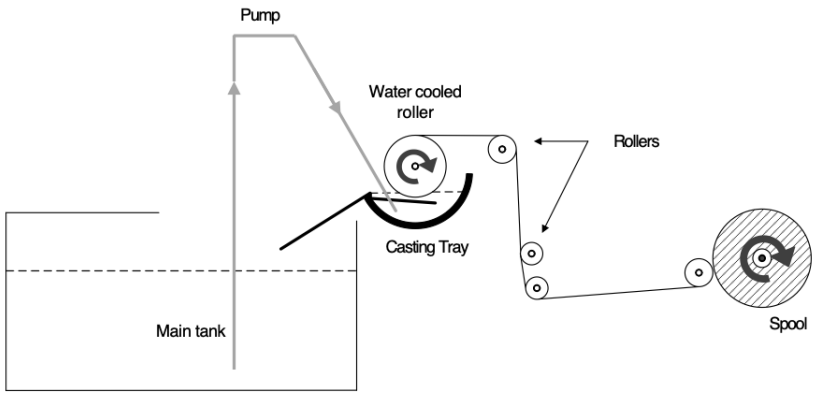

Figure 1.4: Schematic diagram of single drum continuous casting process for sheet lead manufacture

The process starts with scrap lead which consists mostly of old roofing sheets and pipes (also called soft lead). Scrap lead is then melted in a furnace at around 450 $^{\circ}C$ using a natural gas burner. Impurities and dross that arise during the melting process are collected using a mechanical skimmer. The dross collected is stored in metal barrels which are sent for further recovery. Molten lead is then transferred to a refining kettle where it is churned with an oxidising agent such as sodium nitrate for several hours (Harris Process). The scrap lead mostly consists of Antimony, Arsenic and tin as impurities. These elements are more reactive than lead and as a result can be chemically removed by preferential oxidation [19]. The impurities are separated from the lead and get suspended in the flux as sodium arsenate, antimonate and

stannate (tin); any zinc is removed as zinc oxide. The flux and lead are separated, and impurities may be further extracted from the flux. The major product, sodium antimonate, is refined [12]. The refining process results in 99.9% pure lead which is then transferred to a large casting tank. This is the stage where casting of the sheet by direct method begins. The casting tank consists of heating elements that keeps the melt at 400 $^{\circ}C$. The depth of immersion of the drum in the lead bath is a major factor that controls the thickness of the sheet cast. To stabilise the level of molten lead and to eliminate the need to adjust the roll to a changing level, two tanks are provided adjacent to one another but at different heights/levels. A small pump is used to pump molten metal from the casting tank to the tray which is at a higher level. The tray is constructed in such a way that one of its edges is set lower than the other so that the excess melt can overflow through this edge and flow back into the lower tank. With this arrangement of pump and tanks, regardless of the quantity of lead withdrawn as sheet, the level of lead remains a constant in the casting tray [18]. The cast sheet is wound on a spool which is subsequently unrolled and cut into desired dimensions. Figure 1.5(B) shows a process flow diagram for the same.

1.1.1.2 Rolled Lead Sheet

Metal sheet rolling was invented in 1500 s. However, it was only recognized as an alternative technique to traditional sand casting in the early 20^{th} century. Rolled lead sheet has a shiny appearance compared to continuously cast sheet which has a matte finish on one side.

The process starts with melting lead scrap and then refining it. The refined lead is cast in moulds usually made of cast iron. These slabs are then passed through multiple rollers until the desired thickness is achieved [15]. The sheets are then cut to the desired dimensions and packed for distribution as per the process flow diagram

in Figure 1.5(A). The usual thickness of production is 1.32 *mm* (code 3) – 3.55 *mm* (code 8) – thicker rolled lead sheets up to 9.00 *mm* are also produced. Metal in rolling process elongates with the rolling direction, speeding up. This means that the material moves faster on the exit side then on the entry.

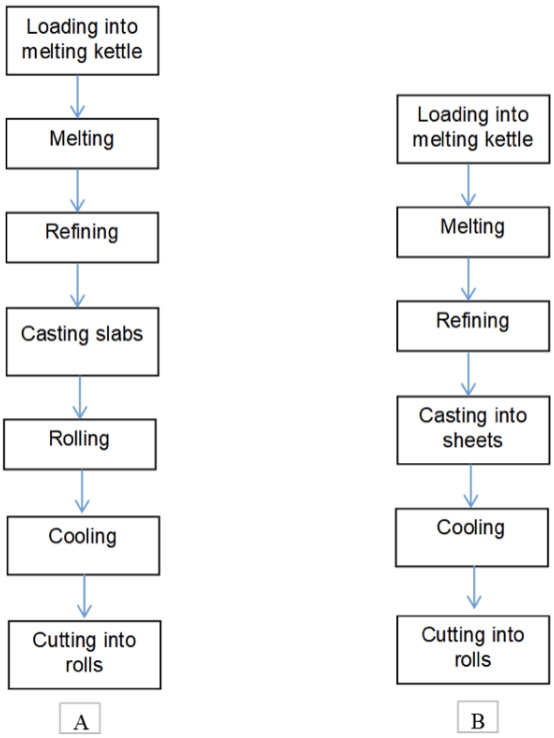

Figure 1.5: Process flow diagrams for (A) Rolling process and (B) DM process

1.1.1.3 Sandcast Lead Sheet

The lead sheet sandcasting process essentially consists of two main stages, namely: (a) pouring molten lead on a sand bed and (b) smearing of the melt surface using a strickle [20]. The process starts with preparing the rectangular sand mould, usually $3m$ - $7m$ long and 0.75 m- $1.3m$ wide. The sandbed surface is flattened using a strickle guided by a screed as illustrated in figure 1.7 and smoothened using a steel floater to avoid any surface undulations. Molten lead is then poured at around

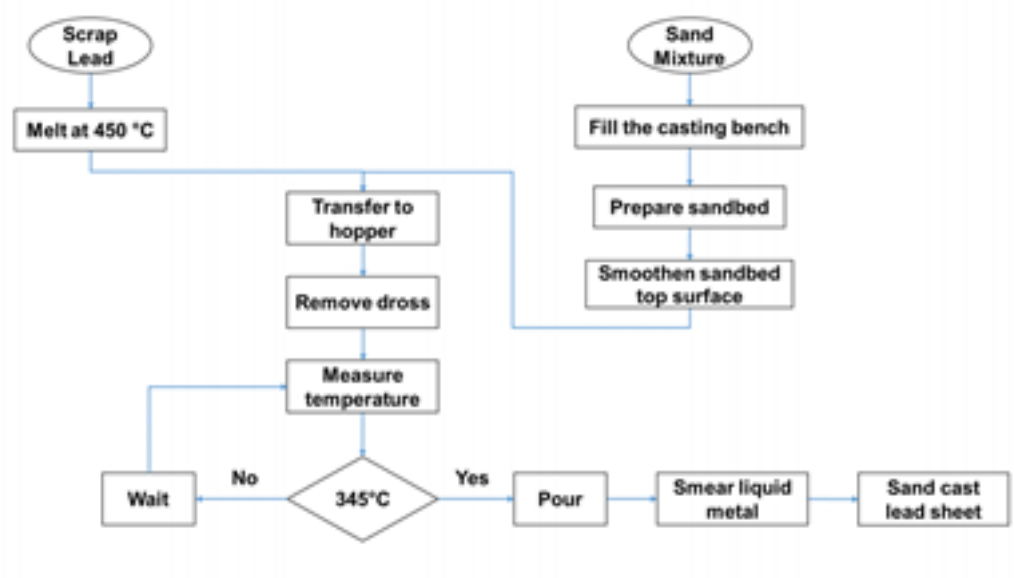

Figure 1.6: Process flow diagram for Sand casting process

350°C using a hopper from the one end of the bed. After pouring, the strickle which is guided by a screed rail is used to smear the flowing melt along the mould figure 1.7(b) and seconds later, the melt solidifies into a sheet.

1.2 Research Motivation and gaps

1.2.1 Sandcast lead sheet

Sand casting of lead sheet is a very traditional process and dates to 5000 BC. Over time, newer processes like rolling and continuous casting have taken over lead sheet manufacture. Despite being the oldest and most traditional method, very little research has been conducted in this area while work has been done on rolled and continuously cast lead sheet. There is no documented knowledge on the process mechanism and physics of open sand casting of sheet lead with respect to effects of process parameters, such as the pouring temperature and strickle velocity on the

(a) Sand bed being levelled using a strickle

(b) Setup for traditional sand casting of sheet lead

Figure 1.7: (a)Sand bed being levelled using a strickle (b)Setup for traditional sand casting of sheet lead

quality of the final cast product. In fact, till nowadays, the control of the process parameters relies solely on the experience and intuition of foundry engineers and operators.

Though numerous studies have been conducted in eliminating defects in cast products, similar studies have not been conducted to identify and eliminate defects in sand cast lead sheets. This also opens an opportunity to investigate the effect of various parameters that affect the quality of sheets and optimise these parameters for minimal defects. Similarly, mechanical and microstructural properties of sheet lead manufactured using conventional methods such as rolling and direct method have been studied previously. Understanding the microstructure and effects of impurities on properties of sand cast sheets would close this gap and would be vital for manufacturers.

Nowadays, the evolution of computing power as well as modelling techniques has made the numerical investigation of casting processes feasible. Many types of sand-casting processes, with the exception of open sand casting of sheet metal have been extensively studied by means of CFD simulations. Reliable numerical models can contribute towards the effective selection of the optimum process parameters without the need to conduct a large number of time consuming and energy intensive experiments.

These days this product is in high demand in the construction industry to renovate heritage buildings like churches and cathedrals that want to preserve the architectural tradition. Hence, research in the areas of material properties, defect elimination and understanding physics of the process are vital for manufacturers.

1.2.2 Continuously cast lead sheet (or DM sheet)

Near Net shaped casting techniques for production of flat products are very impactful for small scale manufacturers economically [21]. The Direct Method or the method of continuous casting of lead sheet is a much more energy efficient process compared to rolling as the latter process involves two stages of processing – casting into slabs and subsequent rolling. Commercially viable continuous casting processes can be very beneficial as they demand lesser energy, reduces lead time, allows production in smaller batches and facilitates lower operating costs [21]. Work has been done previously on comparison of mechanical properties and microstructure of DM sheet with rolled sheet. Some continuous casting processes, which are similar to the DM (used for manufacture of sheet of other metals like Al) have also been modelled. The DM method is a very competent method for manufacture of sheets of metals with a low melting point like lead. Despite being a more energy efficient, faster and simpler process, very little work has been done in understanding the process and the parameters that affect the quality of the product, probably due to the obscure nature of the process when compared to rolling and also due to the niche market for application of sheet lead. Understanding energy consumption and sustainability aspects of the process would be very helpful to the industry. Modelling the process would give us data on process parameters that affect the final thickness of the sheet and methods for process control. The results of the study can also be used for developing and automating the process further.

1.3 Aim and Objectives

After extensive literature review (elaborated in chapter 3) and discussions with foundry engineers on sand casting and continuous casting of lead sheet, the following aim and objectives were established. The focus was to tackle vital issues in the industry pertaining to these processes.

Aim : Improve cast lead sheet manufacture through defect elimination and numerical simulation.

Objectives

1. Understand through literature review and experimentation, sand casting and continuous casting of lead sheet
2. Identify defects in sand cast lead sheet and remedies for them through characterisation and design of experiments; optimise parameters to minimise defects
3. Develop knowledge base of microstructure and mechanical properties of sand cast lead sheet and their comparison with DM sheet.
4. Establish a thermo-physical database and develop a CFD model for both the processes.
5. Identify process parameters that affect thickness of cast sheet and study interrelationships that restrain formation of defects.

1.4 Thesis structure

The main aim of the thesis is to improve casting techniques for manufacture of sheet lead via sandcasting and continuous casting processes by understanding process physics, numerical modelling and defect elimination. In the following chapters previous work done in similar areas, methodologies used and various aspects of the

aforementioned processes would be discussed. The thesis is divided into 8 chapters. Chapter 2 is an extensive literature review on previous work, different methodologies and techniques used. Chapters 3 and 4 look specifically into sandcast lead sheet, microstructure and mechanical properties, defect formation and elimination and understanding effects of different process parameters that cause defect formation.

In chapter 5, two-dimensional Computational Fluid Dynamics (CFD) simulations have been performed to simulate the melt flow and solidification stages of the lead sandcasting process. The effects of process parameters such as pouring temperature, screed velocity and clearance between the screed and the sandbed on the final quality of the lead sheet are investigated. Sheet quality is quantified by measuring the variance and the average of the final sheet thickness over the sandbed length.

Chapters 6 looks into a comparative study between continuous casting and rolling process understanding the process from an energy perspective. An energy audit of the process was conducted, and the consumption is analysed at different stages and compared with rolled lead.

In Chapter 7 a two-dimensional numerical model of the DM process was developed and different process parameters affecting the thickness of the final cast sheet is studied. Effects of parameters like volume flow rate, heat transfer coefficient, speed of rotation of the casting drum and its immersion are investigated.

Finally, Chapter 8 summarises the main conclusions of the study and directions for future work in the area.

1.5 Publications

1. Prabhakar, A., Mielnicka, J., Jolly, M. and Salonitis, K., 2018. Improving Energy Efficiency in Direct Method for Continuous Casting of Lead Sheets. *Energy Technology 2018: Carbon Dioxide Management and Other Technologies*, p.121.

2. Prabhakar, A., Salonitis, K. and Jolly, M., 2019, February. Characterisation of Lead Sheet Manufactured Using Traditional Sand-Casting Technique. In Shape Casting: *7th International Symposium Celebrating Prof. John Campbell's 80th Birthday*(p. 283). Springer.

3. Prabhakar, A., Papanikolaou, M., Salonitis, K. and Jolly, M., 2020. Sand casting of sheet lead: numerical simulation of metal flow and solidification. *The International Journal of Advanced Manufacturing Technology*, 106(1-2), pp.177-189.

4. Prabhakar, A., Papanikolaou, M., Salonitis, K. and Jolly, M., 2020. Minimising Defect Formation in Sand Casting of Sheet Lead: A DoE Approach. *Metals,*10(2), p.252.

5. Prabhakar, A., Papanikolaou, M., Salonitis, K. and Jolly, M. Numerical Simulation of the Single Drum Continuous Casting Process for Manufacture of Sheet Lead- *Manuscript under preparation*

Chapter 2

Literature

A brief literature review and general concepts relevant to this study is described in this chapter.

2.1 Lead

Lead has been used by mankind since thousands of years. It is one of the most easily reducible metals and it is believed that the first production of lead by man could have been achieved by a woodfire on a lead bearing outcrop [5]. The use of lead in the past has been validated by references to writings of Greeks and Roman authors from about 500BC, an example would be the well-known book by Healy on the mining and metallurgy [22]. The Greeks and Romans used lead sheet made by casting on flat stones for several practical purposes like roofing, lining of pipes, protective sheathing for ship hulls etc. It was the romans who developed the practical application of lead, in fact the word plumbing is derived from the Latin word 'Plumbum' for lead [5].

2.1.1 Properties

Lead has a bright silvery and shiny appearance when it is freshly cast. The surface soon becomes grey or dull due to formation of surface oxides, basic carbonates and sulphate films which protect the material from further oxidation. Lead is inert to a range of acids and salts over a wide range of concentrations however the corrosion resistance is owing to the fact that most of its salts and crystals have a low solubility over a wide range of pH values in aqueous solutions, with noteworthy exceptions being the acetate, chlorate and nitrate [5]. It is hence widely used for the storage of acids like sulphuric, phosphoric and chromic acids. The low solubility of lead salts and crystals when compared to other metals makes it a relatively indestructible making it an ideal material to be recycled [5], [10].

Compared to other metals, Lead has a high density (11340 kgm^{-3}), due to its high atomic mass of 207 and Face Centre Cubic structure. Lead is also very dense and possesses a high attenuation coefficient (5.549 cm^2g^{-1} at 100 KeV) especially for high energy X-rays which makes it an ideal material for radiation protection [14]. Lead is also very soft and can be easily manipulated to different shapes due to its high ductility and malleability. It can also be easily recast into different shapes due to its low melting point (327 $^{\circ}C$) [23]. All these properties of lead make it a very suitable material for a wide variety of applications like roofing, flashing, radiation protection and in ballasts. A lot of research has been conducted on properties of lead and its alloys in the past especially related to creep studies [24]–[26]]. The low melting temperature of lead results in poor creep plastic deformation under constant low temperature and stress. Creep occurs in Pure Lead (99.99%) at stresses as low as 0.7 <Pa with elongation of 0.06% after 500 days at 30$^{\circ}C$ [5]. Studies on lead under stress has been used to predict behaviour of other metals at high temperatures as many metals behave similar to lead at temperatures below their melting point [5].

Lead is normally used in temperatures close to its melting point. As a result, it is subject to recrystallisation at low stresses. Mechanical tests like hardness, elasticity modulus etc are hence affected by the rate of application of stress. Usual Brinell hardness is around 3-4 and hence very malleable and soft. The hardness is only minorly affected by presence of common Group 2 impurities like tin, antimony and bismuth up to 0.1% [5]. However beyond 0.1% the hardness and tensile strength increases progressively with addition of antimony [5].

Susan Whillock [27] extensively studied the relationship between mechanical properties like tensile, creep and thermal fatigue behaviour between conventionally rolled and continuously cast lead sheet containing <0.06 wt% copper. It was observed that continuously cast sheets exhibited an increase in UTS with an increase in copper content. It was also observed that the maximum UTS for rolled lead sheets were observed at 0.02-0.03 w% copper. Continuously cast lead sheet was also observed to exhibit good creep resistance which increased with an increase in copper content. This is believed to be due to the large grain size and stable grain boundaries. Rolled lead sheet was found to be less creep resistant and the maximum creep resistance was observed at 0.3 wt% copper. It was also concluded that the thermal fatigue resistance of DM sheet with 0.02-0.05% copper and rolled sheets with 0.03-0.05% copper behave similarly in situations of thermal fatigue. The study also made references to effect of presence of bismuth in DM sheets aggravating the formation of small surface cracks and potentially weakening the sheet at handling temperatures. It was also suggested that the bismuth content should be closely controlled. The study was successful in drawing a comparison between lead sheet manufactured using both methods and has been instrumental in understanding material properties of continuously cast lead sheet which is relatively an obscure product when compared to rolled lead sheet. It was inferred that the continuous casting could be a much bet-

Alloying Element	Acceptable Range of Composition(Weight Percentage)
Copper	0.030 – 0.060
Bismuth	Max. 0.100
Tin	0.050
Silver	0.005
Antimony	0.005
Zinc	0.001

Table 2.1: BS EN 12588:2006 Acceptable range of alloying element composition in lead used for building purposes [28] ANOVA table

ter method for manufacturing sheet lead for construction applications as it is much more economical.

The British Standards specify the alloying composition for the production of lead sheet for the construction industry, table 2.1 [28].

2.2 Rolling

Rolling is a widely used process and more than 95% of ferrous and non ferrous metals are processed using this method [29]. For the manufacture of sheet lead there are three main methods: Rolling (also called milling), continuous casting (also referred to as the Direct Method or DM) and sand casting [17], [20], [24]. Majority of the lead sheet used for construction purposes is produced from recycled lead via rolling, and the process involves casting lead slabs and then rolling them in a mill until the desired thickness has been obtained [24]. Figure 2.1 shows a schematic of a basic rolling process.

In Britain, rolled lead started being produced in early 18^{th} century [16] but the process became competitive to the traditional sand cast lead sheet only by early 19^{th} century.

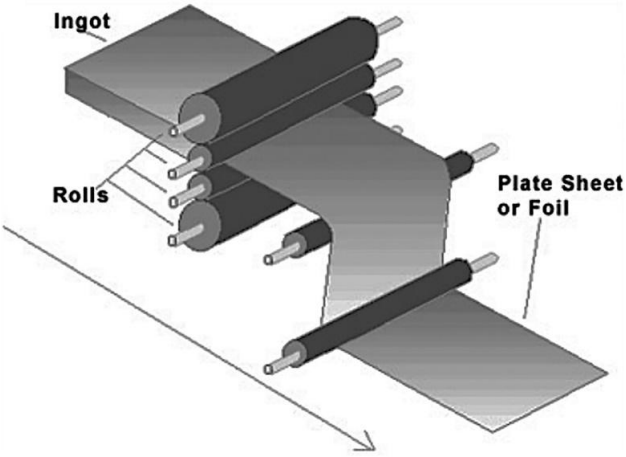

Figure 2.1: Schematic of a basic rolling process[29]

Table 2.2: Standard codes of sheet lead and their corresponding thicknesses

Code	1	2	3	4	5	6	7	8
Thickness (mm)	0.44	0.88	1.32	1.8	2.25	2.65	3.15	3.55

In rolling process for manufacture of sheet lead a billet of approximately 2 tonnes (with 0.03-0.04% copper by wt) is cast in a water cooled mould. The high ductility lead is exploited to reduce the thickness to a code 3 or code 4 (Table 2.2) sheet by passing it through rollers a number of times. The final product is much smoother and shinier than DM sheet as the appearance of the sheet is very much dependant on the surface finish [27]. Lead rolling is also very much preferred as a test material for laboratory modelling of hot steel rolling [30].

2.3 Sandcast lead sheet

Casting, one of the oldest manufacturing processes essentially involves pouring of molten metal in a mould until solidification and dates back to 3600 BC [31]. Green sand casting is one of the most commonly used and preferred methods for manufacturing near net shape parts due to the easy availability of raw materials, its low

cost and recyclability [32]. Sand casting remains to be one of the most widely used casting process. Sand is very resistant to high temperature and this property of sand makes it one of the best materials for casting. Sand is also a relatively cheap material, easily available and can be reused. Sand casting can be very economical due to low cost of moulding materials and ease of preparation of sand mix and mould [33], however can be time consuming at times. Usually the lead used in sand cast sheet contains higher level of impurities whereas the lead used in DM sheets are 99.8-99.9% pure [34].

2.3.1 Casting defects

Formation of defects during casting is very common in foundries. Defects in castings often appear unexpectedly and it can be difficult to identify their source as they can be brought about by a large number of randomly changing production parameters and also due to interactions between alloying elements [35]. At times, defects are caused due to combination effect of more than one parameter [36]. The chances of occurrence of casting defects are high even in extremely controlled processes and hence it is often called as a process of uncertainty [36]. Elimination of defects in castings involves identifying the root cause of the defect and taking necessary steps to reduce the defects.

One of the most common problems encountered in metal casting is the emergence of defects during filling/pouring or solidification. As reported by Campbell [37] the majority of casting defects arise due to poorly designed running and filling systems or improper selection of casting process parameters. Entrainment defects mainly arise due to the presence of turbulence during filling; oxide films submerge into the melt by folding and form oxide bi-films, which often entrap bubbles, sand particles and other inclusions. The presence of turbulence leads to a wide spectrum

of casting defects in the final cast product including bubble trails, gas micro-porosity, hot tears and cold cracks [38]. Besides surface turbulence, there are additional factors leading to defective castings such as hydrogen gas bubbles generated upon solidification due to the lower solubility of hydrogen in the solid phase [36].

Mostly, casting defects are associated with casting parameters. In a study conducted by Jadayil et al., the pouring rate of Aluminium in a green sand mould was observed to affect the formation of surface defects. Increase in pouring rate was observed to increase surface defects and reduced internal defects [39].

Casting defects are of different types. Chaudhari et al. has reviewed causes and potential remedies of different types of casting defects like shrinkage, pouring metal defect, moulding material defects, metallurgical defects and gas defects [40]. Shrinkage defects are caused due to shrinkage of the solidifying metal. They result from the interaction of phenomena such as fluid flow, heat transfer during solidification, feeding flow, deformation of the solidified layers etc [40], [41]. Moulding material defects arise as a result of expansion of the moulding sand when it comes in contact with the molten metal [42]. Typical examples of these kinds of defects are cuts, washes, metal penetration, inclusion etc. Cuts and washes appear as rough regions and areas of excess metal. They arise due to the erosion of moulding sand due to flow of liquid metal. The root cause of this is the low green strength of the moulding sand and high velocity of flow of the metal.

Several defects can be attributed to moulding and the sand mixture. This is because green sand mixture usually consists of several components like sand, clay, water and at times other additives. Defects can arise when one of these constituents are out of balance as each of these constituents serve to reduce or control occurrence of defects. Proportion of bentonite and water affects the bonding strength of sand mould [43].

Elimination of defects in casting is a tedious task considering the number of parameters associated and shortage of skilled workers. Often, casting is considered as a process of uncertainty and even in completely controlled processes, some quality defects are difficult to explain [44].

2.3.2 Defect analysis

There are several approaches to defect analysis like historical data analysis, cause effect diagrams, if-then rules, Design of Experiments (DoE) and trial and error [45]. Dabade et al. proposed a method combining DoE and computer simulations to obtain optimal settings for process parameters for a cast iron component [46]. Guharaja et al. worked on optimising settings of green sand parameters like green strength, mould hardness, moisture content and permeability, using Taguchis optimisation approach to minimise defects in spheroidal graphite cast iron rigid coupling castings [47]. In design of experiments, the most significant process parameters are selected, and different levels are assigned.

Kumar et al. analysed different process parameters of pressure die casting of aluminium alloys to reduce defects to a minimum using Taguchi's method [48]. Design of Experiments and Taguchi's methods are an effective tool in reducing foundry defects by optimising various parameters that affect occurrence of defects [32], [33], [35], [36].

Although previous studies have been focused on various topics related to the manufacturing [49], mechanical properties [24], [25] of lead sheet as well as the numerical modelling of the corresponding sand casting process [50], there is still limited documented knowledge on the relationship between the process parameters and defect formation.

2.4 Design of experiments

The DoE method is an effective tool for reducing foundry defects by optimising various process parameters and can be used to establish a relationship between various input variables (factors) and an output variable (response). It is a systematic method used to understand the relationships between different factors that affect an outcome. Implementation of DoE involves certain steps like selecting factors, their levels, response variable, experimental design, conducting the experiment and analysis of results [51].

Dabade et al. [46] proposed a method combining DoE and numerical simulations to obtain the optimal process parameters for a cast iron component in order to reduce defects. Guharaja et al. [47] optimised the process parameters of a green sand-casting process (green strength, mould hardness, moisture content and permeability) using the Taguchi's optimisation method to minimise defects in spheroidal graphite cast iron rigid coupling castings. In a similar study, Kumar et al. [52] analysed different process parameters of pressure die casting of aluminium alloys to reduce defects to a minimum using Taguchi's method. Five different parameters (solidification time, molten metal temperature, injection pressure, filling time and velocity) were selected while three different levels were chosen for each of these parameters. Experiments were subsequently conducted using different combinations of the process parameters as per the Taguchi's orthogonal array and the parameters were optimised for minimal casting defects. Besides DoE, Artificial Neural Networks (ANNs) have also been used for detecting the root cause of defects in castings. Perzyk et al. [35] trained an ANN using the simulated annealing algorithm in order to efficiently detect the root cause of gas porosity defects in steel castings.

2.4.1 Analysis of Variance (ANOVA)

Analysis of Variance (ANOVA) is a set of statistical techniques used in both trivial and complicated experimental designs. ANOVA is often employed in order to find out how the average value of a dependent variable varies across a set of conditions tested within the same experiment. The various conditions being compared are called independent variables or factors [53]. ANOVA is very useful in DoE where a number of factors may affect a dependent variable, since there is no limit to the number of discrete effects that ANOVA can predict. It can also be used to predict the optimum set of factor values to maximise or minimise the output or dependent variable [54]. The general layout of an ANOVA table is presented in Table 2.3. SS_E and SS_{Trt} are the error and treatment sum of squares respectively. The degrees of freedom for the aforementioned sum of squares are $g-1$ and $N-g$, respectively, where g is the number of treatments and N the total number of observations. The mean sum of squares (MS) is given by the sum of squares divided by the degrees of freedom. The F-statistic (or F-ratio) is equal to the ratio of mean squares of the treatments to that of the error. This quantity is used to test the null hypothesis, i.e., that the means of all the treatments are the same versus the alternative that some of the treatment means differ [53].

Source	**DF**	**SS**	**MS**	**F**
Treatments	*g-1*	SS_{Trt}	$SS_{Trt}/(g-1)$	MS_{Trt}/MSE_E
Error	*N-g*	SS_E	$SS_E/(N-g)$	

Table 2.3: General layout of the ANOVA table

The implementation of the DoE method consists of the following 5 steps, namely: (a) selection of factors and corresponding levels, (b) identification of the response variable, (c) selection of experimental design (d) conducting the experiment and (e) analysis of data.

ANOVA can be of different types viz one-way, two-way or three-way ANOVA depending on the number of factors or independent variables. For example, a three-way ANOVA has three factors and one dependent variable, and each factor can be split into different levels. Three-way ANOVA also uses the same equations for calculation of sum of squares (SS) as that of two-way ANOVA, however these calculations can get complicated and often software like Minitab are used for simplicity. Calculating a two-way ANOVA uses four SS and a three-way ANOVA uses eight SS (SSA, SSB, SSC, SSC, SSAB, SSBC, SSCA and SSABC) where A, B and C represents the independent variables [55].

2.4.1.1 F and P values

In ANOVA, the F value is calculated to understand the effect of variables. In factorial ANOVAs, multiple F values are calculated: one for each effect and one for every combination of effects. To understand the effects or interactions that have a significant effect on the independent variable, the p value is also calculated along with the F statistic. The p value is used to understand the smallest level of significance at which the null hypothesis is being rejected. A smaller p value means that there is stronger evidence in favour of rejecting the null hypothesis [53].

2.4.1.2 R square statistic or Coefficient of Determination

The R^2 statistic or the coefficient of determination is useful for interpreting the results of ANOVA. It represents the percentage of variation in a response variable that is explained by its relationship with one or more predictor variables [56]. R2 values can vary between 0 and1 and are usually specified as percentages from 0% to 100%. Commonly R-square values are considered in regression models. Considering R-square in ANOVA for process improvement problems can be beneficial and

often used by lean practitioners as ignoring R-square can potentially overvalue input parameters, which may not result in significant improvements in the dependent variable [57]. The coefficient of determination can be calculated using the following formula

$$R2 = 1 - \frac{SSE}{SST}$$

Where SSE is the Sum of Squares of Errors and SST is the Sum of Squares of Treatments. R-squared increases as more independent variables are added to the model and this can be disadvantageous as the increase could be artificial without truly improving the models fit. Hence R-squared adjusted is often used. Adjusted R square is an adjusted version of R-squared that has been adjusted for the addition of variables in the model. The adjusted R square value is given by

$$R^2 adjusted = 1 - \frac{(1-R^2)(N-1)}{(N-p-1)}$$

Where R^2 is the sample R-square, p is the number of predictors or independent variables and N is the total sample size. Adjusted R-squared will decrease as variables are added if the increase in model fit does not make up for the reduction in degrees of freedom. Similarly, it will increase as variables are added only if they enhance the model meaningfully [58].

2.5 Continuous Casting

Near Net shaped casting techniques for production of flat products are very impactful for small scale manufacturers economically [59]. One such process is the continuous casting process and is used widely in the manufacture of sheet metal as slabs or strips in a variety of industries like steel, aluminium, copper, zinc, magne-

sium and lead [60]–[62]. Conventional sheet metal production utilises the rolling process where molten metal is cast into thick slabs and passed through a number of rollers to attain the desired thickness. Commercially viable continuous casting processes can be very beneficial as they demand lesser energy, reduces lead time, allows production in smaller batches and facilitates lower operating costs [63]. There are various continuous techniques like single roll (melt drag), twin-roll, single belt (mould-through train), Hazlet etc that are used for production of flat products in different industries depending on the type of metal being cast and the application [64]–[68]. The continuous casting of steel into slabs and billets first appeared in the 1950s and gained popularity over ingot casting. These techniques were further developed and currently a high percentage of the worlds steel and aluminium production is obtained through continuous casting [59].

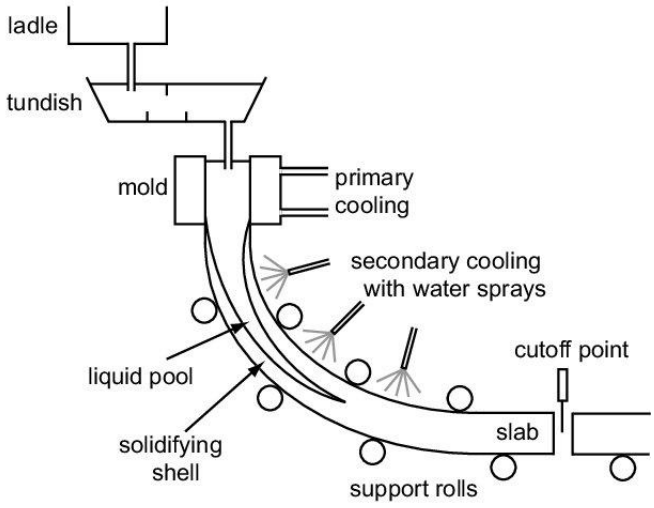

Figure 2.2: Schematic for continuous casting of steel [60].

Continuous casting processes for the manufacture of flat products can be broadly classified into two categories: (A) Casting of ingots and slabs and (B) Casting of thin strips [63]. Slab casters for the manufacture of steel are of different types and they may have either vertical or horizontal configuration. Figure 2.2 shows a basic schematic for the manufacture of steel using a curved mould continuous casting

machine with straightening. The process essentially involves transferring molten steel to the tundish which controls the flow of steel into the mould. The metal continuously solidifies in the mould and is then cooled using secondary water-cooling systems.

Casting of thin slabs or strips is similar to the above-mentioned process but differs with respect to the overall configuration of the caster. The direct strip casting (DSC) process has been commercially used to manufacture strips. The suitability of this process for manufacture of thin strips depends on factors like melting point of the alloy, freezing range, oxidation, heat transfer behaviour etc [59]. The thickness and quality of the final cast sheet are affected by a number of process parameters like surface condition of the rolls, cooling conditions and diameter of the roll as well [68]. Direct strip casting process can be broadly classified into three groups as proposed by Hendricks [61]. Figure 2.6 shows a schematic of different mechanisms categorised into three groups.

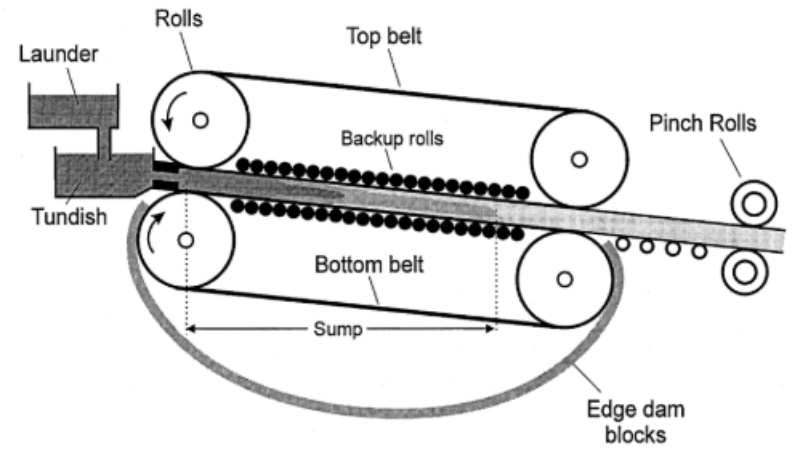

Figure 2.3: Schematic of a typical Hazelett twin belt caster showing configuration of caster and melt feeding

- **Group 1**-Processes in this category make use of travelling conveyor belts with metal either being cast onto the belt or sprayed. A very interesting process in

this group is the Hazelett process in which the melt is introduced between two belts. Figure 2.3 shows a schematic of the Hazelett twin belt caster. Gerber et al [62] conducted a study investigating the influence of process parameters like belt heat transfer, steel superheat, casting speed, and nozzle diameter on the growth of the solidification front within the caster. The results of the numerical model compared well with results available in the literature. The belt heat-transfer and casting speed were the process parameters that influence the development of the solidification front mostly.

The Hazelett caster was initially developed for the manufacture of aluminium but these days also used for steel, copper, zinc and lead industry. There are many advantages to this process like high production rates, lower costs, reduced maintenance etc however the moving mould requires special attention in terms of cooling and surface coatings of belts [59]. The process is capable of manufacturing slabs of 15 to 25mm continuously [64].

- **Group 2**-This group consists of techniques used for manufacture of thin gauge strips/sheet using a single roll. There are several mechanisms for melt feeding as shown in Figure 2.6b. In single roll processes the metal is dragged by the cooling drum/roller. The thickness of the cast sheets is controlled by controlling the speed of rotation of the cooling roll and controlling the contact length between roller and the melt. The Direct Method of manufacture of lead sheet falls under this category where the roller is immersed in a pool of molten metal dragging the metal continuously upon solidification.

- **Group 3**-This group involves twin roll casters in different arrangements. Twin roll casters employ two cooling rolls of equal different diameters. Depending on the alloy being cast, the arrangement could be vertical or horizontal as shown in Figure 2.6c. In the past the process has been studied extensively. Yun

et al [65] studied in detail the different types of defects formed in the final cast products. Several numerical models have also been developed which helped in understanding the complex solidification and rolling process in detail [66], [69], [70].

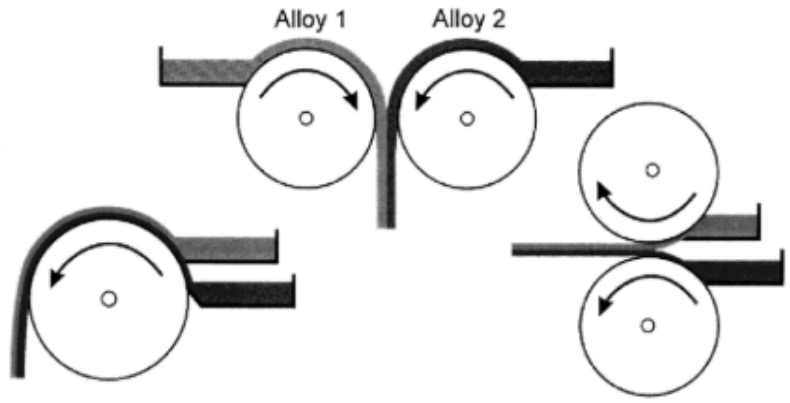

Figure 2.4: Schematic of single roll and twin roll casters for developing clad sheets

Some variations of single roll casting process process has also been developed by Haga et al [71] where one strip is coated on another during casting. A single roll caster and two types of twin roll casters as shown in the figure 2.4 were developed. The mechanism was able to cast thin strips ($2mm$ thick) at a speed of $20m/min$. The study concluded that speed of cooling roll, cooling distance of the base strip, and the temperatures of the melt for the overlay strip were to be prominent factors in final product quality. Twin roll process is slightly more advantageous where the surface finish of the product is important as the process generates sound surfaces due to contact with both rollers [59].

Many studies have been conducted on continuous casting of ferrous and nonferrous alloys. Birat et al [72] experimentally investigated interrelationships between shell thickness and contact time for a number of continuous casting process for manufacture of tin. Sengupta et al [73] studied the effect of water cooling in continuous

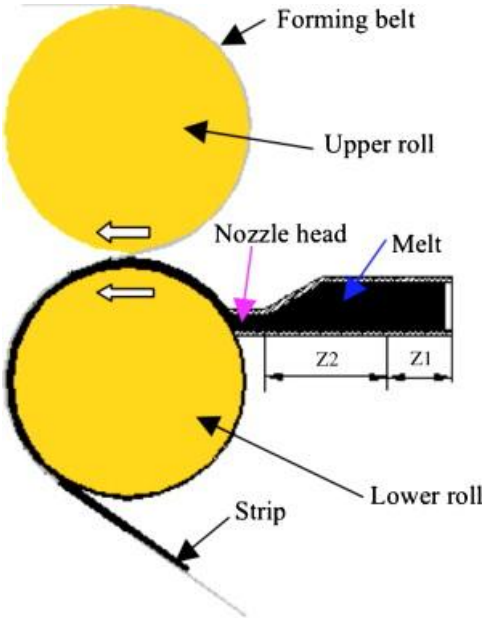

Figure 2.5: Schematic of casting cum rolling apparatus

casting of steel and direct chill casting of steel and aluminium alloys. The water-cooling mechanisms affect product quality by controlling heat removal rate and generating stresses in the final product cast. Zhang et al [74] developed an approach to manufacture metal strips by a casting cum rolling process by using a forming belt and two pinch rolls. Tin, aluminium and magnesium alloys were tested on the apparatus and the results showed that it was possible to produce crack free cast strips of thickness $0.3mm$ to $1.17mm$. However, the authors observed cracks in magnesium possibly due to slow solidification rate and non-uniform temperature and melt distribution. The study also showed that the texture of cast strips was less affected by process parameters and primarily depended on the surface condition of the rolls. It was also observed that the final thickness of the cast strips depended on the temperature of the melt and the speed of rotation of the roll. Figure 2.5 shows a schematic of the process.

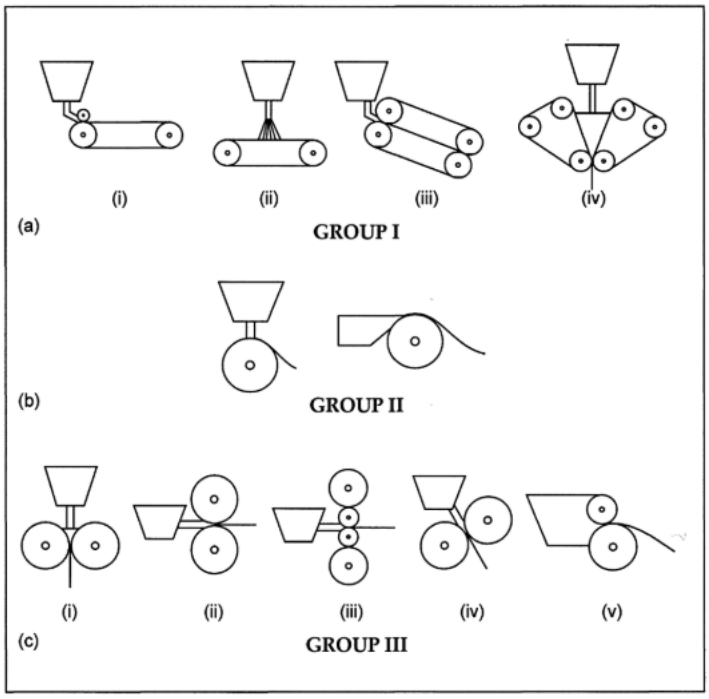

Figure 2.6: Possible strip casting mechanisms classified into different groups-Group1: (i) Single belt caster, (ii)Single belt spray caster, (iii) twin belt inclined caster, (iv)twin belt vertical caster; Group II- Single roll caster showing different melt feeding mechanisms; Group III- (i) vertical, (ii)horizontal, (iii)horizontal, (iv) inclined (iv) twin roll asymmetric arrangements [61]

2.5.1 Direct Method (DM)

The direct method or the single drum continuous casting process for the manufacture of lead sheet has been used since 1951. The process was further developed by broken hill associated smelters company in Australia. Liquid lead does not readily wet most materials or their surface oxides and hence production of lead sheet using this technique is very convenient. Also, the high malleability of lead makes it easy to take-off the cast sheet from the casting drum using relatively simple mechanisms [75]. The process is not very popular as this mechanism of direct strip casting is primarily used only in lead sheets, however, is an efficient and more economical method for production of thin sheets of lead.

Work has been done previously where processes similar to the direct method have been studied and modelled. Shamsi et al [76] developed a two dimensional heat and fluid flow model of the single roll continuous strip casting of steel. The process is very similar to the DM however the melt is fed horizontally from the side as shown in Figure 2.7. The authors examined the effect of processing parameters like the speed of the casting drum, caster drum material, cooling conditions and temperature of the melt. It was observed that the metal head in the tundish had a prominent impact on the thickness of the sheet cast since the level in the melt pool is affected by the head in the tundish.

Guowei et al [68] developed a transient thermal model of the same process. The model predicted the temperature in the solidifying strip coupled with the heat transfer in the rotating drum using explicit finite difference procedure. The cast strip-cooling drum interface was investigated in particular and an empirical function of heat transfer coefficient as a function of contact time, liquid pool depth, superheat, coatings on the drum surface, thickness of the casting drum and material of the drum was developed. It was observed that the heat transfer coefficient decreased with contact time and that the melt superheat affected the strip thickness only marginally.

Laurie et al [67] of Cominco Ltd. published an article in the sixties reporting the fundamentals of the DM process. As per the study the casting process depended on extraction of heat from the melt by the water-cooled drum. The thickness of the sheet produced is controlled by the way heat extraction is altered. For example, slowing the rotation speed, increasing the depth of immersion or using a larger diameter drum results in production of thicker sheets. Likewise, a slower speed of rotation of the drum, shallower immersion or smaller diameter of the drum would result in thinner sheets. Practically, sheets of different thicknesses are obtained by changing parameters like immersion depth and speed of rotation of the drum.

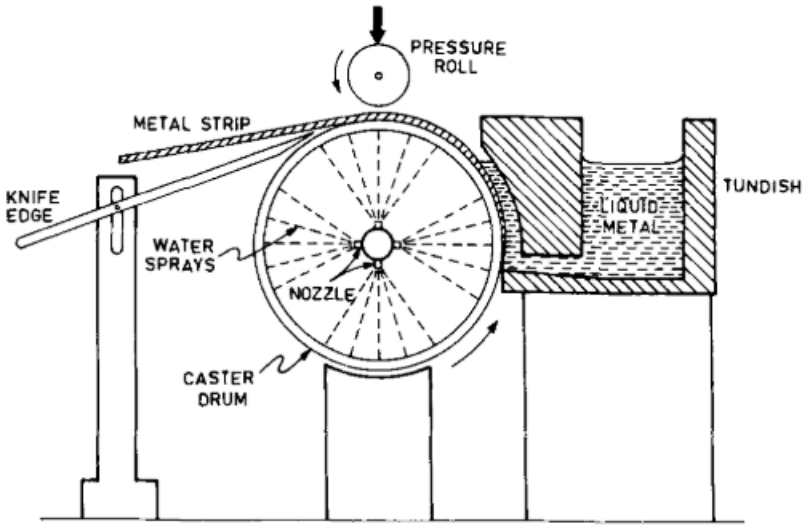

Figure 2.7: Schematic diagram of the single roll strip caster [76]

2.5.1.1 Cooling conditions

The contact time of the hot sheet on the cooling drum before being detached from the drum is another parameter that affects the cooling condition. Usually, the detachment point is kept constant so that the speed of the drum is the only parameter that controls the contact time of the hot sheet with the drum. Similarly, the thermal gradient between the molten lead, drum wall and coolant inside the drum affects the cooling conditions. However, these parameters are not changed during a casting process with a set speed and immersion.

2.5.1.2 Design variables (or Drum)

The conductivity of the drum material and its thickness are important design variables. Higher the conductivity, higher the thickness of the sheet cast. Cooling drums are usually made of Steel, Aluminium and in some cases copper.

2.5.1.3 Cooling rate and water flow

The cooling rate can be controlled by controlling the volume of cooling water. As per a previous study by Cominco Ltd, there is only a marginal effect on sheet thickness up to volume flow rates of 70 gallons/min. It was also found that uneven cooling occurs when velocities are too low. A volume flow rate of 50 gallons/min was considered to be suitable for the process [67].

2.5.1.4 Melt flow rate

The casting tray is continuously fed with molten metal through two feed pipes on both ends. In order to keep the level of metal constant in the tray, the melt is allowed to overflow over a weir. The rate of melt fed through the feed pipes is higher than the rate of solidification of metal on the casting drum in order to keep the level of melt constant. Changes in flow rate can be used to control the thickness of the sheet however this technique is not generally used. A small value of flow rate can result in freeze-ups whereas an excessively high rate can cause variation in sheet thickness. Laurie et al. suggested that the best flow rate is approximately 1-1/3 to 2 times the weight of the metal removed as cast sheet.

2.5.1.5 Melt temperature

An increase in the melt temperature was observed to produce thinner sheets. Hence it is very imperative that the melt in the casting tray is kept at a constant temperature. It also needs to be noted that, variations in temperature of the melt along the tray would result in variation in thickness of the sheet cast. Hence a perfect balance between temperature control of casting try and melt feeding needs to be obtained since feeding of new metal can result in changing the temperature of the melt already present in the casting tray.

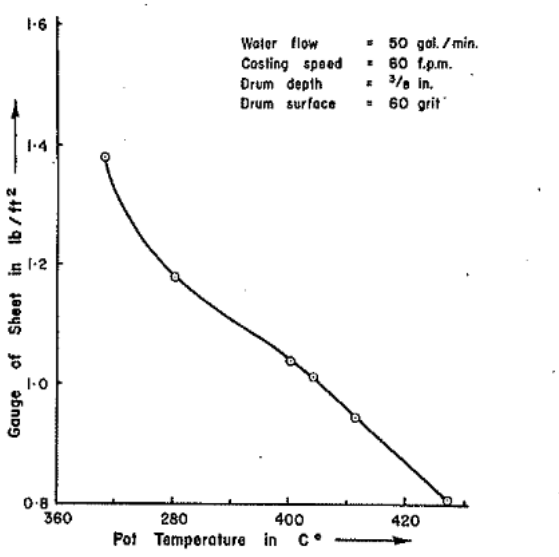

Figure 2.8: Effect of temperature of melt on thickness of cast sheet [1]

2.5.1.6 Quality of cast sheet

The quality of the cast sheet depends on a number of factors apart from the above-mentioned process parameters. Techniques used for creating uniform temperature profiles, vibration of the setup, dross formation and cleanliness of the drum affects the quality of the sheet formed. Vibrations result in ripple formation in the casting tank. Hence isolation of the casting tray is critical. The motor drive of the casting drum should be maintained under smooth working conditions. Localised thickness variations can also be caused due to unclean casting drum and scuffs and scratches on the surface.

2.5.1.7 Production

Some continuous casters make use of pressure rollers to flatten the cast sheet. Sheet is then passed through a series of rollers to keep it in tension and eventually wound on spools. Speed of rotation of spools are kept at the same speed as that of the casting drum and care is taken to avoid telescoping.

2.5.1.8 Surface roughness of cooling drum/roll

The surface of the drum affects the quality of the sheets manufactured and the ability of the drum to manufacture sheets. If the surface contains irregularities like pits or grooves, nucleation is affected appreciably. During DSC, the surface topology of the moving mould is exploited to control solidification microstructure [59].

However, this parameter cannot be changed once the drum is installed. A sand blasted surface was reported to be most suitable for this process and most foundries resort to this method. A finer texture was observed to facilitate casting of thin sheet [67]. Chopra et al[75] studied the effect of surface roughness of the drum and the alloy composition on the heat transfer and hence the thickness of the cast sheet. It is essential to have a rough drum surface to provide certain mechanical bonding between the drum surface and the solidified metal to start up the process. The study experimentally measured temperature transients on an aluminium rod with controlled surface roughness to study the effect of surface roughness on heat transfer. The surface of an aluminium rod was treated with 46 (coarse) and 120 (fine) grit alumina. The study reported that from practical experience, it was observed that with decreasing surface roughness, the thickness of the sheet produced is increased. For a given surface roughness and given alloy composition, the heat transfer coefficient was found to increase with time. It was also observed that the heat transfer coefficient of coarse surface is half of that of fine surface with the exception of Pb-Ca alloy. Also, for fine surface it was observed that, the alloy composition does not have much effect on the heat transfer coefficient for the time range of the casting process. For fine surface this value was between 250-400 $cal/hrsqcmC$ for the time range of practical sheet casting. It was also observed that for coarse surface, the heat transfer coefficient strongly depended on alloy composition. Hence for practical purposes it would be ideal to have the surface of the drum/roll blasted with a fine grit in order to

avoid variability in heat transfer coefficient due to variations in alloy composition.

Bouchard et al [77] studied the effects of surface morphology on the heat transfer and morphology of solidifying shells of a copper alloy. It was observed that rough and grooved surface provided greater heat transfer than polished ones. It was also observed that the solidified shells on rough and grooved surfaces had significant localised variations in thickness, indicating that heat transfer at the substrate- metal interface was not uniform.

Direct strip casting of sheet metal is a very efficient method of producing strips of 1-5*mm* and substantially reduces the need for hot rolling. Hence, the quality of the as cast surface needs to be at least equal to that of hot-rolled products since surface conditioning may jeopardise the economic viability of the process. The work investigated the effect of surface condition of rolls on the heat transfer and surface quality of as cast strips manufactured using a twin roll caster. It needs to be noted that the heat flux and surface conditions of the solidified alloys depend on a number of factors like chemical composition of the alloy, superheat, wetting characteristics of the alloy with the roll surface, fluid flow etc.

2.6 Metallography

Metallography is the study of microstructures of materials [78]. Microstructure inspection is necessary to study grain size and distribution of trace alloying elements like Cu, Zn, Sn, Sb in solidified lead sheets. Microstructure variations can be correlated to variations in mechanical properties of samples of varying alloy content and sheets produced by different processing routes. In order to inspect the microstructure, preparation of surfaces is required.

Surface preparation metallographic inspection generally involves various operations like mounting, cutting, grinding, polishing, etching etc. Lead is very soft in

nature and this property makes it difficult to polish samples to a suitable finish for metallography. Chances of the abrasive material getting transferred to the sample and also the sample getting smeared are high in case of lead. Care needs to be taken as any process that leads to heat generation can alter the microstructure as lead recrystallises even at room temperature [79]. It is very important to ensure that mechanical damage and deformation is avoided during cutting operation. If the sample is cut using a saw, then the operation must be carried out slowly or in a solvent like ethyl alcohol to avoid undue heat. Care must also be taken as lead is prone to oxidation upon contact with air especially during storage of samples.

Ednie [80] worked on various methods of polishing lead alloys used in batteries and found that lead alloy samples were difficult for surface preparation because of their tendency to pick up and embed abrasive particles. Whillock [27] initially attempted electropolishing sections of lead sheet samples and found the method to be unsuccessful and observed that using Silicon Carbide for grinding resulted in particles getting embedded on the sample. Chemical polishing is the technique that is suggested by Whillock as it does not create mechanical damage to samples and microstructure alterations. Scott [34] studied the microstructure of ancient lead that consisted of 1-2% impurities and observed that conventional methods were not convenient or practical to obtain satisfactory etched and polished samples.

2.7 Casting Modelling

Simulations help in understanding effect of different process parameters on process outcomes without the need of conducting expensive experiments and hindering production. The data obtained also helps in improving the process for defect elimination, yield, quality improvement and potential automation of the process.

Nowadays, the evolution of the computing power as well as the modelling tech-

niques has made the numerical investigation of casting processes feasible [81]. The sand-casting process in particular has been extensively studied by means of CFD simulations. Among various topics, defect prediction in sand casting is one of the well-researched areas. A critical review of the existing modelling techniques for the prediction of defects due to air entrainment and oxide formation as well as their benefits and limitations has been provided by Reilly et al. [82]. The authors suggested that, although significant progress has been made with regard to modelling casting defects, simulation engineers should closely collaborate with experimentalists in the future in order to develop computational models for the realistic representation of the mechanisms of defect nucleation and growth. Reis et al. [41] developed their own core code based on the Finite Volume Method (FVM) to predict the formation of shrinkage defects and validated their numerical results against experiments. Their model was proven to be capable of predicting various types of shrinkage defects such as porosity by surface initiation, external and internal porosity. Sulaiman et al. [83] performed a thermal analysis of the molten metal during the filling of a sand mould and compared their results with experimental data. Thermocouples were inserted at different points in the mould and some differences were observed between the experimental and model temperature data. These deviations were attributed to the presence of air in between sand particles that were not accounted in the model. CFD simulations have also been performed for proposing modifications in sand moulds in order to ensure uniform filling and defect-free cast components. In this context, Kermanpur et al. [84] modelled the metal flow and solidification of cast iron in complex multicavity automotive components while their model was validated against experimental observations. More specifically, the authors observed the filling flow patterns obtained from their simulations, identified the areas with increased probability of air entrainment and proposed design modifications which led

to more uniform filling. In more recent investigations, optimisation schemes were coupled with CFD solvers to optimise one or multiple parameters of sand casting processes [85], [86]. Krimpenis et al. [87] focused on the optimisation of the High Pressure Die Casting (HPDC) process with respect to the solidification/filling times and the defects of the final cast product. However, instead of employing implementing optimisation algorithms, they performed Design of Experiments (DoE) to build a database which was subsequently used for training a feedforward Artificial Neural Network (ANN). The trained ANN was capable of fairly predicting the output variables of their model with a mean relative error less than 10%. Their adopted approach is considered to be time efficient as successfully trained ANNs can eliminate the need for performing a large number of simulation runs. Although lead sheet sand casting falls into the category of sand casting processes, the nature of the process is quite different from traditional sand casting as liquid lead solidifies on top of a sandbed instead of inside a mold cavity and it also involves smearing the liquid lead on the sandbed with a strickle. Moreover, the final cast component (sheet) is very thin compared to traditional sandcast components. As a result, CFD modelling of such a process involves a number of challenges related to the mesh generation, free surface flow and turbulence modelling.

2.7.1 Flow 3D

In this section the main theoretical concepts involved in this investigation will be discussed. The commercial CFD software Flow-3D [88] was used to run simulations in this work. Flow-3D employs either finite difference or finite volume approaches to numerically solve the equations of fluid motion and heat transfer. Flow-3D is based on the Fractional-Area-Volume-Obstacle-Representation (FAVOR) method to describe the fluid motion and heat transfer in the vicinity of fluid/obstacle interfaces

and the Volume-of-Fluid (VOF) method to track sharp interfaces [89]. The FAVOR equations for an incompressible and viscous fluid are summarised as follows:

$$\nabla \bullet (Au) = 0 \tag{2.1}$$

$$\frac{\partial u}{\partial t} + \frac{1}{V}(Au \bullet \nabla)u = -\frac{1}{\rho}\nabla p + \frac{1}{\rho V}(\nabla A) \bullet (\mu \nabla)u + g \tag{2.2}$$

$$\frac{\partial H}{\partial t} + \frac{1}{V}(Au \bullet \nabla)H = \frac{1}{\rho V}(\nabla A) \bullet (k \nabla T) \tag{2.3}$$

where:

$$Au = (A_x u_x, A_y u_y, Azuz)$$

$$\nabla A = \left(\frac{\partial}{\partial x} A_x, \frac{\partial}{\partial y} A_y, \frac{\partial}{\partial z} A_z \right)$$

and,

$$H = \int C(T) dT + (1 - f_s) \bullet L$$

In Equations 2.1, 2.2, 2.3, A_i is the fraction of the open area in the i^{th} direction, u_i the velocity component in the i^{th} direction, T the fluid temperature, μ the fluid viscosity, V the open volume fraction, H the fluid enthalpy, ρ the fluid density and p_i the pressure component in the i^{th} direction. The symbols L, C and f_s refer to the latent heat, specific heat and solid fraction respectively. The temperature of the mold

is given by:

$$\frac{\partial T_m}{\partial t} = \frac{1}{\rho C_m V_c}(A_c) \bullet (k_m \nabla T_m) \tag{2.4}$$

where the subscripts m and c refer to the mold and complementary quantities respectively. The heat flux at the metal mold interface is calculated according to:

$$q = h(T - T_m) \tag{2.5}$$

where h is the heat transfer coefficient at the interface.

The Volume-of-Fluid (VOF) method employed in this study is widely used for tracking free surfaces at the interface between liquid metal and surrounding air. According to this algorithm the free surface can be tracked based on 3 main principles:

1. The fluid fraction is a function of the position and the time $(F = F(t,r))$. Its value is equal to 1 at the fluid region, 0 at the void region while $0<F<1$ at the free surface region.

2. The donor-acceptor advection method is employed for the reconstruction of the free surface [90]. According to this method the free surface is constructed based on the values of F (Equation 2.6) in the computational cell and the surrounding ones.
$$\frac{\partial F}{\partial t} + \frac{1}{V}\nabla \bullet (AuF) = 0 \tag{2.6}$$

3. The boundary conditions at the free surface are zero normal and tangential stresses.

The FAVOR method allows use of fully structured computational grids that are much easier to generate than the usual deformed grids used by most other CFD pro-

grams. The method was developed in order to define obstacles of general shape inside grids comprising of rectangular elements [91]. In this method, for each rectangular brick element, the fractional areas of each of the faces of the element that are open to flow and the open volume of the block, is defined. These volumes are then included in the finite volume equations of mass, momentum and energy [89]. Rectangular grids are easier to generate, and indices for neighbouring elements are known. It also makes it easier to compute the fractional areas and volumes. This method is advantageous due to the flexibility it offers in modelling. For example for heat transfers between solids and liquids, the method offers high accuracy of solutions by enabling a good approximation to the areas of the fluid-obstacle interface inside each rectangular brick element [89].

When compared to body fitted mesh approaches or deformed grids, the deformation is used to fit a bounding solid surface by moving the nodes of elements closer to the surface Fig 2.9. In FAVOR method, an element is allowed to cut through the block and its location is recorded in terms of the fractional area and volume of the element that are not a part of the solid and this technique has the same effect in terms of numerical approximation as the traditional body fitted approach. In FAVOR method, these areas are stored as a fraction of the original area of the face element, however in body fitted approach, these areas are computed using the coordinates of the nodes defining the faces. FAVOR method is also more advantageous when compared to body fitted approach as the later kind of grids are more difficult to construct and takes significant amount of time to establish a well behaved grid whereas FAVOR grids are easier to construct and the fractional areas and volumes are easier to compute and automate the computation. FAVOR method also is advantageous in problems involving porous media [92].

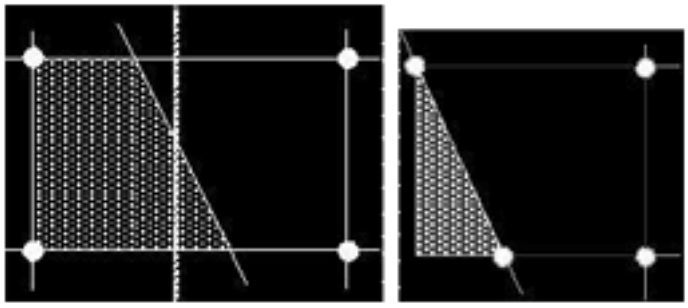

Figure 2.9: FAVOR (Left) and Body Fitted Cell (Right). Shaded area represents solid region[8]

Surface Tension

The surface tension forces inside a cell are calculated based on the curvature of the free surface, and the magnitude of the normal component is divided by the area of the free surface to give the additional pressure. The additional pressure given by the surface tension model is basically added on to the cells that have a free surface. The surface tension forces combined with the gas pressure and viscous normal force must be equal to the continuous stress across the free surface of the molten metal. It can be expressed as

$$p_{fs} = p_g + \sigma K + 2\mu \frac{\delta u_n}{\delta n} \tag{2.7}$$

where p_fs is the interface fluid pressure, p_g the gas pressure, σ the coefficient of surface tension, K the curvature of the free surface, μ the dynamic viscosity, n the normal to the free surface unit vector and $u_n = u.n$

Chapter 3

Characterisation Of Sand Cast Lead Sheet

3.1 Introduction

The sheet produced using the sand-casting method looks very different from rolled and machine cast sheet in appearance. The upper side, or the side that is exposed to the atmosphere, has a shiny mottled appearance with presence of numerous white patches (Figure 3.1- A). On the other hand, the sand side (surface that is in contact with the sand bed) as shown in Figure 3.1- B retains the texture of the sand bed and has a dull appearance similar to the case of DM sheets where one of the surfaces retains the texture of the casting drum [27].

Usually the lead used in sand cast sheet contains higher level of impurities whereas the lead used in DM sheets are 99.8-99.9% pure [34]. Use of pure lead (refined) in sand casting is observed to result in formation of interference colours on the top surface and the mottled appearance (as in Figure 3.1– C) is not observed to be promi-

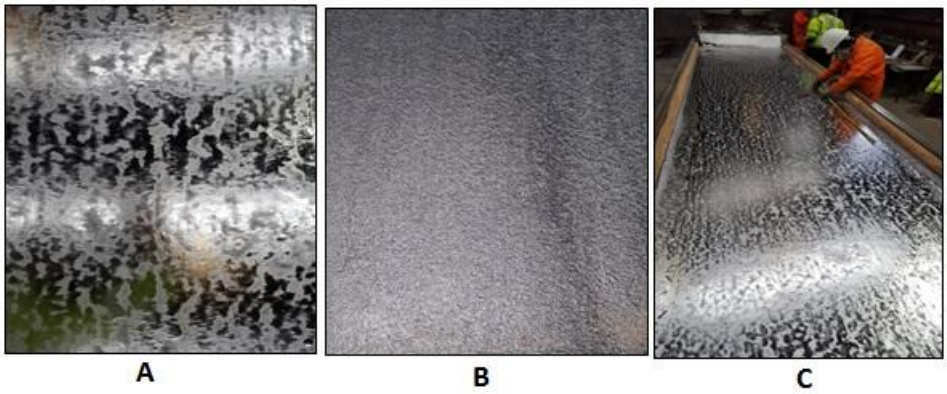

Figure 3.1: (A)-Top surface of sand cast lead sheet (50cm x 90cm) ; (B)-Sand side of sand cast lead sheet (50cm x 90cm); (C)- Sand side of sand cast lead sheet (50cm x 90cm)

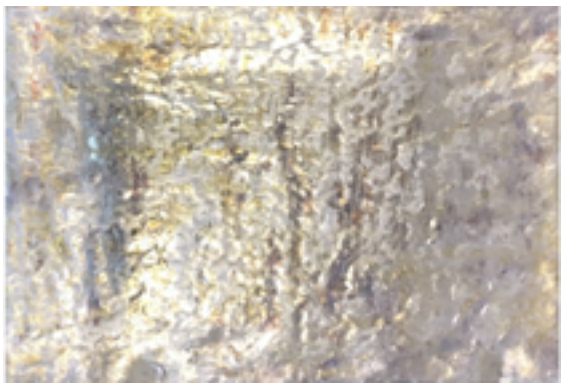

Figure 3.2: Surface of sandcast lead sheet (90cm x 50cm) when pure lead is used (99.97%)

nent. The interference colours are due to oxidation are related to the thickness of the oxide film [93]. The pattern (as observed in Figure 3.1-A) is observed to form when the melt consists of a mix of refined lead and scrap lead. Since unrefined scrap is mixed with pure lead, every cast has a different chemical composition.

Lead sheet used for roofing purposes should not only be visually attractive, but also should possess good mechanical properties. Understanding the microstructure and is therefore very important. Previously published work on continuously cast lead sheet and milled sheet [5] has contained extensive research on the microstructure and mechanical properties of continuous cast lead sheet and rolled lead sheet. Whillock

investigated relationships between mechanical properties such as tensile, creep and thermal fatigue behaviours, and microstructure for rolled and continuous cast lead sheet at different concentrations of copper [27]. However, not a lot of research has been conducted in understanding properties and metallography of sand cast lead sheet. Sand cast lead sheet contains more impurities when compared to DM or rolled sheet and Lead is highly sensitive to changes in properties with the presence of even trace amounts of alloying elements. Variations in grain size and hardness values of lead have been reported when only traces of other elements present [34]. For example, the addition of Sb is found to increase the tensile strength and hardness of lead progressively [5].

3.2 Materials and Methods

3.2.1 Experimental Design

Three different ratios of pure lead to unrefined scrap were used to manufacture sand cast sheet (Table 3.1) on a sand bed that is $7m$ X $1.3m$. A $6cm$ thick layer of silica sand was used. 99.98% lead ingots and secondary lead scrap which consists mainly of lead from batteries, building and construction industry were used for sand casting. Temperature of melt was fixed at $350°C$ for all casts. 99.98% pure DM sheet of $1.8mm$ thickness (Code 4) manufactured using direct method was also used to compare hardness values in this study.

As described in Table 3.1, samples A1 to A4 were manufactured using sand casting and A5 was manufactured using direct method. Material mix for A4 is unknown since it is sourced from the market and is used for comparison purposes only.

Sample Name	Material mix	Method of manufacture
A1	*Lead ingots*	Sand Casting
A2	*50:50 Lead ingots: Scrap*	Sand Casting
A3	75:25 Lead ingot: Scrap	Sand Casting
A4	Similar material available in the market	Sand Casting
A5	Refined lead	Direct method

Table 3.1: Sample names, composition and manufacturing method

3.2.2 Metallographic preparation of samples

Pb alloys are difficult to polish to a finish suitable for metallographic inspection due to its softness [94]. Grinding of samples smears the metal and deposits abrasive grit from the grinding paper onto the surface of the specimen. Care needs to be taken as any process that leads to heat generation can alter the microstructure as lead recrystallises even at room temperature [79]. Care must also be taken as lead is prone to oxidation upon contact with air. There are different methods available in the literature [17], [27], [94] for metallographic preparation of lead samples, however most of the techniques proved to be practically difficult when tried to reproduce.

Samples were grinded using 600 and 1200 grit silicon Carbide (Sic) paper. Cutting oil was used to lubricate the grinding process. This also helped prevent lead from sticking on to the paper and forming a glaze that could drag and distort the surface of the sample. After 1200 grit paper, 6 microns and 1-micron diamond paste were used on a chemically resistant cloth to reduce mechanical damage and excessive smearing of the sample. Polishing was performed using 0.04-micron colloidal silica and soap. Finally, samples were chemically polished for 2-3 seconds with a mixture of 70ml hydrogen peroxide and 30 ml oxalic acid and immediately rinsed with water. Etching was performed using a solution of 9g ammonium molybdate, 15g citric acid and 80 ml distilled water. Samples were cleaned in an ultrasound

bath in between steps.

3.2.3 Characterisation

The samples in the study were studied using a Nikon Opti phot image acquisition system equipped with Leica Application suite for optical imaging and a Phillips XL30ESEM environmental scanning electron microscope (ESEM) equipped with an energy dispersive spectroscope (EDX). The optical imaging was carried out under 10x magnification. Elemental analysis of samples was conducted using Petromax DCM2752 mass spectrometer. Analysis was conducted at ten different points on each sample and the average was taken. To measure hardness values of samples, a Zwick Roel hardness tester was used.

3.3 Results

3.3.1 Elemental analysis

As mentioned previously, a combination of pure and unrefined scrap lead is used to manufacture sand cast lead sheet in order to achieve the patterned surface. As a result, the impurity content on each cast sheet varies. An elemental analysis of the scrap used for the cast showed presence of mainly copper (Cu), zinc (Zn), tin (Sn), antimony (Sb), bismuth (Bi) and silver (Ag) whose concentrations vary with the scrap supplied. Table 3.2 shows the average percentage and standard deviation (SD) of each of these elements out of 80 different scrap batches.

Figure 3.3 shows elemental analysis and different impurity contents in each of the samples used for this study. Analysis was conducted at ten different points on each sample and the average taken. Presence of copper improves creep resistance properties of DM sheets [27]. Hence DM sheet are manufactured with small amounts of

copper as it is evident from Figure 3.3- E. The sample manufactured using 75% pure ingots and 25% scrap have almost similar impurity content as pure ingots. Yet, there are differences in the appearance of the final cast product. As mentioned before, use of pure ingots is observed to result in the formation of a colourful patina on the top surface.

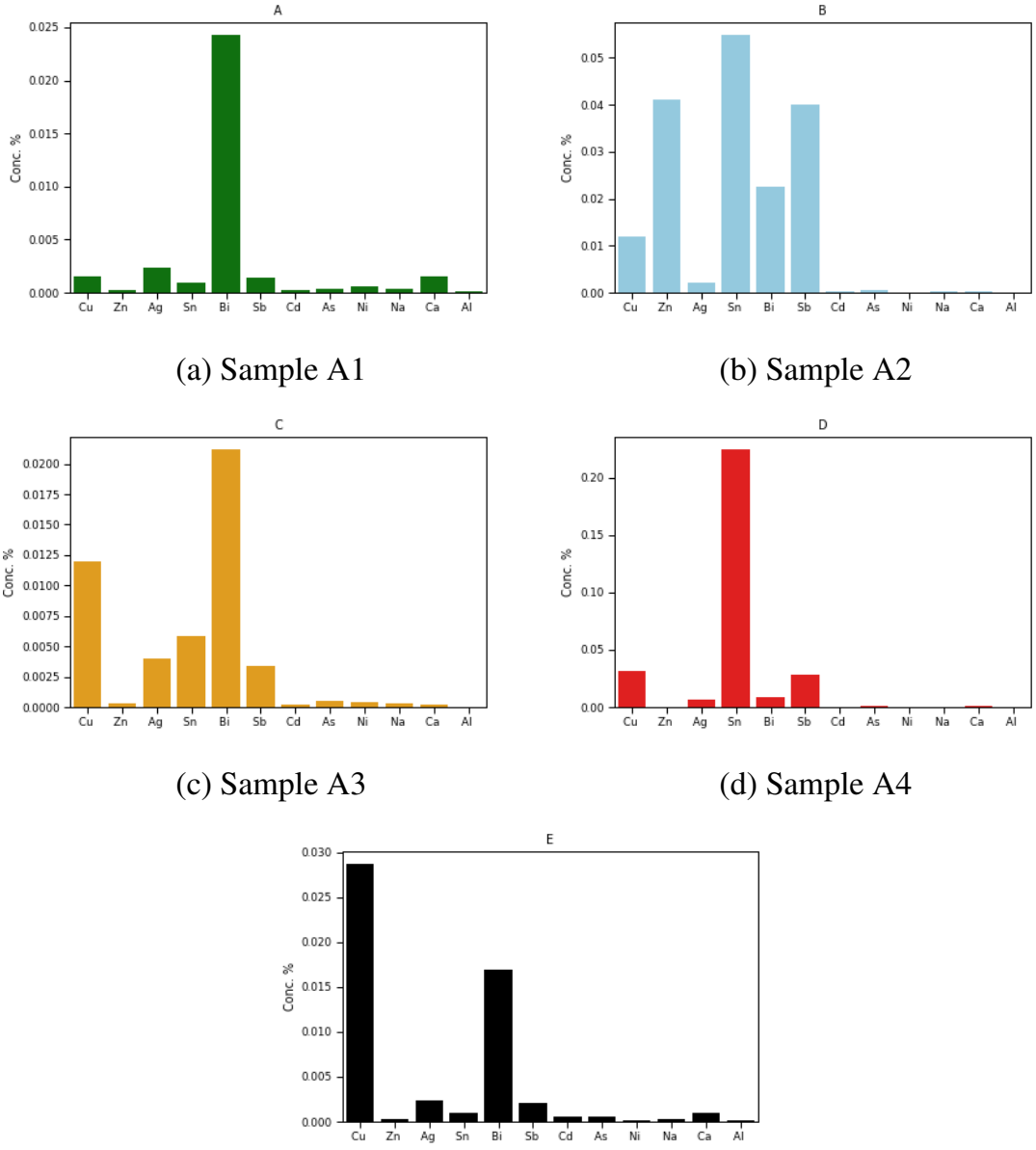

(a) Sample A1

(b) Sample A2

(c) Sample A3

(d) Sample A4

(e) Sample A5

Figure 3.3: Elemental composition of different samples

	Cu (%)	Zn (%)	Sn (%)	Sb (%)	Bi (%)	Ag (%)
Mean	0.0283	0.0029	0.086	0.0315	0.0179	0.0041
SD	0.0255	0.0101	0.0011	0.079	0.0030	0.0184

Table 3.2: Mean and standard deviation (SD) values of common impurities obtained from elemental analysis of 80 different scrap melt batches

3.3.2 Microstructure

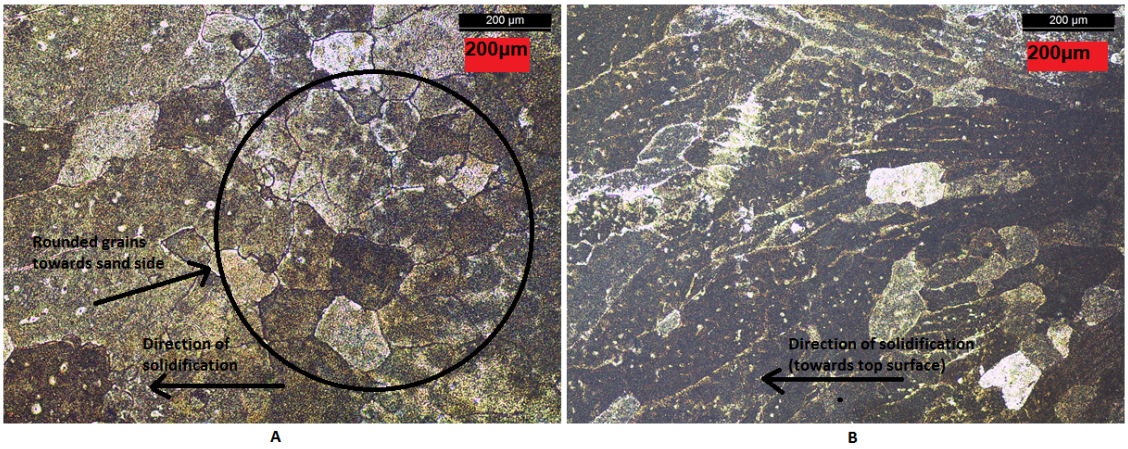

Figure 3.4: Micrographs of a cross-section of sand cast lead sheet (S2); (A) Grains at the edge corresponding to sand side (B) Long branched grains oriented towards the top side

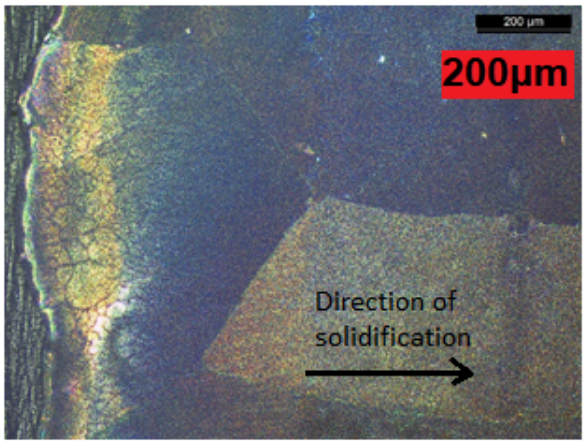

Figure 3.5: Micrograph of a cross- section of sample A4 showing long and large grains oriented towards the top side of the sheet

Sand cast lead sheet samples were grinded, polished, etched and observed under a microscope. The grains were observed to be small and circular in shape near to the sand side of the sheet (Figure 3.4– A) which branched into large long grains oriented towards the top surface of the sheet (Figure 3.4- B). This indicates the presence of temperature gradient during solidification and is partly in line with the observations of Rocca et al. who investigated ancient gallon-roman lead sarcophagus which potentially could have been manufactured via sand-casting technique [3]. Some areas near the top surface of the sheet were observed to have small circular grains. Sample A4 also possessed a similar grain structure but the grains were observed to be larger in size as shown in Figure 3.5.

3.3.3 SEM analysis

Top surface of sand cast lead sheet was observed under SEM to understand the differences in morphology of the dull and shiny texture that appear during solidification. And elemental analysis in the area showed presence of mainly lead, carbon and oxygen in the region. As it can be observed from Figure 3.6- A and Figure 3.7, the dull area has a branched rounded structure compared to the smooth surface of the shiny/grey area.

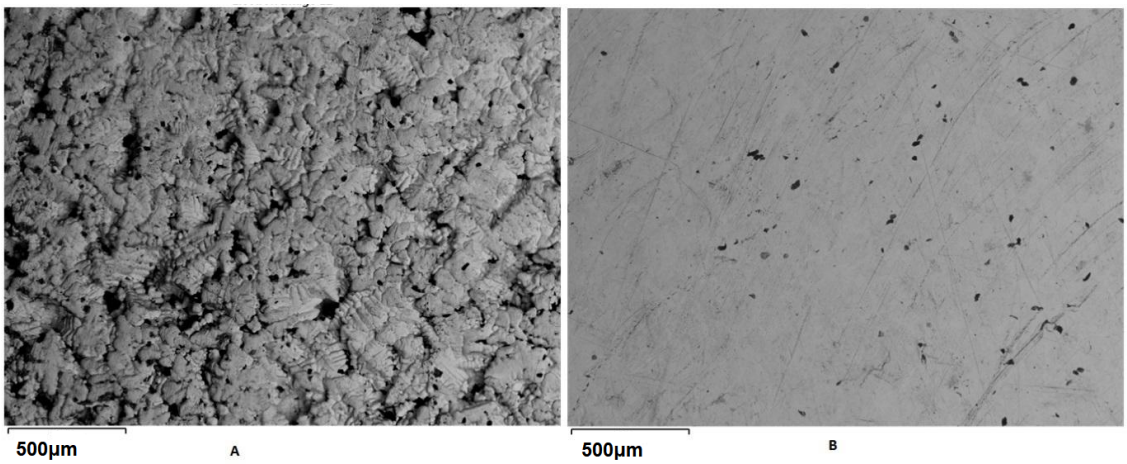

Figure 3.6: SEM images of dull and shiny patches on top side of sand cast lead sheet; (A) Dull/Whitish areas (B) Shiny/Grey area

SEM images of A4 revealed a patch like appearance on the surface. The sample consisted of mainly copper and tin as impurity. Elemental mapping was performed in the region and it showed presence of copper rich areas as shown in Figure 3.8.

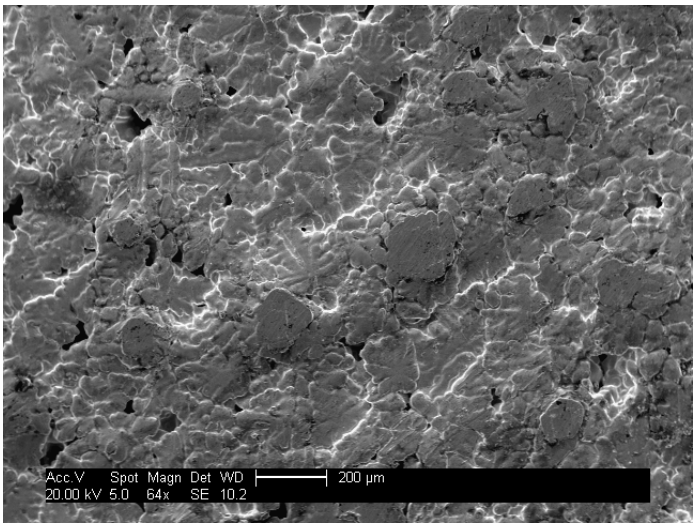

Figure 3.7: Secondary Electron image of the dull area showing dendrites with oxide concentrated at boundaries.

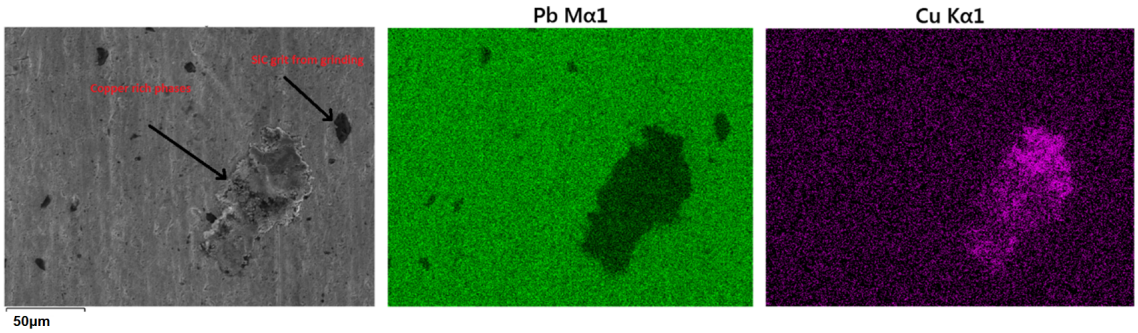

Figure 3.8: SEM Images of S3 and elemental maps showing copper rich areas

3.3.4 Hardness

The samples were cut and grinded using a 1200 grit Sic paper in water to prepare a flat surface for hardness testing. 25g load was used for 15 seconds along the cross section of samples. 10 tests were conducted for each sample and the average value was taken. Table 3.3 shows the hardness values of different samples.

Sample number	Vickers Hardness Number	Percentage of lead
A1	4.9	99.97
A2	4.1	99.83
A3	4.7	99.95
A4	4.8	99.70
A5	5.1	99.95

Table 3.3: Hardness values of samples

3.4 Discussion

Lead is one of the most recycled materials and as a result scrap consists of mostly lead from batteries, building and construction industries. This is often clean though refining may be required [12]. The melt used in sand cast lead sheet is often a mixture of pure (refined) lead and scrap lead to attain the pattern on the surface. The

addition of scrap results in formation of the patterned surface which appear as white and dark (or dull and shiny) patches on the top surface. From SEM observations, white (or dull) areas are observed to appear so, due to rounded and branched dendrites with oxides and carbonates concentrated in those areas, potentially due to an increased surface area. The region on the top surface of the melt which is smeared by the screed is flat and solidification occurs due to contact with the screed which could potentially be the reason of occurrence of rounded grains in some areas on the top edge of the cross-section as observed.

From literature, it was found that addition of even trace amounts of impurities to lead alters its properties [1]. Addition of 1.25% antimony increases its tensile strength from 17Mpa to 29MPa [95]. However, such prominent differences were not observed in hardness values of the collected samples probably due to the effect getting neutralised by other impurities.

Dilute alloys sometimes have unstable growth conditions [27]. The rough sand surface results in a number of nucleation sites for solidification [96]. Solute particles that have low solubility in lead are rejected to the regions ahead of the sand interface. A low concentration of solute close to the sand surface results in formation of circular grains, potentially due to moderate undercooling. The impurities of the melt used in the study contains copper in the range of 0.03% by weight. As per the lead copper phase diagram, the lead -rich eutectic occurs at around 0.06% by weight of copper. At 326°C. Though the eutectic composition has been confirmed at 0.06% Cu (by weight), previous studies suggest that a fully eutectic structure is not usually observed at this composition [27]. Phase diagrams are generally valid only for equilibrium conditions and solidification in real life is often not slow enough for equilibrium to attain especially in a process like sand casting of lead sheet. While observing microstructures of DM lead sheet with 0.06% copper (by wt) Whillock [24]

explained a kinetic barrier with respect to the formation of a eutectic microstructure and this barrier was associated with the formation of copper particles since nucleation of solid lead was observed to occur readily. A high nucleation rate of lead was argued to be the reason for the difficulty in nucleating copper particles.

Cellular, sometimes dendritic structure is a feature of dilute alloys due to unstable growth conditions as a result of constitutional supercooling [97]. With the progress of the solidification interface, pure lead freezes and solute is rejected into the liquid ahead of the interface. In copper lead systems, rejection of copper is primarily due to the difference in atomic sizes of copper and lead atoms as the incorporation of solid copper atoms into the solid lead is energetically unfavourable resulting in low solid solubility. Where there is moderate undercooling, a smooth interface advances through the liquid as can be observed with respect to the initial columnar growth [27]. As the concentration gradient of the solute builds up ahead of the interface, and solute concentration increases, the freezing point of the liquid is depressed, and the interface becomes unstable as the degree of undercooling increases.

Since the concentration of solute particles increases with distance from the sand interface (due to solute particles being pushed away from the sand interface), it is believed that dendritic solidification is forced to happen due to severe undercooling. This is in line with microstructure observations in the previous section. Whillock had observed similar results during solidification studies of continuously cast lead sheet with varying amounts of copper as impurity [24].

The hardness values of all samples were almost similar to that of continuously cast sheet. There are slight variations in hardness values which could be due to the presence of impurities. Further study needs to be conducted to understand effect of these trace impurities on other properties like tensile and thermal fatigue.

Chapter 4

Defects in Sandcast Lead Sheet

4.1 Introduction

One of the most common problems encountered in metal casting is the emergence of defects during filling/pouring or solidification. As reported by Campbell [37] the majority of casting defects arise due to poorly designed running and filling systems or improper selection of casting process parameters. Entrainment defects mainly arise due to the presence of turbulence during filling; oxide films submerge into the melt by folding and form oxide bifilms which often entrap bubbles, sand particles and other inclusions. The presence of turbulence leads to a wide spectrum of casting defects in the final cast product including bubble trails, gas microporosity, hot tears and cold cracks [98]. Besides surface turbulence, there are additional factors leading to defective castings such as hydrogen gas bubbles generated upon solidification due to the lower solubility of hydrogen in the solid phase [99]. Moreover, the presence

of sand casting defects are also dependent on the moulding and sand mixture [43]. This is because green sand mixture usually consists of several components such as sand, clay, water while the proportion of the aforementioned constituents affects the bonding strength of the sand mould. Defects on the product surface may arise when one of these constituents are out of balance due to sand expansion.

Figure 4.1: Sand side of cast sheet with grooves (60cmX100cm)

Just like any other cast product, sand cast lead sheets are also found to have defects. Defects in castings often appear unexpectedly and it can be difficult to identify their source as they can be brought about by a large number of randomly changing production parameters and also due to interactions between alloying elements [35]. At times, defects are caused due to combination effect of more than one parameter [52]. Elimination of defects in casting is a tedious task considering the number of parameters associated and shortage of skilled workers. Often, casting is considered as a process of uncertainty and even in completely controlled processes, some qual-

ity defects are difficult to explain [44]. This chapter focusses on a specific surface defect type occurring at the sand side of the sand cast sheet. The defect type under investigation has a groove like appearance (Figure 4.1) and appears along the cast sheet (in the direction of flow of the metal) and can range from 2 cm to 30 cm in length and will be addressed as 'grooves' throughout this thesis. The objective of the current investigation in this chapter is to identify the main process parameters affecting the formation of grooves and propose remedies leading to the reduction or elimination of the aforementioned defect type. Since these sheets are used for roofing applications, which involves bending and manipulation of the sheet, cracks are often initiated at these locations. It also gives a perception of poor quality and leads to rejection.

4.2 Materials and Methods

4.2.1 Materials

For the purpose of this experiment, silica sand of two different grain sizes (AFS 50 (approx. 280 micorns) and 70 (approx. 195 microns) sourced from Tarmac UK) and bentonite clay were used. The sand moulds were prepared by mixing silica sand (95-98%) with water (2%) and bentonite clay (0-3%) depending on the case under examination. Moreover, two types of melt were used: (a) pure lead and (b) a 50:50 mix of scrap with pure lead. Scrap lead primarily consisted of old roofing sheets, flashings and lead pipes. A SPECTROMAXx stationary metal analyser (with a resolution of 0.0001%) was used to determine the elemental composition of the scrap lead as shown in Table 4.1. Pure lead (99.9%) was obtained by melting scrap lead and then refining it using Sodium Nitrate and Caustic soda. Lead was melted in 120-ton steel kettles and mixed in a smaller 5-ton kettle prior to casting.

	Cu (%)	Zn (%)	Sn (%)	Sb (%)	Bi (%)	Ag (%)
Mean	0.0283	0.0029	0.086	0.0315	0.0179	0.0041
SD	0.0255	0.0101	0.0011	0.079	0.0030	0.0184

Table 4.1: Mean and standard deviation (SD) values of common impurities obtained from elemental analysis of 80 different scrap melt batches.

4.2.2 Defect Analysis

This investigation is focused on a surface defect type, hereby This investigation is focused on a surface defect type, hereby addressed as 'grooves', appearing on the sand side of sand cast lead sheets as shown in Figure 4.1. As it can be observed, the nature of this defect type is different from surface roughness which can be effectively controlled by AFS grain fineness number of the sand. These defects are formed along the direction of the flow and may range between $2cm$ and $30cm$ in length while their root cause has not been identified in the literature yet. Since lead sheets are used for roofing applications, which involve bending and manipulation of the sheet, cracks are often initiated at these locations. Moreover, grooves give the perception of poor quality and lead to rejection by customers.

There are several factors which could potentially influence the quality of cast lead sheets and promote the formation of grooves. Hence, based on process observation, literature review [43], [52], [100] and the experience of foundry engineers, all the possible factors affecting the quality of sheets were categorised based on a 5M model (Man, Material (Melt), Machine (Mould), Method, Measurement) and environment [51] (see Table 4.2).

Initially a qualitative approach (visual examination) was followed; a set of screening experiments was conducted to check the influence of different process parame-

No	Process parameters	Classification as per 5M
1	Temperature of Melt	Material
2	Melt Composition	Material
3	Sand	Machine
4	Water content	Machine
5	Velocity of screed	Method
6	Angle of inclination of sand bed	Machine
7	Use of screed	Method
8	Ambient temperature	Environment
9	Bed preparation	Man

Table 4.2: Factors potentially affecting the quality of cast sheets

ters on the formation of grooves and narrow down the factors affecting defect formation. The formation of grooves was hardly affected by altering the pouring temperature of the molten metal. Increased moisture content resulted in the formation of new defects such as blow holes. To investigate the effect of the stress induced by the screed rail on the metal during the process on the formation of defects, trials were conducted by casting sheets without the use of a screed rail. Trials were also conducted by altering the inclination of the sandbed as well. It was inferred that the screed rail and inclination of sandbed did not have much of an influence on the formation of grooves when other operating conditions were set. Experiments were also performed using 99.9% pure lead and unrefined scrap. According to naked-eye observations the use of scrap melt led to additional defects due to the presence of impurities, as expected. With regard to the concentration of grooves per unit area, which was the observable in this investigation, slightly higher values were observed in the case of unrefined scrap melt. Finally, it was observed that coarser sand resulted in poor surface finish, as expected. The initial screening experiments performed were used for the final selection of 3 factors affecting the formation of grooves which were subsequently used in the DoE analysis, as it will be discussed

in Section 4.2.3.

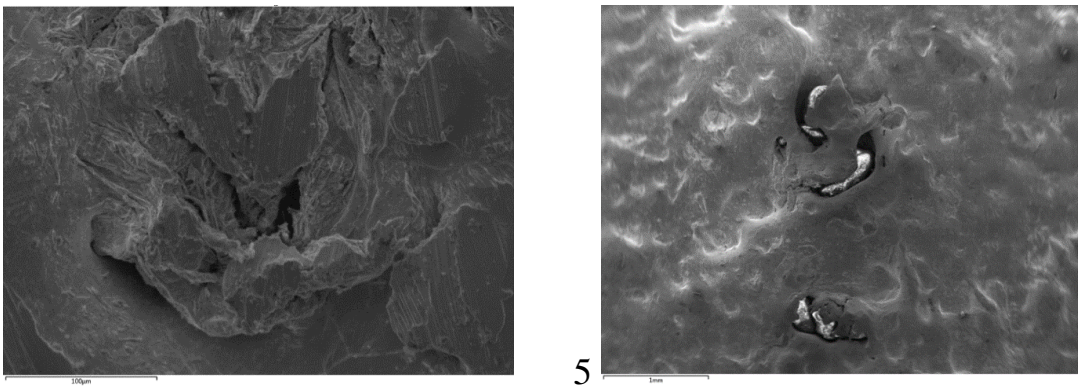

(a) (b)

Figure 4.2: SEM images of (a) the groove defect at 350x magnification and (b) a sand inclusion at 26x magnification.

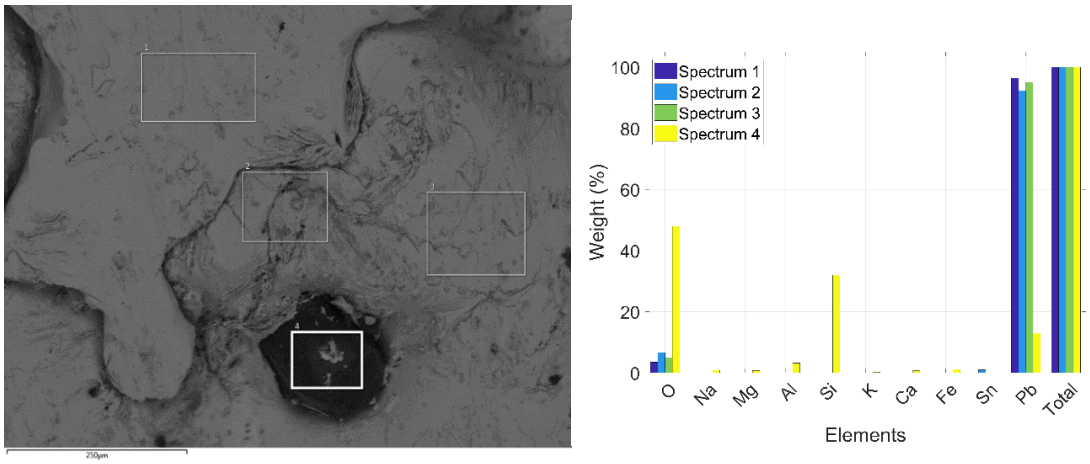

(a) (b)

Figure 4.3: (a) SEM Image of sand inclusion at magnification 150x and (b) Spectral analysis of the corresponding regions (1-4)

In order to thoroughly investigate groove formation, microscopic analysis of the defects was carried out. 20*mm* x 20*mm* square samples were cut out from the central part of defective sheets. Since defects were observed to be uniformly distributed over the surface of the sheet, the aforementioned sample was considered to be indicative of the properties of the whole sheet. The samples were cleaned with ethyl alcohol (ethanol) at concentration 70% and the sand side of the samples was observed under

a Scanning Electron Microscope (SEM) with an Electro Dispersive Spectrometer (EDX). A Phillips XL30ESEM environmental scanning electron microscope was used for this purpose. The results from the EDX confirmed the inclusion of sand particles in the vicinity of grooves as illustrated in Figure 4.2 and Figure 4.3. Based on this observation, it was assumed that the composition of the mould material may have an effect on defect formation.

4.2.3 Design of Experiments

The implementation of the DoE method consists of the following 5 steps, namely: (a) selection of factors and corresponding levels, (b) identification of the response variable, (c) selection of experimental design (d) conducting the experiment and (e) analysis of data. In this study, the experimental factors were selected based on literature review, process observation and operator interviews. As discussed in the previous section, according to SEM observations and screening experiments, it was concluded that defects were caused as a result of poor mould properties. Green sand mould consists of sand, water and a binder (usually clay) to bond the sand particles together. A good casting is produced when there is a good balance between the components of a green sand mixture. Hence, the effect of these parameters on the formation of defects on the surface was investigated. Moreover, the use of pure lead does not result in the mottled appearance on the top sheet surface which is one of the most characteristic and desired properties of cast lead sheet [20]; thus, most foundries use a mix of pure (refined) and scrap lead. This factor was also included in the study as defects could also be caused due to the melt quality or interaction between the melt and the mould. Table 4.3 summarises the experimental parameters and their corresponding levels that have been used in this study. The factors used for the DoE analysis were ‘sand’ (based on their AFS fineness number) (A), ‘bentonite

percentage' (B) and 'type of melt' (C). Each factor was set to two levels equivalent to the high and low values of the corresponding experimental variables.

Factors	Type	Low level	High level
A: Sand AFS (Dimensionless)	*Numeric*	*50*	*70*
B: Clay (%)	*Numeric*	*0*	*3*
C: Melt	Categoric	Pure	50:50 Mix of refined and scrap lead

Table 4.3: Factors and their levels

After identifying the various factors and their levels, a suitable experimental design was established. Considering the relatively small number of factors, a full factorial design was preferred. In full factorial designs all possible combinations of factors are tested in order to identify the statistically significant ones. Full factorial designs are very effective especially when the number of factors is relatively low due to the small number of experiments needed to be conducted. The design layout was formed as per the parameters defined in Table 4.3 while the run order was randomised in order to minimise systematic errors. All trials were replicated twice and a total of sixteen experiments was conducted. The experimental design is shown in Table 4.4. A square sample ($0.5m$ x $0.5m$) was cut out from the middle section of the cast sheet and the total length of defects per unit area was measured using a digital calliper or a ruler depending or their length; as mentioned in the previous subsection, their length can exceed $30cm$. The total length of defects per unit area was considered as the response variable (Y) of the DoE analysis.

Standard Order	Run Order	A: Sand AFS (Dimensionless)	B: Bentonite (%)	C: Melt (Composition)	Response: Y (1/mm)
1	*1*	*50*	*0*	Pure	620
15	*2*	*50*	*3*	50:50	105
2	3	70	0	Pure	538
16	4	70	3	50:50	99
3	5	50	3	Pure	110
12	6	70	3	Pure	70
9	7	50	0	Pure	640
8	8	70	3	50:50	96
4	9	70	3	Pure	65
6	10	70	0	50:50	582
13	11	50	0	50:50	712
14	12	70	0	50:50	600
7	13	50	3	50:50	105
11	14	50	3	Pure	95
10	15	70	0	Pure	548
5	16	50	0	50:50	685

Table 4.4: Experimental Design

Minitab 18 was used for the analysis of the collected results. As mentioned in the Literature section, the main objective of using a full factorial DoE is to estimate the main and interaction effects with a significant influence on the response variable. In this study a 95% confidence interval was assumed while the factor effects were considered to be statistically significant for $P \leq 0.05$.

4.3 Results and Discussion

Experiments were conducted on a $7m$ long casting bench under identical conditions at a foundry based in Derby, UK. Each mould mixture was prepared in a rotating sand mixer while the melt was prepared in a furnace next to the casting bed at 450°C. The melt was then transferred to a hopper where any dross formed was removed. A k-type thermocouple with a temperature range of -200 °C to 1250 °C sourced from Omega Engineering Ltd was dipped in the melt in order to constantly monitor the temperature before pouring at 345 °C. The pouring temperature was held constant for all trials. As illustrated in Table 4.5, the factors and interactions whose P-values are less than 0.005 have a significant effect on the response variable Y. Moreover, the sand-melt interaction and the three-way interaction between sand, clay and melt were considered to be insignificant and were hence neglected since their P values were greater than 0.005. The R-squared (R2) statistic is indicative of the variation of the response variable due to the variation of the input variables; larger values of R2 adjusted indicate models of greater predictive ability [101]. Predicted and adjusted R2 values were found to be equal to 99.92% and 99.85% respectively and in agreement with each other. Thus, the values obtained in the experiments are considered satisfactory for the validation of ANOVA.

ANOVA can also be validated through the normal probability plot of residuals (or error) which is a graphical technique for assessing whether a data set is ap-

Source	DF	Adj SS	Adj MS	F-Value	P-Value
Model	7	1119746	159964	1412.48	0.000
Linear	3	1111617	370539	3271.87	0.000
Sand	1	14042	14042	123.99	0.000
Clay	1	1092025	1092025	9642.60	0.000
Melt	1	5550	5550	49.01	0.000
2-Way Interactions	3	7552	2517	22.23	0.000
Sand*Clay	1	5776	5776	51.00	0.000
Sand*Melt	1	12	12	0.11	0.751
Clay*Melt	1	1764	1764	15.58	0.004
3-Way Interactions	1	576	576	5.09	0.054
Sand*Clay*Melt	1	576	576	5.09	0.054
Error	8	906	113		
Total	15	1120652			

Table 4.5: ANOVA table

proximately normally distributed. If the data points of a normal probability plot lie on the vicinity of a straight line, it can be assumed that the residuals are normally distributed. In Figure 4.4 the plotted data points fall on a straight-line indicating compliance to the normality assumption.

A Normal Probability Plot is a plot of the theoretical percentiles of the normal distribution plotted against observed sample percentiles. The theoretical pth percentile of a distribution is a value such that $p\%$ of the measurements fall below the value. If the data is normally distributed, then the theoretical percentiles of the normal distribution versus the observed sample percentiles should be a straight line. Observed sample percentiles are expressed as a Z score (or normal score). Z score is calculated as

$$z = \frac{x - \mu}{\sigma} \tag{4.1}$$

Where x is the raw score, μ is the mean of the population, and σ is the standard

deviation of the distribution. Since we are interested in the normality of residuals, a normal probability plot of the residuals is created. To plot the normal probability plot, the residual values are ordered from minimum to maximum and a rank order number (i) is assigned. The cumulative probability is calculated as

$$z = \frac{p_i - 0.5}{n} \tag{4.2}$$

Where n is the number of data points. For each value of probability, the corresponding z values are obtained and plotted.

The normal probability plot of the effects shows the standardized effects with respect to a distribution fit line for the case when all the effects are zero. The standardized effects are basically t-statistics that test the null hypothesis that the effect is zero. The plot also helps us in understanding the direction of the effect.

Pareto Chart depicts the absolute values of the standardised effects in a decreasing order of the magnitude of the effect. The chart also plots a reference line to show statistically significant effects depending on the significance level (α)[102].

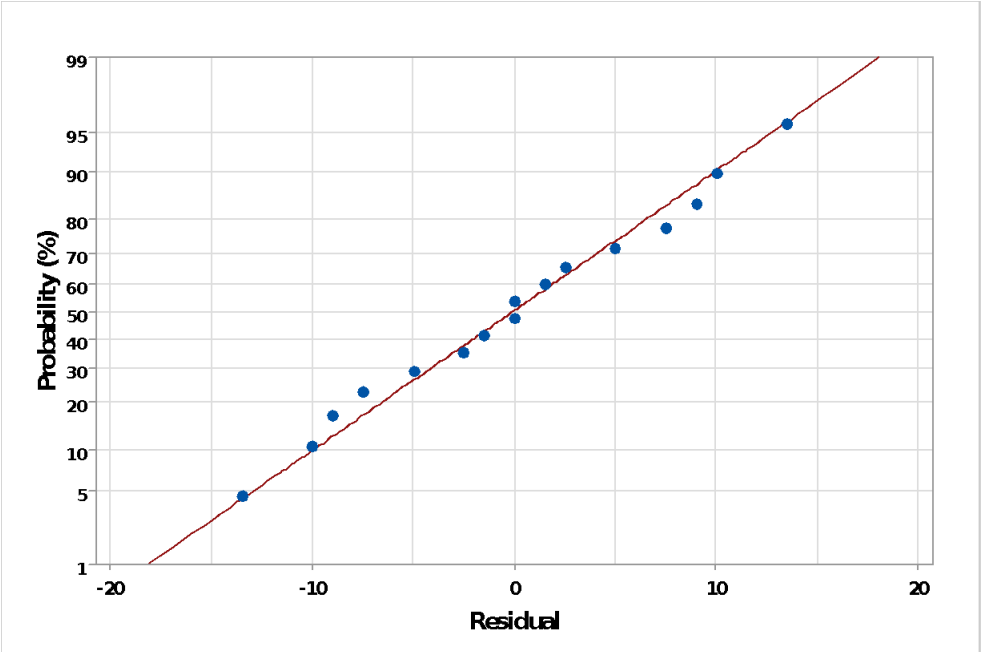

Figure 4.4: Normal probability plot of residuals

Significant effects can be identified from the normal plot of the effects as shown in Figure 4.4. All the effects lying in the proximity of the straight line are insignificant while the ones lying far from it are statistically significant. The response variable is increased when the positive effects change from low level to high level while negative effects have the inverse effect on the response variable. Those effects further from $x = 0$ are more significant [103]. A Pareto plot was also generated to evaluate the significance of the main and interaction effects as shown in Figure 4.5. The vertical red line at 2.3 is called reference line; any effects with bars reaching beyond this value are considered significant. From the Pareto and normal probability plots of the effects, it is evident that the most significant effect is B (clay content in the moulding mixture). Other significant effects influencing defect formation are A (sand type), C (melt composition), AB (sand-clay interaction) and BC (clay-melt interaction). It can also be observed that AC (sand-melt interaction) and ABC (three-way interaction between sand, clay and melt) are insignificant and consequently have negligible influence on the formation of defects.

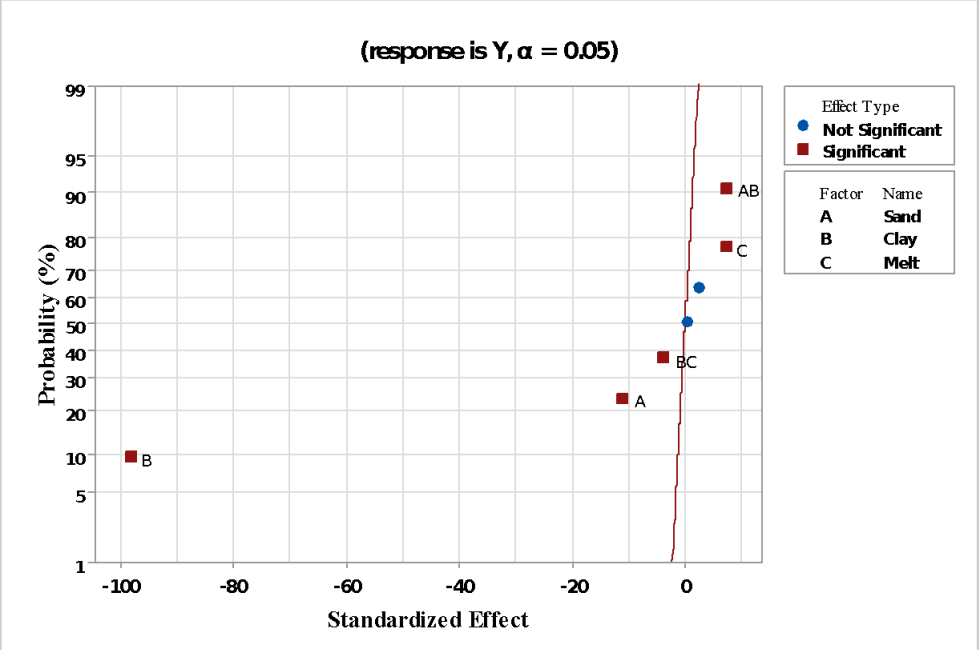

Figure 4.5: Normal probability plot of the effects

The main effects of the three factors considered on the formation of defects on the cast sheet have been plotted in Figure 4.6. As it can be observed, the clay content of the moulding mixture is the most significant among the 3 factors examined while defects have been found to reduce significantly with an increase in bentonite content. This is because a good casting is produced when there is a good balance between the components of the green sand mixture. Lead is a metal with a high density and has a high value of 3.22% for contraction on solidification [37]. Expansion defects are very common in castings and they originate in part due to expansion of the sand grains which get heated by the molten metal [100]. Silica sand expands to a greater extent when compared with other sand like zircon, olivine and chromite [104]. Apart from expansion, these defects are also reliant on moisture. When the molten metal flows over the sand bed, the moisture in the mould is converted to steam and this steam permeates through the sand grains in the mould. At the point when the steam reaches a temperature lower than $100^{\circ}C$, it condenses, and a wet layer is formed. This wet layer is weaker than the green sand or the hot dry sand. However, when the hot sand expands due to the heat absorbed from the molten metal, this wet layer shears to allow expansion and ridges of sand spread into the mould cavity and thereby grooves are formed on the cast sheet. This phenomenon is intensified due to the contraction of the solidifying metal and erosion of sand. Addition of a binder holds the sand particles together thereby reducing this effect and explains the reduction in formation of these defects.

Grooves were also found to reduce with an increase in the AFS grain fineness number. Fine grained sand helps to attain a better surface finish owing to lower metal penetration into the mould but needs more binder content. However, a low permeability might result in formation of gas defects. Coarse grains provide higher permeability but may allow metal penetration. As a result, there should be a balance

between these parameters to attain the best results [105].

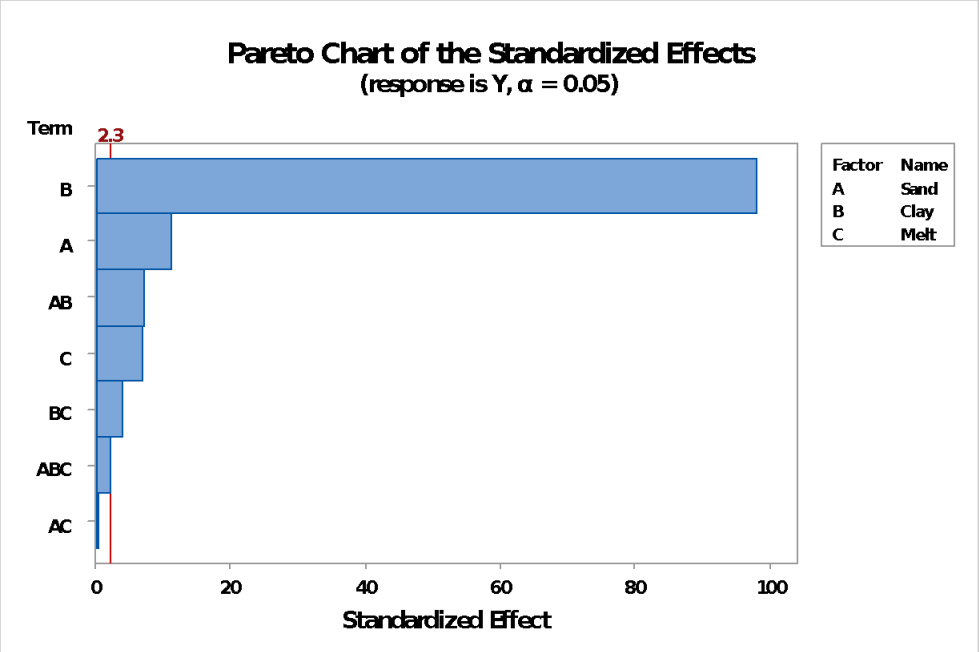

Figure 4.6: Pareto chart of Standardised effects

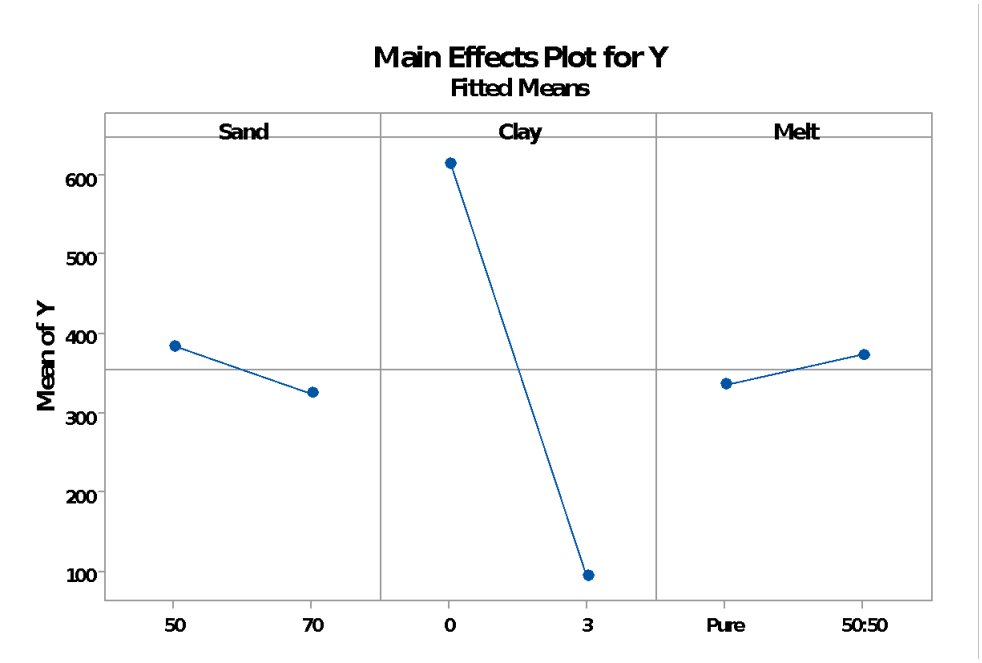

Figure 4.7: Effect of process parameters on defect formation

Finally, the use of 50:50 mix of refined to unrefined lead increases the formation of defects as expected. This is because of the already existing inclusions in the 50:50

mix which contribute to the formation of additional defects. The optimum settings for minimal defects are obtained for a combination of 70 AFM sand, 3% Bentonite and pure melt.

4.4 Conclusions

Sand casting of lead sheet is a traditional method for manufacturing premium lead sheet for roofing applications in heritage buildings. Similarly, to all casting processes lead sheet casting suffers from the presence of defects. In this investigation the focus has been laid on a surface defect type, hereby addressed as 'grooves', appearing on the sand side of cast lead sheets. The main conclusions drawn from this investigation are summarised below:

- The majority of the defects produced in lead sheet casting industry can be attributed to mould properties and moulding materials. This paper substantiates the fact that green sand casting provides better surface quality and finish as compared to traditional sand mixtures used in sand casting of lead sheet.
- The trials conducted with the green sand mixture showed an improved surface finish and substantial reduction in the grooves produced on the sand side. Addition of bentonite in the sand mixture results in a substantial reduction of groove defects in sand cast lead sheet.
- Grooves are reduced for higher AFS grain fineness numbers. Fine grained sand contributes to superior surface finish owing due to the decreased lead penetration into the sand.
- The quality of the melt also affects the formation of the grooves. Pure lead should be favoured over a mix of refined and scrap lead.

- Groove defects in sand cast lead sheet can be minimised by 90% for a combination of 70 AFS sand, 3% bentonite and pure melt.

Chapter 5

Numerical Modelling of Sandcasting Process

5.1 Introduction

Nowadays, the evolution of computing power as well as modelling techniques have made numerical investigation of casting processes feasible [81]. The sand casting process in particular has been extensively studied by means of CFD simulations. Among various topics, defect prediction in sand casting is one of the well-researched areas. Although lead sheet sand casting falls into the category of sand casting processes, the nature of the process is quite different from traditional sand casting as liquid lead solidifies on top of a sandbed instead of inside a mold cavity and it also involves smearing the liquid lead on the sandbed with a strickle. Moreover, the final cast component (sheet) is very thin compared to traditional sandcast components. As a result, CFD modelling of such a process involves a number of challenges related to the mesh generation, free surface flow and turbulence modelling

Despite the extensive application of CFD in metal casting, the lead sheet casting process has not yet been numerically investigated according to the authors' best knowledge. This investigation aims to shed light on the effects of three main process parameters (pouring temperature, strickle-sandbed clearance and strickle velocity) on the final quality of sandcast lead using a two-dimensional CFD model. This is the first attempt to investigate the lead sheet casting technique via numerical simulation. A CFD model was developed to simulate the filling and solidification stages of the process. The final quality of the sheets was quantified by measuring their roughness and average thickness. The developed CFD model was validated using temperature data at the fluid-sandbed interface collected from real-time experiments.

5.2 Methodology

5.2.1 Simulation Setup

As stated in the introduction, the lead sheet casting process consists of two main sub-processes: (a) pouring the molten metal onto a sand bed and (b) smearing of the melt surface using a strickle. As illustrated in the flow chart of Figure 5.1, the process starts with melting a mixture of scrap lead and refined lead in a furnace at $450^{\circ}C$. Molten metal is then poured into a hopper where the dross is removed. Meanwhile, the casting bench is filled with a green sand mixture which is subsequently levelled and smoothened to attain a flat surface. The temperature of the metal is being constantly measured using a thermocouple and pouring starts when the lead temperature has reached $345^{\circ}C$. Temperatures lower than this value might lead to premature solidification (liquid lead might not reach the end of the bed), while higher temperature might lead to sheets with increased surface irregularities and thickness lower than the desired value, as it will be shown in the results section. In this investigation the

focus is laid explicitly on the pouring and solidification stages of the process.

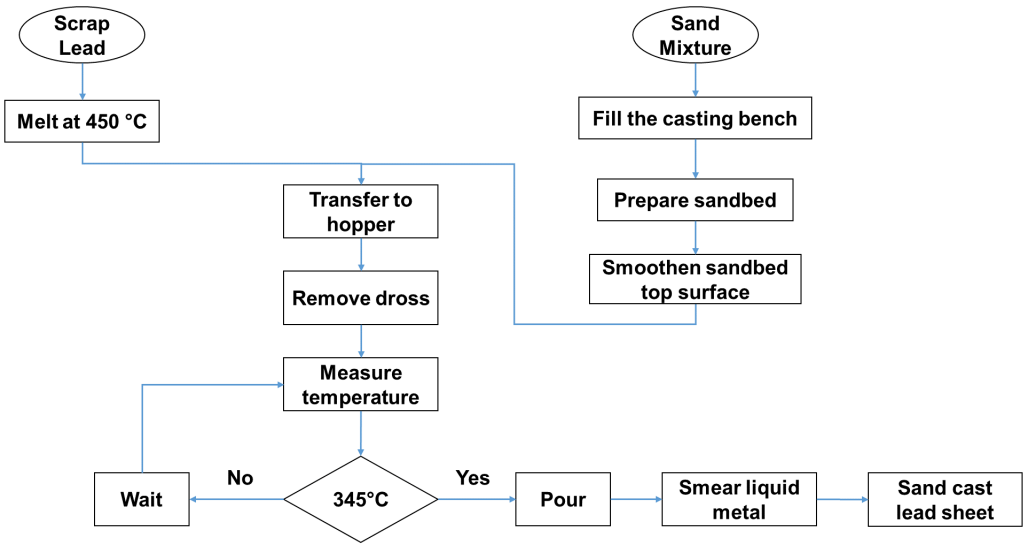

Figure 5.1: Process flow chart of the lead sheet casting process

As illustrated in Figure 5.2(a), a typical sand-casting setup for sheet lead manufacture consists of 3 components: (a) a sandbed, (b) a wooden strickle and (c) an inclined plane made of steel. The dimensions of each component are depicted in Figure 5.2(b). For the simulation setup a 3m long sandbed was considered. This value was selected because it is large enough to provide an accurate estimate of the lead sheet quality while maintaining the computational cost within acceptable limits. Moreover, as it will be presented in the following sections both the flow and temperature fields are stabilised after the first 1 m of the horizontal section of the sandbed. The CFD model was limited to two directions in favour of computational efficiency since the flow and temperature fields are not expected to change in the transverse direction (y-direction). Moreover, the effects of the sandbed walls with respect to heat transfer and shear stress are not dominant across the transverse direction considering that the contact area of liquid lead with the walls is very small compared to the corresponding one with the sandbed.

Component	Material
Sandbed	Silica Sand
Inclined Plane	Stainless steel
Strickle	Wood

Table 5.1: Component materials

Density* (kg/m^3)	10,600
Viscosity* ($Pa.s$)	0.0027
Specific Heat* ($J/(kg.K)$)	143
Thermal conductivity ($W/(m.K)$)	33
Heat transfer coefficient (lead/void) ($W/(m^2.K)$)	30
Heat transfer coefficient (lead/sandbed) ($W/(m^2.K)$)	1000
Heat transfer coefficient (lead/strickle) $[W/(m^2.K)]$	1000
Heat transfer coefficient (lead/inclined plane) ($W/(m^2.K)$)	8000
Melting point ($^\circ C$)	327.5

Table 5.2: Lead (Pb) properties [106]

The material properties corresponding to each component were taken from the Matweb online materials database [106] while the heat transfer coefficients at the interfaces of the molten metal and each component were set according to [107]. Based on the measurements taken during the experiments conducted, the initial temperature for each component was set equal to $15^\circ C$, as well as the room temperature. Metal pouring was simulated using a rectangular metal source placed on top of the inclined plane while the velocity normal to the metal source area was selected to be constant during the first 2.5 seconds of the simulation and equal to $1.14 m/s$. The value of the velocity was calculated according to equation (7) and selected so as to satisfy a mass flow rate ($\dot{m}$) equal to $392 kg/sec$ as suggested by the experimental setup.

$$u = \frac{\dot{m}}{\rho A} \tag{5.1}$$

Temperature (K)	Specific heat capacity (J/kgK)
298.15	129
400.15	132
500.15	137
600.55	142
600.55	148
700.15	147
800.15	145
900.15	143
1000.15	140
1100.15	139

Table 5.3: Lead Temperature v/s Density

Subsequently, the source was removed and the strickle was displaced vertically up to the point of the desired clearance between the strickle and the sand bed. Then the strickle was assigned a constant velocity ranging from 1-1.6m/s, depending on the case under examination, parallel to the sand bed (x-direction). The lead properties used for the simulation setup are listed in Table 5.2. The values of the properties denoted with a star (*) refer to the melting point of lead and have been considered to be dependent on the lead temperature during the simulation [108]. The dependencies have been shown in the table 5.3 and 5.4.

A rectangular mesh was utilised in order to solve the mass, momentum, energy and heat transfer equations. Due to the enhanced resolution required at the interface between the sandbed and the liquid lead (boundary layer), an increasingly finer mesh was introduced at the vicinity of the aforementioned area as illustrated in Figure 5.3. In order to achieve high accuracy, the cell size across the direction normal to the sandbed was set equal to 0.5mm in order to have at least 4 fluid cells along the minimum cross section of the setup; this corresponds to the clearance between the sandbed and the strickle, which ranges between 2.5 and 4mm. In order to maintain

Temperature (K)	**Specific heat capacity (J/kgK)**
298.15	11350
473.15	11150
573.15	11000
598.15	10700
673.15	10600
873.15	10370
1073.15	10220

Table 5.4: Lead Temperature v/s Specific heat capacity

an aspect ratio equal to 3 across the simulation domain, the maximum dimension of the cells was consequently set equal to $1.5mm$. The final constructed mesh consisted of 237,168 cells in total. The mesh was confined to the solid components of the simulation domain (inclined plane, sandbed and strickle) with an overlap length equal to $5cm$. Symmetry boundary conditions were applied across all the mesh boundaries, except of z_{max} where a pressure boundary condition was applied and x_{max} which was defined as an outflow boundary. Finally, a no slip condition was applied at the mold/lead and strickle/lead interfaces.

The developed model accounted for surface tension which was considered to be equal to $\gamma = 0.439kg/s^2$ while a full flow shrinkage model was used in favour of computational accuracy [109]. Moreover, the Renormalized Group (RNG) model was employed for modelling turbulence [110]. For each simulation performed the fluid momentum and continuity equations were solved, while a first-order method was used for the approximation of the momentum advection.

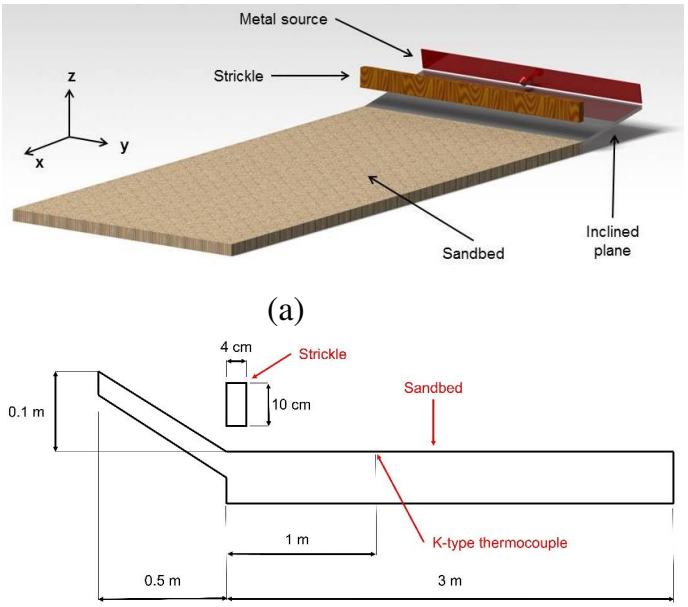

Figure 5.2: (a) Schematic illustration and (b) sketch of the simulation setup

5.3 Model verification

Experiments were conducted on a $7m$ long sand bed at a foundry based in Derby UK, with a 99.9% pure recycled lead charge. When conducting experiments, it was essential that the liquid melt was smeared using the strickle before it completely solidified to attain a flat top surface; any delays would result in premature solidification and consequently sheets with higher thickness than the desired value. On the other hand, the strickle motion should not commence very early as this would result in additional melt solidifying on top of the flat surface already created by the strickle motion. During the process, shims were used in between the strickle and the screed rail to adjust the clearance between the sand bed and the bottom surface of the strickle.

The verification of the CFD model was based on the comparison of the cooling curves of liquid lead obtained from experimental and numerical results respectively. This strategy has been also been used in past investigations for validating numerical

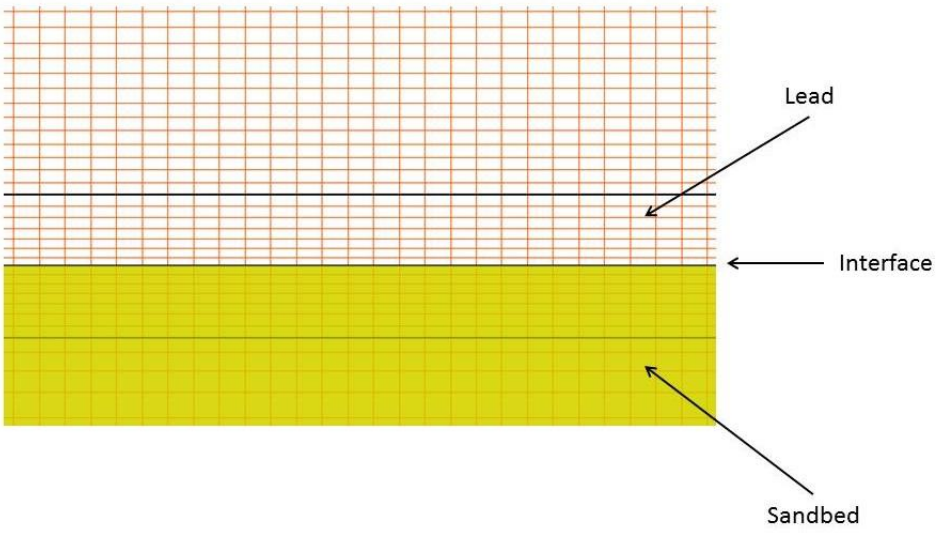

Figure 5.3: Mesh resolution

models against experimental ones [111], [112]. Similar cooling curves between the experimental and numerical results would be indicative of the appropriate selection of heat transfer coefficients, material properties and solidification models employed. To obtain the experimental temperature measurements, one K-type thermocouple was inserted from beneath the sand bed and placed at the sandbed/lead interface at a distance equal to 1 m from the end of the inclined plane (Figure 5.2(b)). An 8-channel thermocouple data acquisition module (Pico TC-08) coupled with the software PicoLog 6 was used to collect temperature data at equally spaced time intervals of 1 second. In order to meaningfully compare the experimental results with the numerical ones, the simulation parameters (pouring temperature, clearance, strickle motion onset time and speed) were set so as to accurately replicate the experimental conditions.

In Figure 5.4, the collected temperature data are plotted as a function of time along with the temperature of a probe of the simulation domain with the identical position, located at the interface between the sandbed and the lead. Moreover, it has to be noted that t=0 corresponds to the time when the strickle starts moving

while both the experimental and simulation results correspond to a lead sheet with thickness equal to 4*mm*. It is evident the numerical results are in very good agreement with the experimental ones; thus, the model is considered to be adequate and accurate enough to describe the particular manufacturing process.

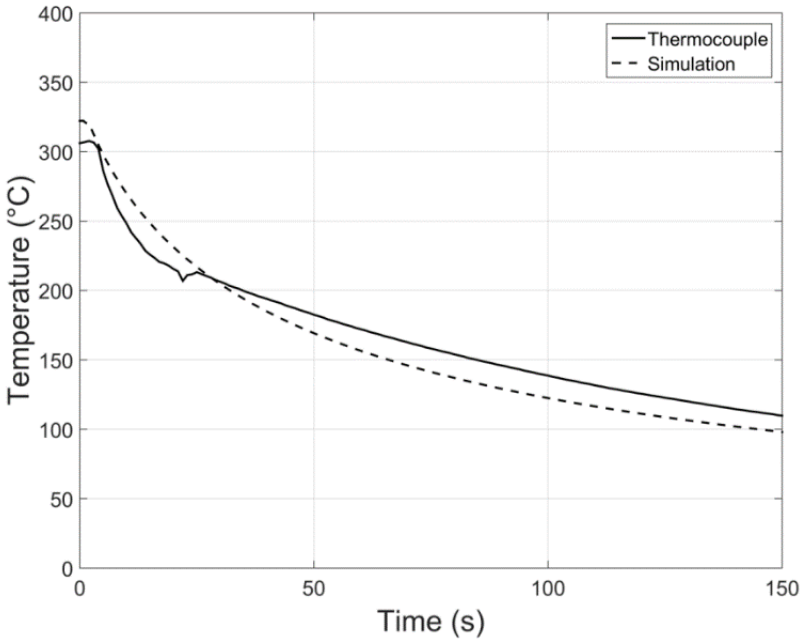

Figure 5.4: Lead interface temperature vs time (numerical vs. experimental results)

5.4 Results

5.4.1 Introduction

The most significant challenge of the lead sheet sand casting process is controlling the thickness of the lead sheet. We performed sand casting experiments to manufacture 3 different codes (standardisation of thickness) of lead sheet. The pouring temperature values were selected based on the interviews with the craftsmen and foundry engineers of Midland Lead. The obtained thickness readings at 5 equally

spaced (by 20cm) along the longitudinal (x-) axis points located at the centre of the bed are listed in Table 5.5. It can be observed that although the mean thickness values are close to the desired one, there are fluctuations around the mean value.

Table 5.5: Experimental thickness readings for various thickness codes

Code	6	7	8
Thickness (mm)	2.65	3.15	3.55
Pouring temperature($^{\circ}C$)	355	347	342
Reading 1	2.37	2.94	3.44
Reading 2	2.45	2.91	3.58
Reading 3	2.28	3.21	3.68
Reading 4	2.77	3.11	3.37
Reading 5	2.81	3.18	3.49
Average	2.54	3.07	3.51
Variance (mm^2)	0.046	0.015	0.012

It is therefore crucial to identify the effects of each process parameter on the final quality of the lead sheet in order to minimise thickness fluctuations on the final product. This section aims to demonstrate how common casting parameters affect quality, which is quantified on the basis of average sheet thickness and its standard deviation, by means of numerical modelling. The effect of clearance between the strickle and sand bed, melt temperature and speed of motion of strickle is presented in this section.

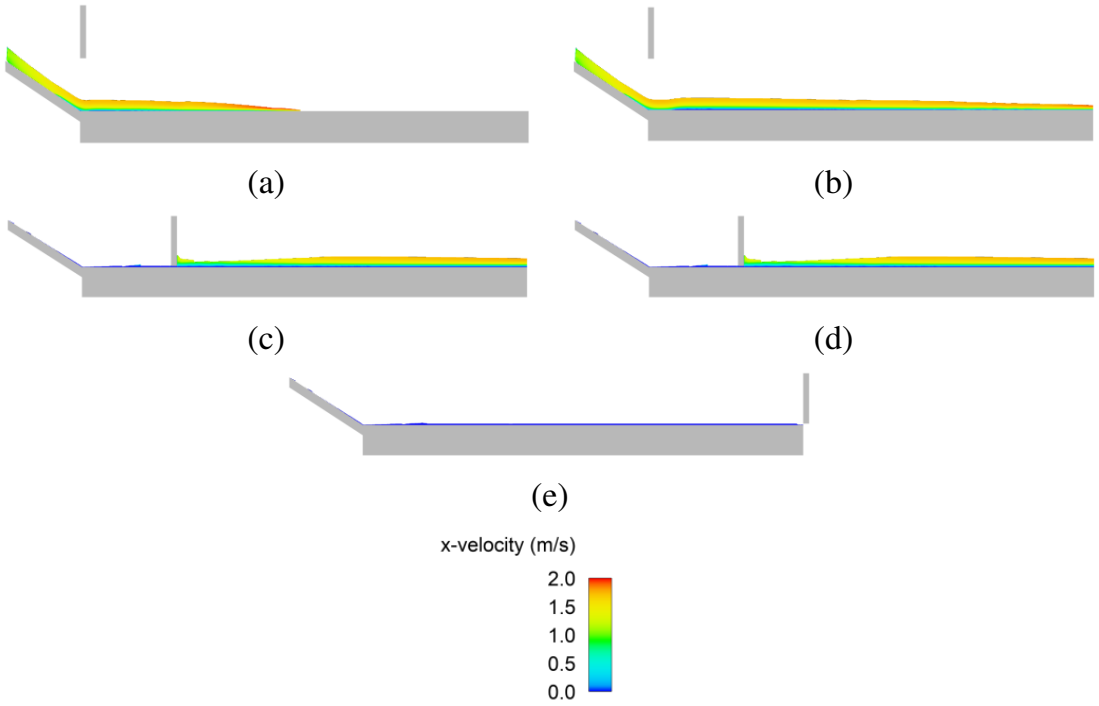

Figure 5.5: Velocity profiles at (a) t=1.2 s, (b) t=2.4 s, (c) t=3.6 s, (d) t=4.8 s and (e) t=6 s

The velocity profiles of the liquid lead are demonstrated in Figure 5.5 for evenly spaced time intervals. It can be observed that the maximum velocity is located at the metal front which reaches the end of the bed within the first 2.4s. The x-velocity is zero at the liquid-solid interface due to the no-slip boundary condition imposed, while it gradually increases towards its maximum value located at the free surface. The strickle starts moving along the x-axis at $t = 3s$ and smears the melt. When the strickle exits the simulation domain, the fluid is stationary and has a uniform thickness along the sandbed with the exception of the first 0.75 meters of the sandbed. This is because of the additional non-solidified metal flowing over the inclined plane after the strickle starts moving. This observation is in agreement with experimental results and will be further discussed in the following sections.

5.4.2 Clearance

As mentioned in the introduction section, craftsmen control the lead sheet thickness by adjusting the clearance between the sandbed and the strickle. The thickness profiles for 4 different values of the clearance c are illustrated in Figure 5.6. It has to be mentioned that the lower limit of the axis corresponds to the end of the inclined plane ($x = 0.5m$), while the strickle velocity was set to $1m/s$.

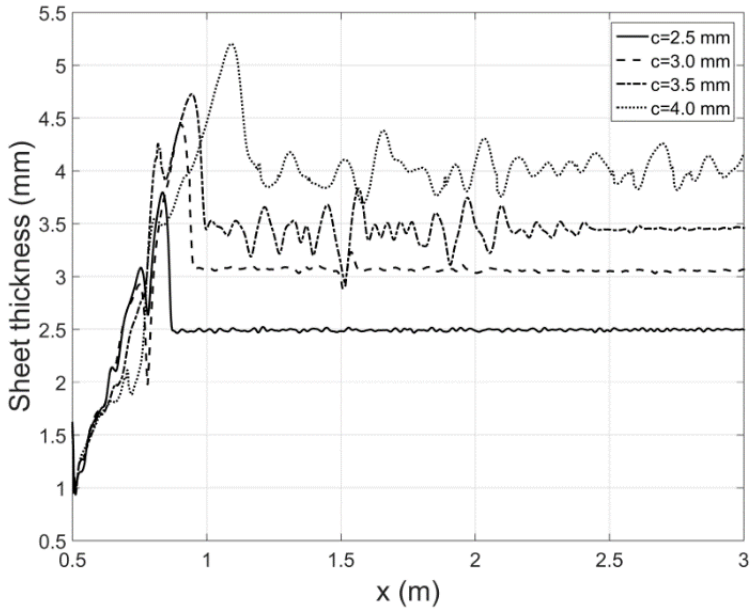

Figure 5.6: Thickness profiles for various values of clearance

It is evident that the sheet thickness gradually increases along the sandbed until it obtains a constant value for all cases examined. This region is characterised by the presence of hills and valleys and this behaviour is attributed to the fact that it lies in the proximity of the metal source which hinders immediate solidification due to the continuous flow of metal over the inclined plane. As we move away from this region the temperature of the liquid lead drops and a solid substrate is formed as illustrated in Figure 5.7.

Despite the fact that higher clearance may lead to higher sheet thickness variance,

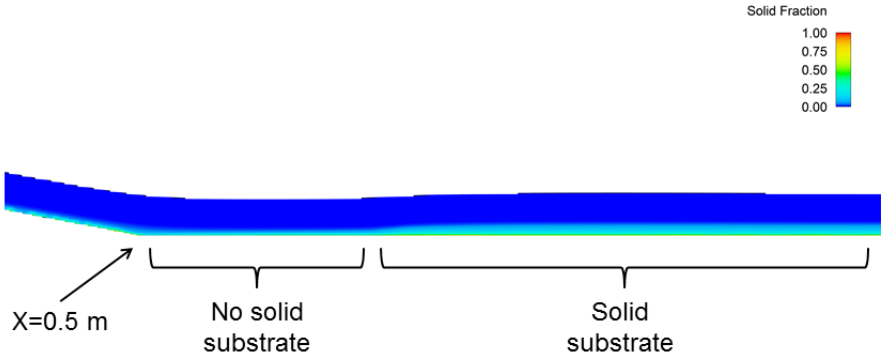

Figure 5.7: Solidification profile

the average sheet thickness, which has been calculated similarly to the variance, can be effectively controlled by the clearance as illustrated in Figure 5.9.

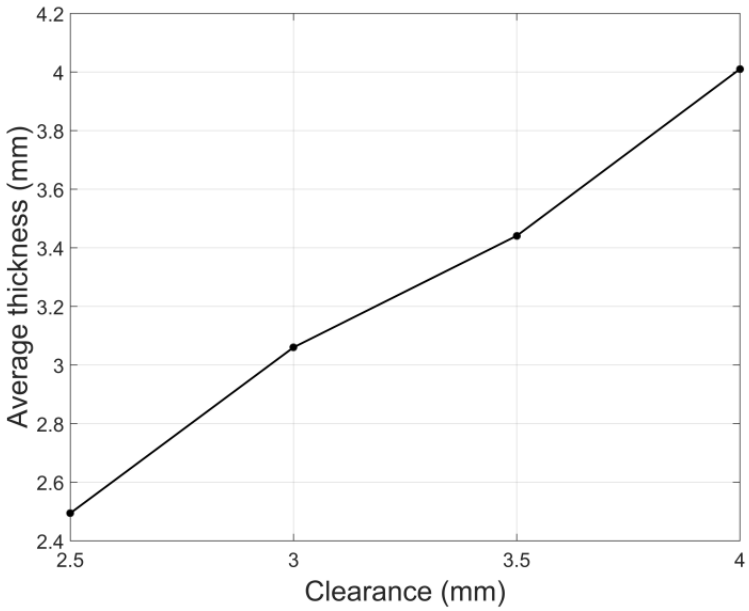

Figure 5.9: Average thickness vs clearance

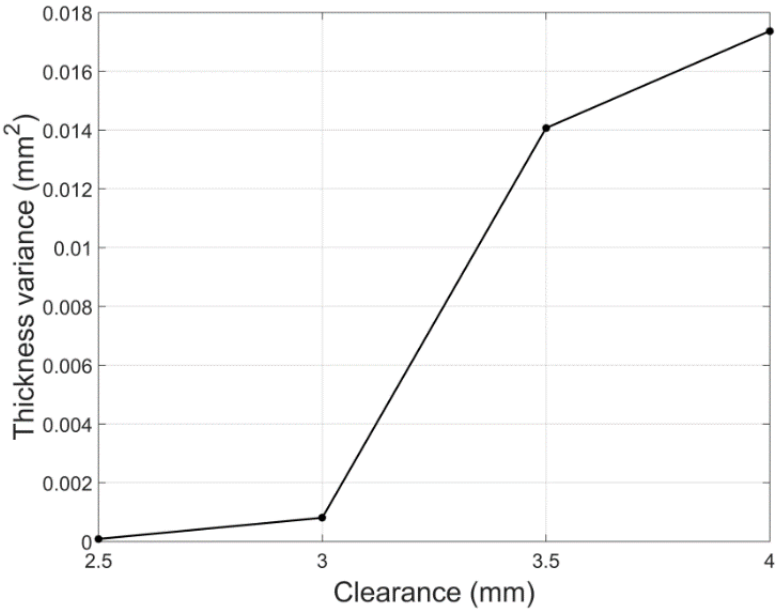

Figure 5.8: Thickness variance vs clearance

As depicted in Figure 5.6, it is clear that more uniform sheet thickness can be achieved for lower values of the sheet thickness. This is because at the sandbed/lead interface the temperature is lower compared to the free surface. Consequently, the fluid viscosity decreases as we move away from the sandbed/lead interface and the sheet thickness becomes increasingly irregular. This in agreement with [113] in which an increase of the wrinkle (small amplitude surface wave) height is documented for lower values of the fluid viscosity. In Figure 5.8 the variance of the sheet thickness is plotted as a function of clearance. The variance for each case has been calculated over the cells that belong to the region where the thickness profile has been stabilised ($1.25m$ <x <$3m$). As expected, variance increases with clearance as the distance of the free surface from the interface increases due to the increased height wrinkles. This observation suggests that for higher sheet thickness the strickle should start moving at a later stage in time so as to ensure that the solid substrate has been further extended along the y-direction and thus the viscosity has reached a higher value.

5.4.3 Strickle velocity

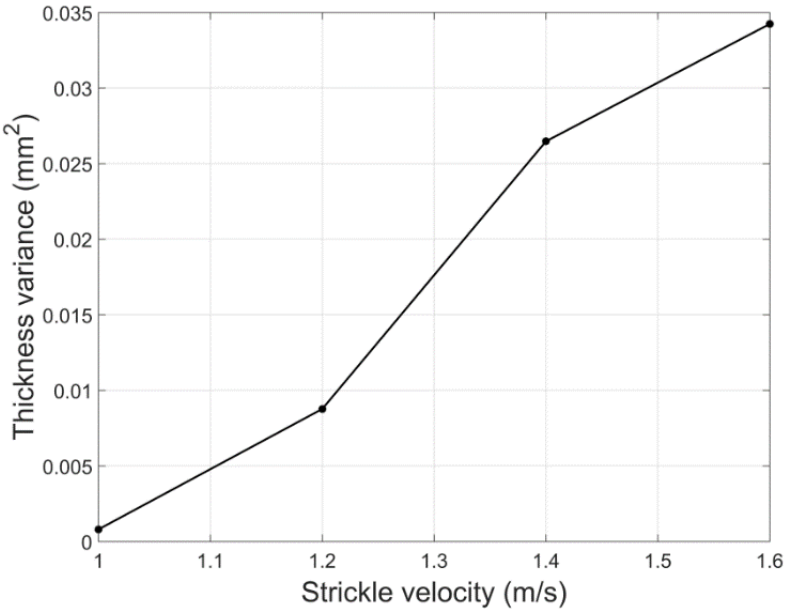

Figure 5.10: Thickness variance vs strickle velocity

In this section, the effects of the strickle velocity on the quality of the lead sheet will be discussed. 4 values of the velocity have been examined: (a) $v_s = 1m/s$, (b) $v_s = 1.2m/s$, (c) $v_s = 1.4m/s$, and (d) $v_s = 1.6m/s$, while the clearance was set to $3mm$. The corresponding thickness profiles are illustrated in Figure 5.12. As it can be observed, the x-coordinate for which the sheet thickness obtains an approximately uniform thickness is larger for higher values of the strickle velocity. This is because the lead surface being in contact with the strickle acquires the same velocity with the strickle due to the no-slip boundary condition imposed. As a result, for higher strickle velocities, additional time is required for the liquid lead to be decelerated under the effect of the shear forces; consequently, the sheet thickness becomes constant for a larger value of the x-coordinate. Moreover, it is apparent that the sheet thickness is more uniform for lower values of the strickle velocity as verified in Figure 5.10. This is because surface wrinkles with higher amplitude are generated for

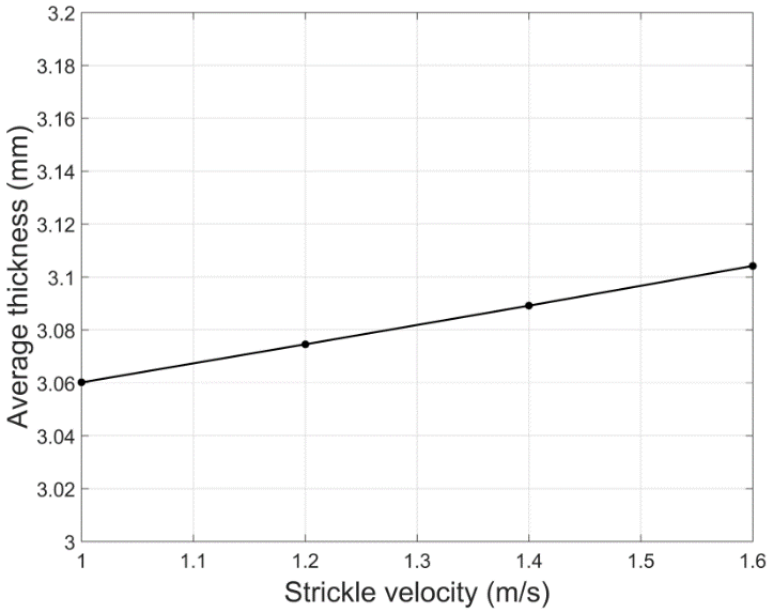

Figure 5.11: Average thickness vs strickle velocity

higher values of the shear velocity, similarly to the observations reported in [114]. If the aforementioned surface wrinkles have not come to equilibrium by the time solidification occurs, additional thickness fluctuations and consequently higher thickness variation appear in the final cast sheet.

By observing the thickness profiles of Figure 5.12 someone cannot distinguish any distinct effects of the strickle velocity on the average sheet thickness. In order to extract safer conclusions, the average sheet thickness ($1.25m$<x <$3.5m$) was calculated and plotted against the strickle velocity as shown in Figure 5.11 . It appears that the average sheet thickness is increasing linearly with the strickle velocity although it is not significantly affected by its value. This is because of the fact that the shear stress is higher for higher values of the strickle velocity and consequently a larger portion of the liquid metal follows the motion of the strickle. As a consequence, additional material is layered on top of the smeared surface. The displacement of the thickness peak towards the end of the bed as well as the increase of its amplitude for higher values of the strickle velocity, as illustrated in Figure 5.12, are attributed

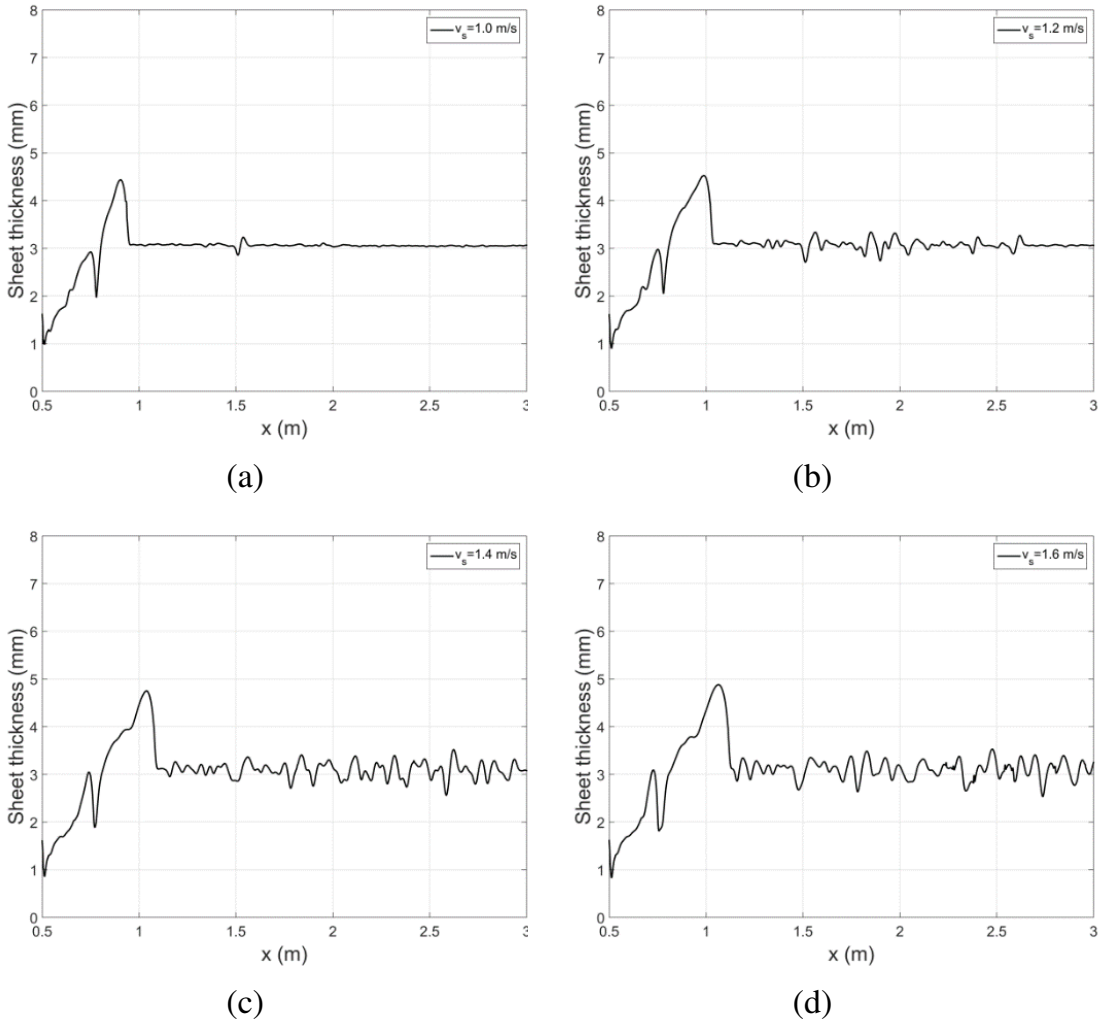

Figure 5.12: Thickness profiles for (a) vs=1 m/s, (b) vs =1.2 m/s, (c) vs =1.4 m/s, and (d) vs =1.6 m/s

to the same reason.

By comparing Figure 5.8 and Figure 5.10 it can be concluded that the strickle velocity has a more significant effect on the thickness variance compared to clearance. It is therefore very significant that the craftsmen walk with a constant and relatively low speed alongside the bed. It is also highly likely that any strickle velocity fluctuations will also lead to variations in the sheet thickness.

5.4.4 Pouring temperature

In this section, the effects of the lead charge pouring temperature (T_P) on the quality of the lead sheet thickness will be discussed. In the previous section, it has been pointed out that higher temperature of the melt should be associated with increased irregularity of the final lead surface due to the lower viscosity. For the same reason a similar trend is observed in Figure 5.13 which demonstrates the thickness profiles obtained for 4 different values of the pouring temperature: (a) $T_P = 345°C$, (b) $T_P = 350°C$, (c) $T_P = 355°C$ and (d) $T_P = 360°C$.

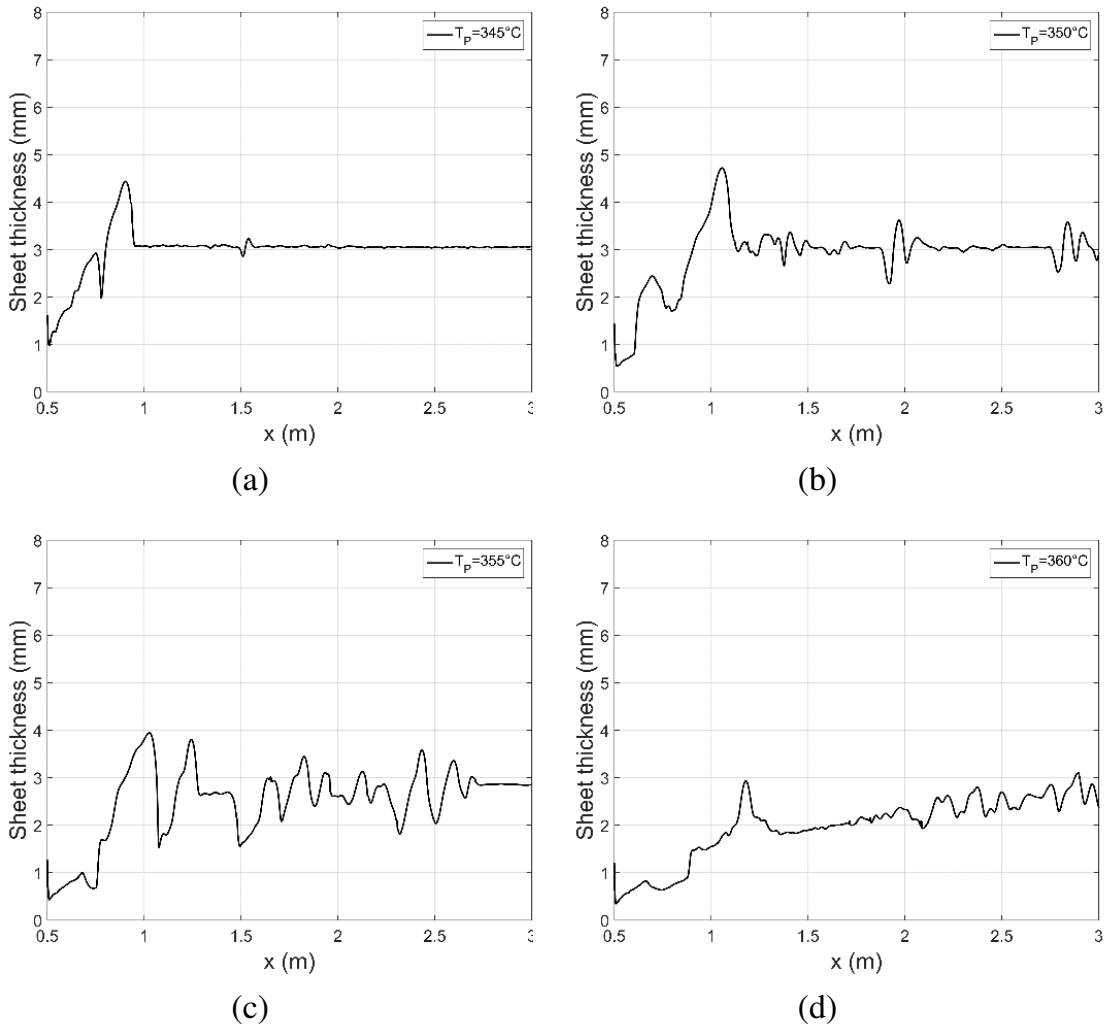

Figure 5.13: Thickness profiles for(a) $T_P = 345°C$, (b) $T_P = 350°C$, (c) $T_P = 355°C$ and (d) $T_P =^{\circ} C$.

It is evident that the average sheet thickness decreases with higher pouring temperature. However, in the case of $T_P = 360°C$ the sheet thickness is much lower than the desired value ($3mm$). This is because of the increased fluidity due to the lower viscosity of the molten lead. Due to the higher temperature and the consequent delayed solidification phase the liquid is decelerated at a later stage in time. This leads to lower average sheet thickness compared to lower pouring temperatures (Figure 5.14). This result is in agreement with the conducted experiments which report that the average sheet thickness reduces with the pouring temperature and that it is impossible to obtain the desired thickness profiles for pouring temperatures higher than $355°C$.

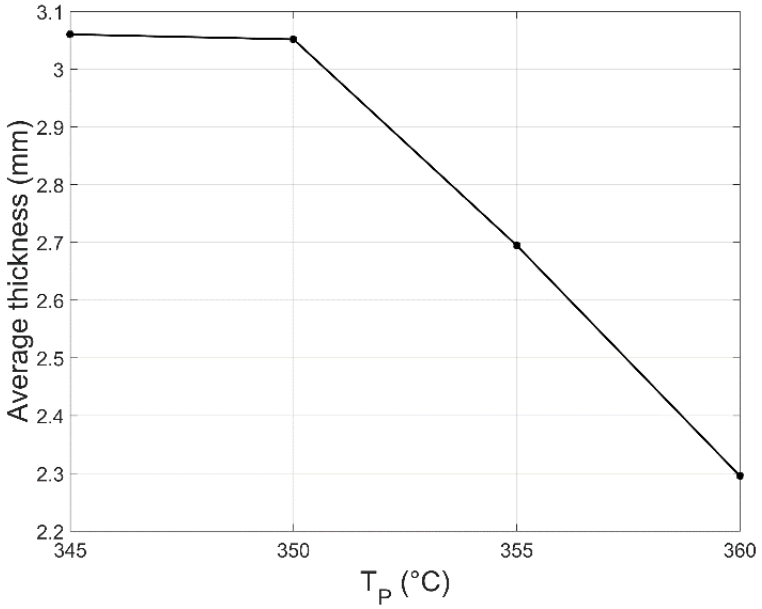

Figure 5.14: Average sheet thickness vs pouring temperature

By observing Figure 5.13(a), (b) and (c), it can be seen that increased pouring temperature leads to more irregular lead sheet thickness profiles. This is because increased fluidity induces additional surface wrinkles. However, in Figure 5.13(d) it appears that the surface irregularities are decreased compared to Figure 5.13(c). This is attributed to the delayed solidification phase which allows the fluid to equilibrate

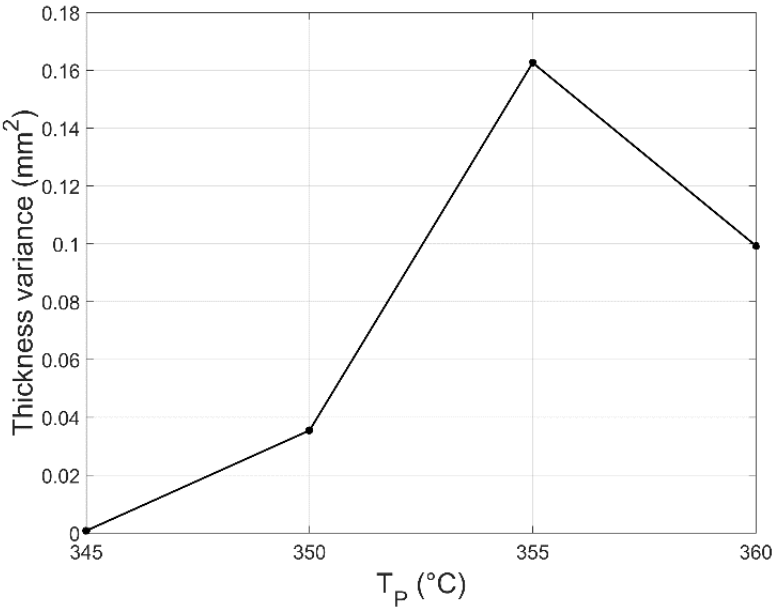

Figure 5.15: Thickness variance vs pouring temperature

under the effects of surface tension and gravity and obtain a smoother thickness profile (Figure 5.15).

By comparing the variance profiles (Figure 5.8, Figure 5.10 and Figure 5.15 for the 3 process parameters under investigation (clearance, strickle velocity and temperature respectively) it can be concluded that temperature can potentially have the most detrimental effect on the quality of the final product. The value of the pouring temperature should be therefore carefully selected as very low temperature will lead to premature solidification but on the other hand very high temperature will lead to either additional surface irregularities or a mean thickness lower than the desired value.

5.5 Conclusions

This investigation is the first effort to bridge the traditional lead sheet sand casting process with numerical simulations. A 2-dimensional CFD model was devel-

oped to simulate the melt flow and solidification of lead during the sand casting process.Simulation results are in good agreement with experimental observations. More specifically, it is observed that the clearance between the sandbed and the strickle can be effectively used to control the sheet thickness for a specific range of pouring temperature values. The average sheet thickness increases with higher values of the strickle velocity and decreases with pouring temperature. However, an increase in any of the above-mentioned parameters leads to an increase in the thickness variance. Moreover, the variation is relatively low for thinner lead sheets. This behaviour is attributed to the lower viscosity of lead in the areas far from the sandbed/lead interface. This issue can potentially be solved by delaying the commencement of the strickle movement in order to allow a thicker solid substrate to be formed along the normal direction. Finally, it is observed that the initial 0.5 - 0.75m of the cast sheet has in general lower thickness compared to the rest, high variation and consequently cannot be used for practical applications. This result is in agreement with experimental observations.

Chapter 6

Direct Method- Energy Studies

6.1 Introduction

Sustainability aspects in material processing industries are widely discussed these days. Metal processing is highly energy consuming and contributes significantly to carbon dioxide emissions. This sector is being examined these days as emission reduction is a key driver for finding more energy efficient solutions. Foundries are one of the most energy intensive industries. The average energy burden for the foundry sector in UK is $55 GJ/tonne$ which is more than double the target burden of $25.7 GJ/tonne$ as per the climate change agreement published by the UK government [115]. Metallurgical processes like melting, refining and casting have a crucial impact on environment and as a result assessing and controlling the emissions and energy consumptions are of supreme interest for continuous improvement initiatives.

The foundry industry is one of the most energy consuming sectors. The type of

material is also a crucial factor that influences the amount of energy used. Secondary lead production requires much less energy than primary lead production with the former taking up 5-10GJ per tonne of lead, and the latter 7-20GJ per tonne [12].

A modern casting process consists of different stages like melting, refining, moulding, pouring, etc. The cost of a process increases with increase in energy intensiveness [116]. In most foundries, melting, holding and refining consume majority of energy (around70%). Melting and holding incurs a lot of energy loss which depends on a number of factors like, type and design of the furnace, insulation, frequency of metal charging, etc [116]. Most furnaces are not very efficient, in fact there are very few furnaces with efficiencies more than 50% [117].

There are several factors that affect energy consumption. The current study compares energy consumption of the DM process with that of the rolling process. The energy data for the DM has been sourced from a foundry based in the UK. However, the values for rolling process have been theoretically calculated. It is assumed that the melting and refining values are the same for both process, since these activities stay unchanged irrespective of the process. The same rule accounts for cutting and transporting the spools, hence this data is omitted.

6.2 DM Process

Data analysis and theoretical calculations were made based on thermodynamic properties of lead as well as from literature. The theoretical quantity of energy required to rise 1 tonne of pure lead from room temperature (22°C) to its melting point, melt it and raise to the temperature of 440°C can be calculated as 0.077GJ as per the equation below.

$$E = H_m + [(T_m - T_s) * C_p s] + [(T_p - T_m) * C_p l] \tag{6.1}$$

Property	Value
Heat of melting (H_m)	$22.4kJ/kg$
Specific heat of solid lead(Cps)	$0.126kJ/kg/^{\circ}C$
Melting point (T_m)	$327.5^{\circ}C$
Specific heat of liquid lead(C_pl)	$0.14kJ/kg/^{\circ}C$
Thermal Conductivity	$35W/(m.K)$

Table 6.1: Properties of lead

Figure 6.1 below presents utilization of the machines in the direct machine casting process as per data received from a foundry in the UK. The refiner and scrapper are the most energy consuming segments of the process.

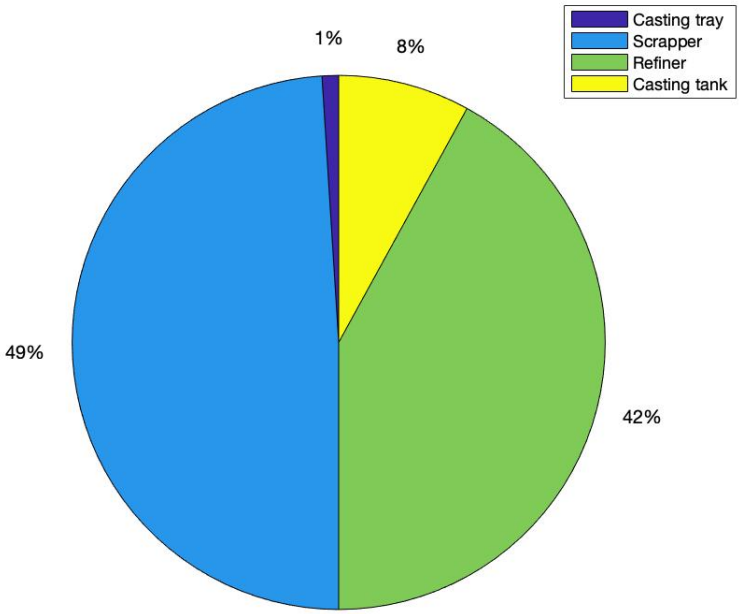

Figure 6.1: Energy usage by different entities in DM

The main parts of the DM process are the scrapper, refiner, casting tank and the tray. Table 6.2 shows the consumption at each stage of the process sourced from a Midland Lead in a calendar month. The company produced 316 spools of cast lead

weighing 2010 tonnes.

Figure 6.2 below presents utilization of the machines in the direct machine casting process as per data received from a foundry in the UK. The refiner and scrapper are the most energy consuming segments of the process.

The main parts of the DM process are the scrapper, refiner, casting tank and the tray. Table 6.2 shows the consumption at each stage of the process sourced from a Midland Lead in a calendar month. The company produced 316 spools of cast lead weighing 2010 tonnes.

Table 6.2: Energy data for DM process collected from a foundry based in UK for a calendar month

Element	**Stage**	Energy usage (GJ)	Energy usage per tonne (GJ/t)
Scrapper	Melting	529.57	0.263508
Refiner	Refining	452	0.224915
Casting tank	Holding	91.19	0.045375
Casting tray	Casting	12.13	0.006037
Total		1084.91	0.539836

6.3 Rolling Process

Metal in rolling process elongates with the rolling direction, speeding up. This means that the material moves faster on the exit side then on the entry. The rolling calculations have been conducted based on equations for roll force and torque in flat-rolling [118]. The needed data are initial thickness of the billet (h_o), desired thickness (h_f), width of the material (w), number of revolutions per second of the rolls (N) and roll radius (R). At first roll-billet contact is given by the formula:

$$L = \sqrt{R(h_o - h_f)} \tag{6.2}$$

The roll force is calculated by the formula:

$$F = LwYavg \tag{6.3}$$

Where Y_avg is the average true stress. The total power is estimated by the equation:

$$P = \frac{2nFLN}{1000} * 10^6 KW \tag{6.4}$$

Where N is the number of rotations per second. Since billets are not milled to the required thickness in one pass, multiple rolling approach has been applied. It assumes that with each pass the billet reduces its thickness by a percentage of its original thickness. The sheets are assumed to be constrained from the sides which means there is no change in the width of the sheets. The only parameters that change during the rolling process are length and thickness. This method produces multiple energy values which sum up to total energy of the process. The following assumptions are made to theoretically calculate the energy consumed.

Data	**Value**
Initial thickness	$50mm$
Pass reduction level	25%
Length	$6m$
Width	$1.4m$
Roll velocity	$0.3m/s$
Roll radius	$0.519m$
Average true stress (Y_avg)	$16MPa$

Table 6.3: Assumed data for theoretically calculating the energy consumed in rolling process

Changing the length can be captured by comparison to the volume of the material, which stays the same though the whole process. Information regarding the

velocity of the rolls enables calculating the time needed to roll given length. Next, multiplying the power by time gives the energy value presented in kJ. Density and volume provide the information about the mass of the material and the energy per tonne can be determined.

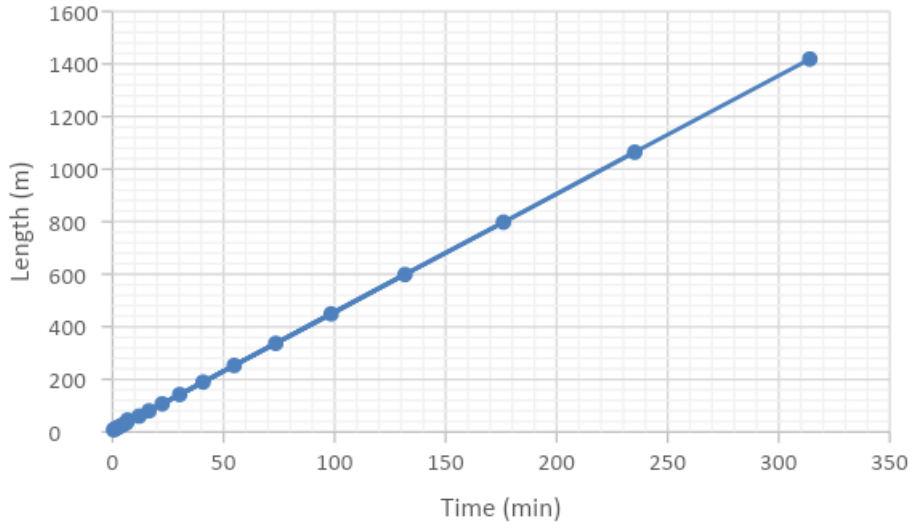

Figure 6.2: Length of rolled sheet (l) Vs total time taken (T)

The maximum reduction in thickness (d) that can be attained is related to the coefficient of friction (and radius of the roll (R) as per the following equation:

$$d = \mu^2 R \tag{6.5}$$

Higher the value of μ, higher the reduction in thickness that can be attained. However, a higher coefficient of friction would result in higher consumption of energy.

Pass	**Initial thickness ho (m)**	**Final thickness hf (m)**	**Change in thickness**	**Contact length L (m)**	**Force (MN)**	**Power (W)**	**Length of sheet (m)**	**Time (s)**	**Energy (kJ)**
							6	20	
1	*0.05*	0.0375	0.0125	0.08054	1.804208	527.52	8	26.6666	14067.2
2	0.0375	0.028125	0.009375	0.06975	1.56249	395.64	10.66667	35.5555	14067.2
3	0.028125	0.021094	0.007031	0.06040	1.353156	296.73	14.22222	47.4074	14067.2
4	0.021094	0.01582	0.005273	0.05231	1.171868	222.547	18.96296	63.2098	14067.2
5	0.01582	0.011865	0.003955	0.04530	1.014867	166.910	25.28395	84.2798	14067.2
6	0.011865	0.008899	0.002966	0.03923	0.878901	125.183	33.71193	112.373	14067.2
7	0.008899	0.006674	0.002225	0.03398	0.76115	93.8872	44.94925	149.830	14067.2
8	0.006674	0.005006	0.001669	0.02942	0.659176	70.4154	59.93233	199.774	14067.2
9	0.005006	0.003754	0.001251	0.02548	0.570863	52.8115	79.90977	266.365	14067.2
10	0.003754	0.002816	0.000939	0.02207	0.494382	39.6086	106.5464	355.154	14067.2
11	0.002816	0.002112	0.000704	0.01911	0.428147	29.7065	142.0618	473.539	14067.2
12	0.002112	0.001584	0.000528	0.01655	0.370786	22.2798	189.4158	631.385	14067.2
13	0.001584	0.001188	0.000396	0.01433	0.32111	16.7099	252.5543	841.847	14067.2
14	0.001188	0.000891	0.000297	0.01241	0.27809	12.5324	336.7391	1122.46	14067.2
15	0.000891	0.000668	0.000223	0.01075	0.240833	9.39932	448.9855	1496.61	14067.2
16	0.000668	0.000501	0.000167	0.00931	0.208567	7.04949	598.6473	1995.49	14067.2
17	0.000501	0.000376	0.000125	0.00806	0.180625	5.28712	798.1964	2660.65	14067.2

Table 6.4: Calculation of energy consumed in rolling process

6.4 Cost analysis of DM method

As per Table 6.2, the overall energy consumed in the DM process is $539836 kJ/t$. The energy consumed by the DM machine consisting of the main tank and the tray is $51412 kJ/t$. The total energy consumed in reducing thickness from 0.05 m to $0.000376 m$ is theoretically calculated to be $239142.4 kJ$. The energy required per tonne for the rolling process can be calculated as $50210.46 kJ/t$. This value is almost similar to the actual consumption of the DM process as per the energy audit from the foundry. The actual energy consumed in the rolling process would be much higher than the theoretically calculated values due to wastage through friction and loss of energy. Hence the Direct Method of casting can be considered to be a more energy efficient process than rolling process.

	Gas used (kWh)	**Gas rate (£)**	**Electricity (kWh)**	**Electricity rate (£)**	**Total cost (£)**
Scrapper	147103.16	0.017202			2530.47
Refiner	125558.96	0.017202			2159.87
DM tank			25330.86	0.075811265	1920.37
DM Tray			3370.20	0.075811265	255.50
					6866.20

Table 6.5: Actual cost analysis of DM

There is a large difference between theoretical and actual energy consumption values in case of the DM. Though the theoretical value can never be achieved, this difference can be considered an opportunity for improvement. Table 6.5 and Table 6.6 show a cost analysis of DM. The scrapper and refiner are gas kettles and consume energy at a cost rate of £0.017202 per kWh. Direct casting machine is powered by

electricity. The electricity rate is variable throughout the day but for simplicity the average cost has been taken.

Based on the actual cost data for the process, calculations can be made for the theoretical value of energy needed to melt and produce the same amount of lead that was manufactured via DM in a calendar month and this is calculated to be $155.23GJ$

This enables approximating energy values for each of the machines and possible cost. Mentioned calculations are shown in Table 6.6

The huge difference between actual cost of energy of the DM and the cost estimated according to theoretical energy consumption shows that there is a potential for large amount of savings. Though reducing the energy consumption to attain the theoretical value of $0.077GJ$ is impossible,

	% Energy used	Energy consumed (GJ)	Energy in kWh	Type	Gas rate (£)	Average electricityrate (£)	Total cost (£)
Scrapper	*48.81*	75.7743427	21512.40	Gas	0.017202	-	370.0563
Refiner	*41.66*	64.6767050	18361.77	Gas	0.017202	-	315.8592
DM tank	8.41	13.0481862	3704.39	Electricity	-	0.075811265	280.8345
DM tray	1.12	1.736023107	492.86	Electricity	-	0.075811265	37.3642
							1004.114

Table 6.6: Theoretical cost analysis of DM

6.5 Energy improvement techniques for DM

There are several techniques for saving energy in foundries. Techniques like insulating furnaces, preheating scrap, reducing losses through convection, etc. are widely used. The following are two important areas of improvement in the DM method of lead casting:

6.5.1 Reducing wastage

Operational material efficiency (OME) is the ratio between the good casting shipped to customer and the total metal melted [119]. Improving the true yield is possibly the simplest way in which foundries can save energy, as this method focuses on increasing good casting production and reducing the total metal melted [120].

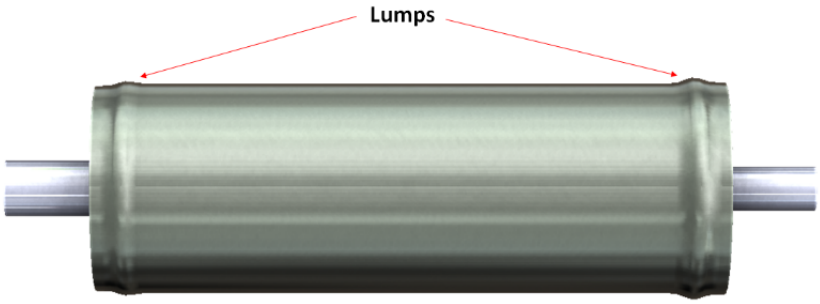

Figure 6.3: Accumulation of edge deformation resulting in formation of lumps on DM spools

Casting in general results in formation of waste which are removed by machining. In many casting systems, wastage can be over 50% which are machined [120]. The DM process on the other hand is a distinct casting process in which the metal solidifies over the rotating drum layer by layer and wastage is substantially less compared to other casting processes. However, at times deformations can occur at the

edges of the spool as shown in Figure 6.3. This accumulation results in formation of a bulge or lump which is machined off and is re-melted, refined and recast to utilise materials resourcefully. However, this results in increased energy costs, labour and emissions. A reduction in the amount of material that needs to be machined can be considered as an opportunity to improve OME thereby making the process more energy efficient.

Mass of spool (*kg*)	**Mass of lump** (*kg*)	**Energy required to recast** (*GJ*)
6136	1603	3.312434
6302	1144	3.402046
6098	1421	3.29192
6072	2091	3.277884
6152	1271	3.321071
6225	1551	3.360479

Table 6.7: Analysis of lumps on a batch of 6 spools

An analysis of the amount of wastage per spool in a day is shown in Table 6.7. Therefore, if the true yield of the casting can be improved, less metal will be required to produce the casting and the energy consumption for recasting could be reduced. Techniques to reduce these defects to the minimum would result in large energy savings and a higher OME can be attained.

6.5.2 Heat recovery and preheating of scrap

Pre-heating of scrap can be very effective. It is very advantageous as it could remove any moisture and organic materials in the scrap, thereby preventing explosions in the furnace and reduce energy required for melting. Techniques like using flue gases from the melting furnace are being used by foundries these days [120]. In the DM process, the dross formed during melting is filled in metal barrels and is sent to a rotating recovery furnace. The metal barrels are loaded into the furnace which is

heated to a temperature of over 420 °C and rotated. Recovery rates up to 65% are obtained. The barrels are taken out and then allowed to cool. Selvaraj et al. conducted studies on an innovative approach to preheat the scrap by using heat released by castings when they cool. The study reported 2.83% energy savings using this approach in which heat from the cast metals is recovered during cooling and used to preheat scrap [121]. A similar approach can be applied to use the heat from the recovery furnace and can be used to preheat scrap lead

Chapter 7

Numerical Simulation of DM process

7.1 Introduction

With the advancement of computing technologies, these days, it has been possible to develop numerical models that are very powerful in analysing various physical phenomena that occur during casting processes. Numerical solutions give an in depth understanding of fluid flow, solidification and heat transfer that occur during casting. Such simulations help researchers improve the process by conducting experiments and optimising casting parameters without hindering the real process thereby saving huge amounts of energy, raw materials and labour.

As mentioned in the introduction section, the Direct Method for manufacture of sheet lead involves a water-cooled drum which is immersed partly into a tray containing molten lead. The temperature difference between the surface of the drum and the melt pool results in solidification of a thin sheet. Molten lead is continuously

fed to the tray at about $360^{\circ}C$ from a reservoir of molten metal as shown in the schematic Figure 7.1. In order to maintain the level of the melt in the tray, the melt is made to overflow over a weir on one side of the tray while the drum continuously casts the sheet out. The tray consists of a baffle plate which blocks any dross formed during the filling process from floating to the top of the tray.

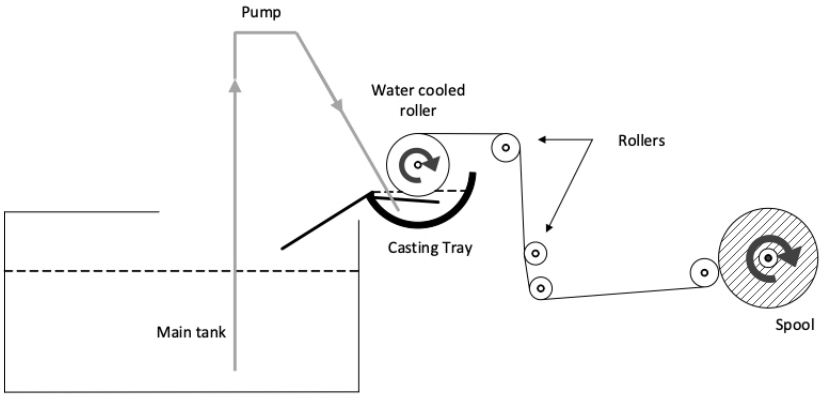

Figure 7.1: Schematic of the DM process

This chapter focuses on effects of three main process parameters (temperature of melt, speed of rotation of the casting drum and immersion of the casting drum within the melt etc.) on the thickness of the cast sheet. This is the first attempt to investigate the direct method for manufacture of cast lead sheet via numerical simulations. A numerical model was developed in order to simulate the process. Special emphasis was placed on effects of melt flow rate into the casting tray, heat transfer coefficients, melt temperature, speed of rotation and immersion of casting drum on the average sheet thickness. The developed CFD model was validated using thickness data of cast sheets measured during experiments.

7.2 Simulation Setup

As illustrated in Figure 7.1, a typical set up of the DM process consists of (a) cooling drum and (b) the holding tray. Sheets of different thicknesses are manufactured primarily by adjusting the speed of rotation of the drum and the immersion of the drum. Essentially, the contact time of the cooling drum and the melt is controlled by adjusting these parameters. In order to make adjustments to the immersion of the drum in the melt, the tray is rotated about a pivot using a screw mechanism while the position of the drum is maintained constant. Figure 7.2 shows different immersions of the drum within the melt at different tilt positions of the tray when the meniscus of the melt is at the same level as the weir on the side of the tray.

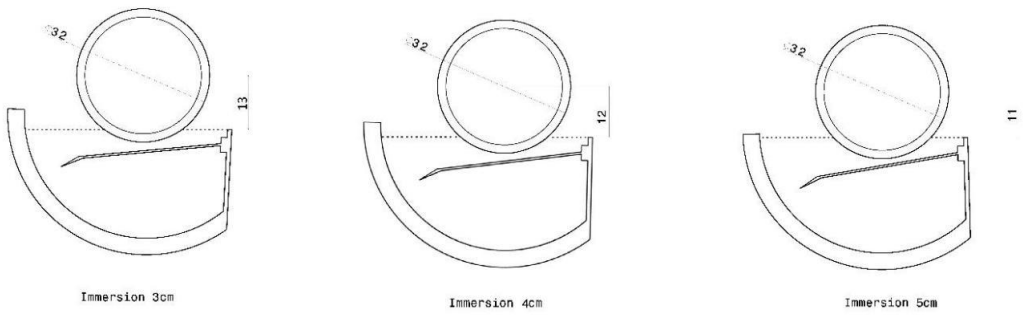

Figure 7.2: Schematic of the simulation setup at different immersion levels of (a) 3cm, (b) 4cm and (c) 5cm obtained by altering the angle of tilt of casting tray

For the simulation setup a cooling drum of $0.32m$ diameter made of stainless steel was selected. The CFD model was limited to two directions in favour of computational efficiency and the flow and temperature fields are assumed to not change in the transverse (x) direction. The material properties corresponding to each component were taken from the Matweb online materials database [108] while the heat transfer coefficients were set according to literature and experimental results [75] and the temperature of the cooling drum was set to $400K$ to simulate uniform cool-

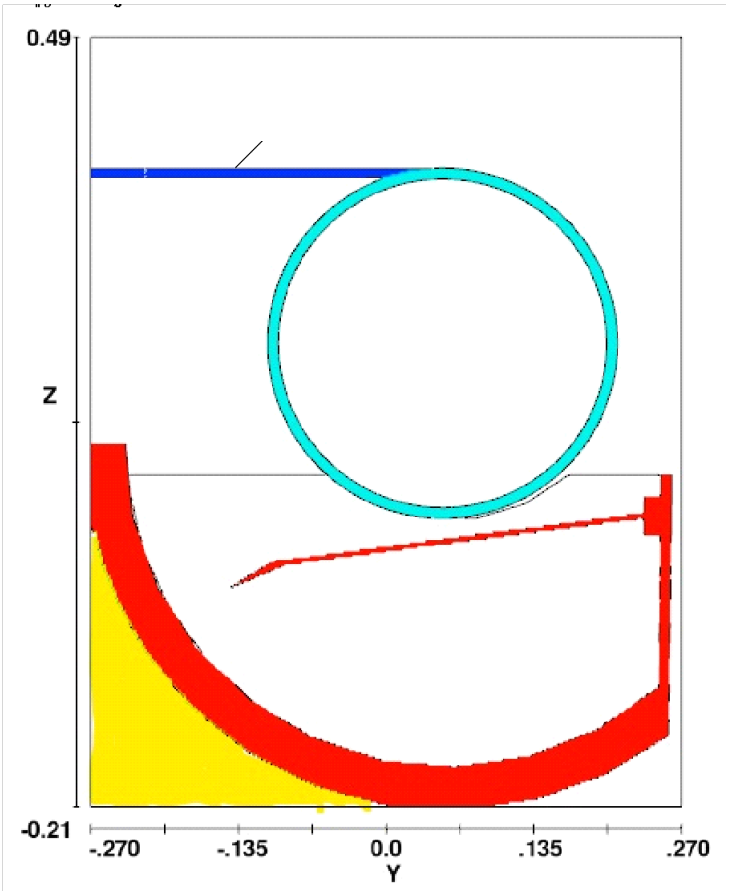

Figure 7.3: Schematic of the DM simulation setup

ing. Melt feed into the tray was simulated by placing a metal source rate placed at the bottom of the tray. Simulations were tried with three different mesh sizes of 0.5mm, 1mm and 2mm. The exit thickness is the output variable and was measured for all three mesh sizes dynamically over the same period of time (10 seconds). Even though there was substantial difference in output thickness between 1mm and 2mm when compared to experimental results, there was negligible variation observed over the thickness between 1mm and 0.5 mm and the experimental values. To reduce computational time and cost, mesh size of 1mm was used as it was able to replicate the observations of experimental values closely as a trade-off between accuracy and efficiency. In all cases the models were observed to converge and capture the trend obtained in variation in thickness observed as per the real process.

Since our goal is to understand the trend in the change in thickness with respect to various other process parameters, and the focus was not on accuracy of the output thickness, this approximation was adopted. A rectangular mesh was utilised in order to solve mass, momentum, energy and heat transfer equations. A mesh size of $1mm$ was utilised and the final constructed mesh consisted of 379620 cells. In order to reduce the computational costs, a domain removing element was added to the setup as shown in Figure 7.3. Symmetry boundary conditions were applied at mesh boundaries along the x axis while pressure boundary conditions were used at the remaining mesh boundaries except Ymin where an outflow boundary condition was used. The developed model accounted for surface tension which was considered to be equal to $\gamma = 0.439kg/s^2$ [122]. For each simulation performed the fluid momentum and continuity equations were solved, while a first-order method was used for the approximation of the momentum advection. The commercial computational fluid dynamics (CFD) software Flow-3D [88] was used to simulate the process. A flat plate of $0.01m$ thickness was used to facilitate the motion of the solidified sheet out of the domain as shown in Figure 7.3. Simulations were run for 10 seconds as the process gets stabilised within the first 3-5 seconds as it will be presented in the following sections. The results obtained were in accordance with experimental data obtained from the casting machine at ML Operations.

7.3 Results

7.3.1 Effect of Volume flow rate

This section investigates the effect of volume flow rate into the melt pool on the thickness of the cast sheets. High values of volume flow rate were selected to understand the potential impact and simulations were run at simulations were run at

flow rates of (a) $V_1 = 0.0008m^3/s$ and (b) $V_2 = 0.001m^3/s$ at 60 RPM while the immersion depth of the casting drum was set at $d = 4cm$. Looking at the thickness profiles as shown in Figure 7.4, it was observed that the thickness only marginally varied at high volume flow rates. This can be explained based on the outflow of the excess melt over the weir on the side of the casting tray as it will be explained in this section.

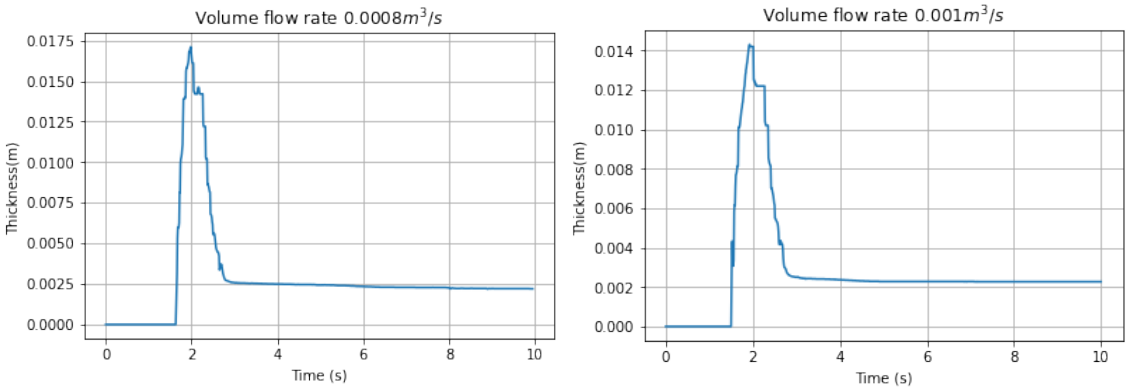

(a) $0.0008m^3/s$ (b) $0.001m^3/s$

Figure 7.4: Thickness plots at volume flow rates

To understand the impact of depth of immersion at high volume flow rates, simulations were run at immersion levels of (a) $d1 = 3cm$, and $d2 = 4cm$ at 35 RPM while the volume flow rate was set at $V = 0.001m^3/s$. It was observed that controlling the thickness of the sheet at really high-volume flow rates was difficult. As it can be seen from thickness profiles in 7.5., immersion was observed to not sufficiently affect the thickness of the cast sheet at $V = 0.001m^3/s$. Ideally, an increase in immersion should increase the contact surface area with the liquid melt. However as observed from the plots, the effect of immersion was not very prominent.

When the flow rate of the melt into the tray is high, the height of the overflowing molten metal from the edge of the tray increases. This results in an increased immersion effect. As shown in Figure 7.6 for a setting of the tray (tilt position) to obtain an immersion of $3cm$, during casting the effective immersion is around $5.8cm$ due to

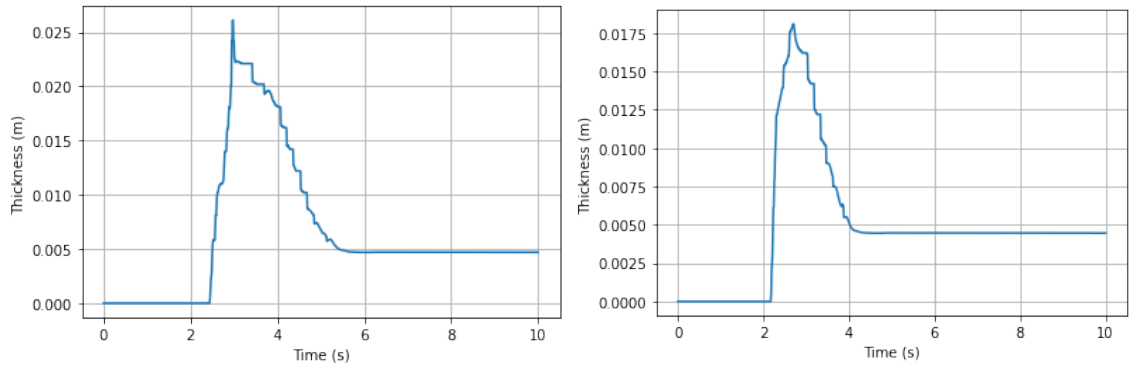

(a) 3*cm* (b) 4*cm*

Figure 7.5: Thickness profiles at high volume flow rate of 0.001, 35*RPM* and immersions

the additional height of the overflowing liquid metal. Different immersion levels are obtained by different tilt positions of the tray, and the volume flow rate is kept constant (and not generally controlled in most foundries). Also, the height of the liquid over the weir does not increase beyond a certain height due to an increase in velocity at higher flow rates. As a result, the area of the contact surface of the drum within the liquid metal at different immersions is not altered much. This results in lack of thickness control by varying the immersion levels when the flow rate of melt is high. Hence it is very important to control the flow rate of the melt into the casting tray. It can also be concluded that, the melt flow rate could create a combination effect with immersion of the drum if the flow rate is not controlled and could potentially nullify the effect of immersion depth of the casting drum into the melt. A high-volume flow rate could also result in high velocities profiles creating disturbances around the surface of the liquid causing unwanted variation in thickness profiles. Laurie et al. [67] suggested that, volume flow rate be set to approximately twice the amount of the removal rate of solidified sheet for best results in practical cases

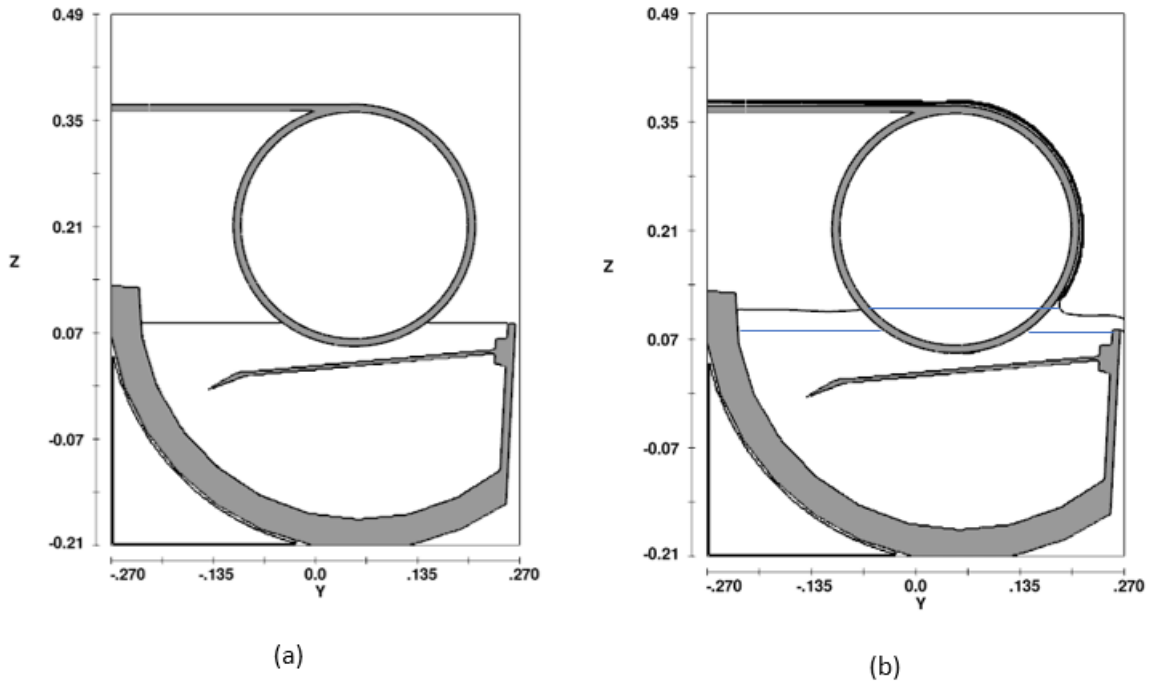

Figure 7.6: (a) Tilt position of tray with 3cm immersion (b) Actual immersion of 6cm due to high melt flow rate

7.3.2 Effect of immersion of casting drum

In this section, the effects of immersion levels of the casting drum in the molten metal pool will be discussed. Three values of immersions have been examined: (a) $d_1 = 3cm$, (b) $d_2 = 4cm$ and (c) $d_3 = 5cm$ while the speed of rotation of the drum was set to 60 RPM. Simulations were run at a low volume flow rate of $0.0005m^3/s$. The volume flow rate was selected to ensure that the molten metal just overflows over the weir at the same time ensuring that the immersion levels are not higher than anticipated.

By observing the thickness profiles of Figure 7.7, one cannot distinguish the effects of immersion on average sheet thickness. In order to extract safer conclusions, average thickness values after stabilisation was calculated and plotted against immersion values as shown in Figure 7.8. It can be observed that the average thickness values increase with an increase in immersion depths. A higher immersion results

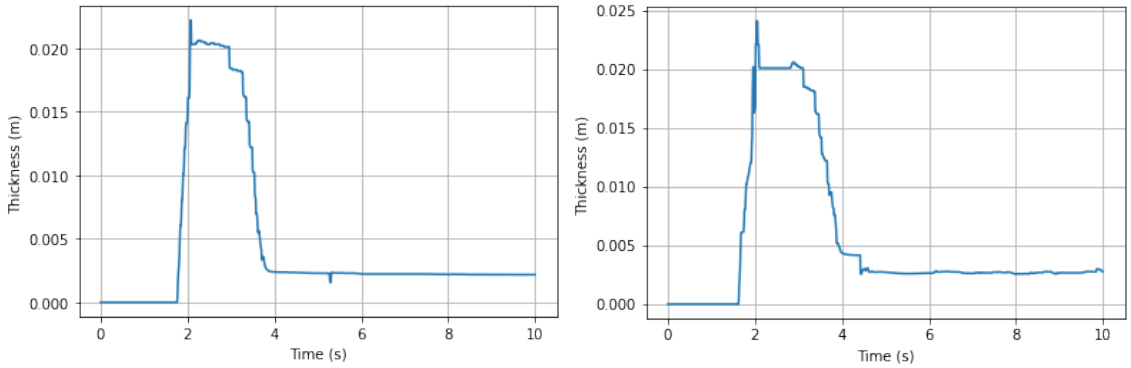

(a) 3*cm* (b) 4*cm*

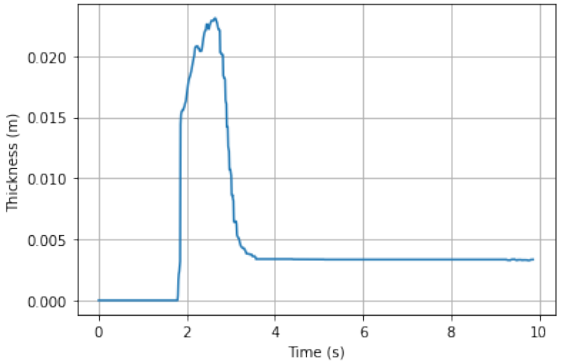

(c) 5*cm*

Figure 7.7: Thickness plots at 60*RPM* at immersions

in a higher contact time of the drum surface with the melt resulting in additional material solidifying on the surface of the drum.

7.3.3 Effect of heat transfer coefficient between drum and melt

Simulations were run for high volume flow rate at different values of heat transfer coefficients. Figure 7.9 shows the average thickness of the sheet obtained after stabilisation (at around 5*s*) at different heat transfer coefficients for an immersion of 4*cm* and 60 RPM. As expected, the thickness was observed to increase with an increase in value of heat transfer coefficient.

Simulations were also run at 80 RPM at two different heat transfer coefficients of

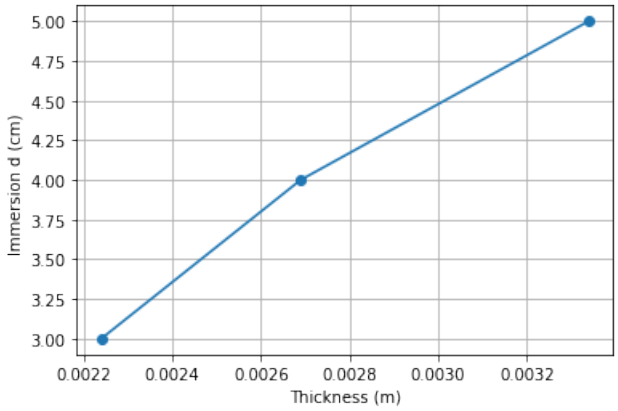

Figure 7.8: Average thickness of cast sheet at different immersion levels

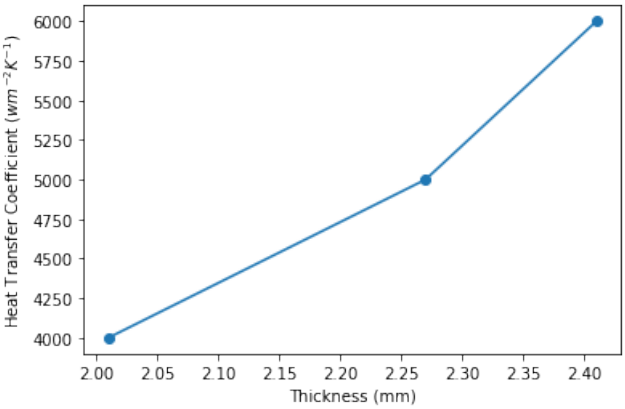

Figure 7.9: Thickness vs Heat transfer coefficient at 4*cm* immersion and 60*RPM*

5000 and 8000 respectively. As shown in the thickness profiles obtained in Figure 7.10, it can be observed that the thickness almost doubles when the heat transfer coefficient increases to 8000. This large increase is due to the high value of heat transfer coefficient, combined with an increased immersion effect caused due to the high volume flow rate.

Heat transfer coefficient is an important parameter in Direct Method for casting lead sheets. As per a study conducted by Chopra et al. [75], by measuring temperature transients in a cooling substrate dipped in molten lead, it was observed that there is no unique value of heat transfer coefficient for a given surface roughness and alloy composition. Heat transfer coefficient was observed to increases with contact

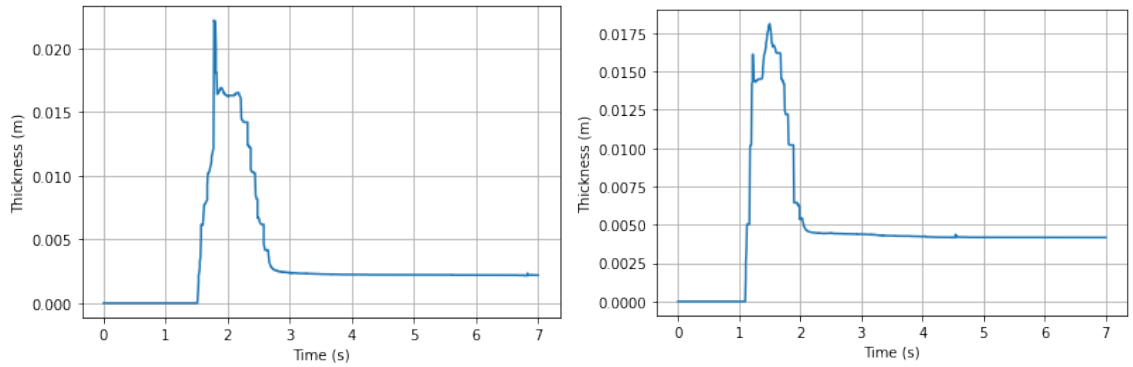

(a) $5000wm^{-2}K^{-1}$ (b) $8000wm^{-2}K^{-1}$

Figure 7.10: Thickness variation at 80 rpm at heat transfer coefficient

time of the substrate and melt. In practical applications, the drum is surface treated by sand or shot blasting in order to facilitate nucleation. The rough surface also provides the necessary friction to drag the solidified material and helps in starting up the process. Most foundries use manual sand blasting to prepare the surface of the drum. This can result in uneven roughness across the width of the drum and can cause variations in thickness of the cast sheet across the drum. Hence special care must be taken while preparing the drum surface to ensure uniform roughness. Care must also be taken to ensure that the melt used is clean and devoid of any impurities as presence of small amounts of impurities can also affect heat transfer coefficient and result in variations in thickness between batches.

7.3.4 Effect of melt temperature

In this section, the effect of melt temperature on the sheet thickness is investigated. In the real process the temperature in the casting tray is usually kept constant at around $640K$ by the help of heating elements. Simulations were run at three different temperature values of (a) $T1 = 630K$, (b) $T2 = 640K$ and (c) $T3 = 645K$ and (d) $T4 = 650K$ at 60RPM and a heat transfer coefficient of $h = 5000wm^{-2}K^{-1}$ while immersion was kept constant at $d = 4cm$. Figure 7.11 shows the thickness profiles

obtained at these settings respectively.

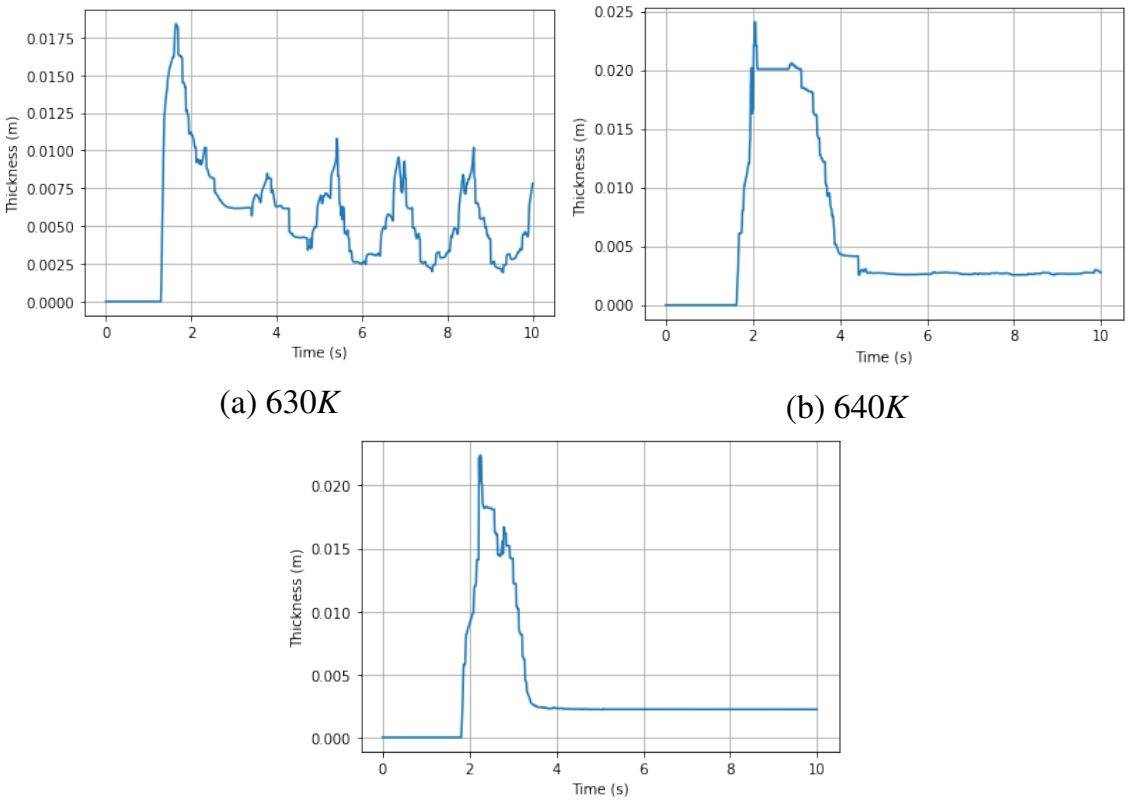

(a) 630K

(b) 640K

(c) 645K

Figure 7.11: Thickness profiles at temperatures

As it can be observed from Figure 7.11 (a) at a lower temperature of 630K, the thickness profile obtained is highly unstable. This is due to high solidification rates due to the low temperature of the melt resulting in a decrease in the level of melt. The drum drags a high volume of solidified material creating a reduction in level which is then supplemented by the mass flow source which continues like a cycle. Figure 7.12 shows snapshots of the solid fraction at time intervals $t1 = 6s$ and $t2 = 7s$ corresponding to the troughs and crests observed in the thickness profile shown in Figure 7.10(a).

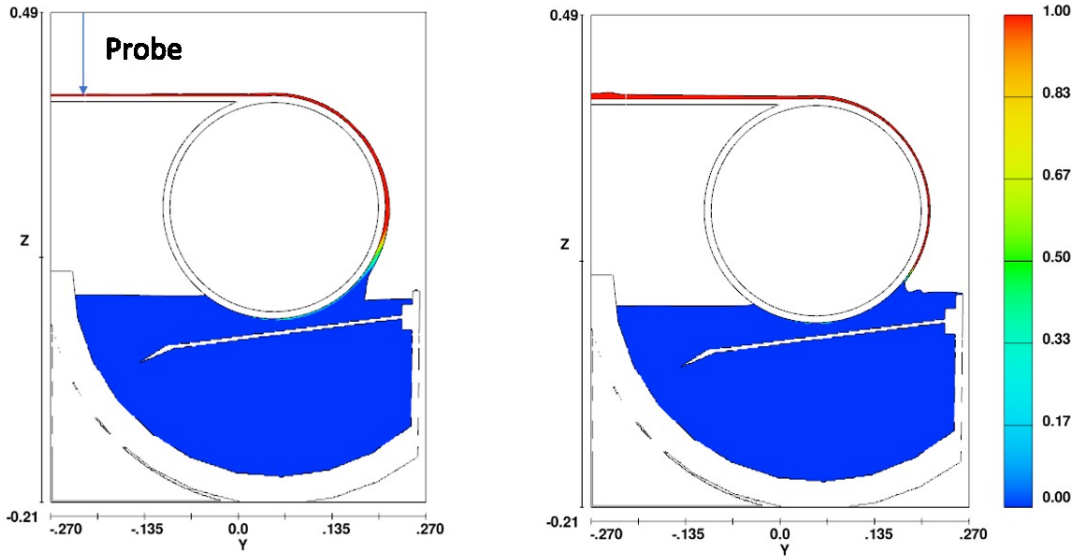

Figure 7.12: Snapshots of solid fraction at time (a) $t_1 = 6s$ and (b) $t_2 = 7s$

An increase in temperature from $640K$ to $645K$ resulted in a drop in average thickness of the cast sheet from $2.69mm$ to $2.22mm$ as shown in Figure 7.11 (b) and (c). Increasing the temperature further resulted in the drum being unable to cast the sheet over it probably due to the inability of the drum to pick up the lead. This is in line with observations from experiments conducted at higher melt temperatures. As mentioned previously, the drum is sand blasted to ensure uniform roughness in order to facilitate solidification of thin sheets and provide the necessary friction to pull the sheet out. The present model does not take surface roughness into consideration and thereby it was not possible to cast sheets when temperature was set higher than $650K$.

7.3.5 Effect of speed of rotation

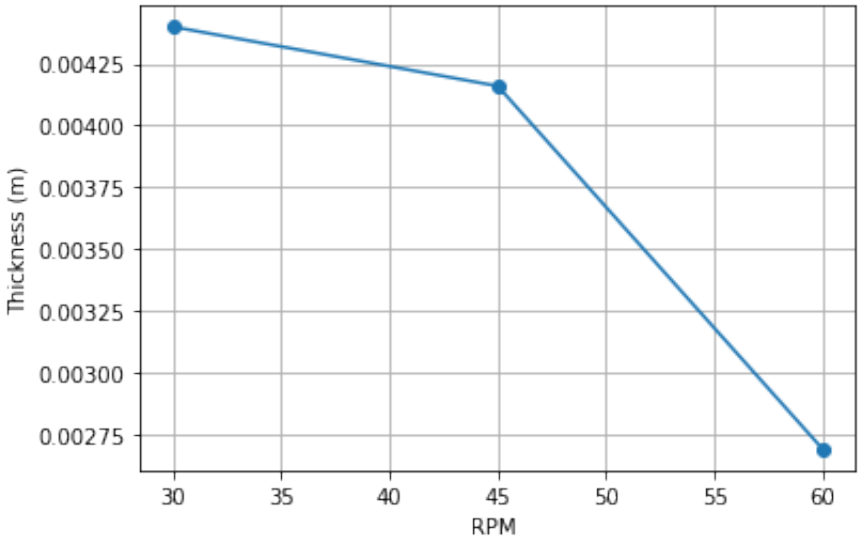

Figure 7.13: Average thicknesses of sheet produced at various casting speeds

The effect of speed of casting drum is investigated in this section. Simulations were performed at three different speed of rotation of the casting drum: (a) 30RPM, (b) 45 RPM and (c) 60 RPM at 4cm immersion. The average value of the thicknesses obtain after stabilisation are plotted against the RPM values as shown in Figure 7.13. As expected, the thickness is observed to reduce with an increase in speed of rotation of the drum due to a decrease in contact time of the cooling drum with the melt. This is in line with observations from experiment and data available from literature [67]. Also, it can be observed that the speed of rotation of the drum can be very effective in controlling the thickness of the cast sheet substantially.

7.3.6 Conclusions

A 2- dimensional numerical model was developed for the single drum continuous casting process for manufacture of sheet lead. The study is a first effort to model the process and investigate the effects of different process parameters. Simulation

results were observed to be in accordance with experimental results. The following conclusions were drawn from the investigation

- Volume flow rate of the melt into the casting pool plays a crucial role in the ability to control the thickness of the cast sheet. A high volume flow rate resulted in a higher contact area between the melt and the casting drum causing an increased immersion effect than anticipated. Hence it is very important to control the volume flow rate of the melt into the casting pool.
- Heat transfer coefficient has a significant effect on the thickness of the cast sheet and hence process parameters that affect heat transfer coefficient (like surface roughness of the casting drum) should be controlled in order to avoid variation in thickness across the width of the drum.
- The thickness of the cast sheet can be effectively controlled by adjusting immersion and RPM
- The temperature of the molten metal needs to be monitored continuously as good quality castings can only be obtained in between a certain temperature range. Lower melt temperature can result in highly variable thickness profiles while a higher temperature can result in the drum being unable to cast the sheet.

Chapter 8

Discussion

The research project was funded by ML Operations, a sheet lead manufacturer based in Derbyshire along with Innovate UK and Cranfield University. The company focusses on Continuously Cast lead sheet and sandcast sheet and has about 25% market share in UK. The current research project was launched as a strategic decision to improve the processes within the company. The thesis essentially looks into aspects of two processes viz Sand casting of lead sheet and the single drum continuous casting process. The focus has been on understanding what process parameters affect the quality of the sheet especially thickness. Both these processes are relatively traditional and very little research has been conducted in this space.

Sandcast lead sheet is primarily used in the construction industry for renovation of heritage buildings, churches, state homes etc. Though there are other types of lead sheets like continuously cast and rolled sheet, which are superior in quality and also cheaper, architects prefer using sandcast sheet to preserve the heritage of these buildings. The distinct appearance of sandcast lead sheet, where one surface has a mottled appearance and the other a rough sand finish is a very important quality aspect to the end consumer as sandcast sheet is considered to be a premium product

and is distinguished from other types of lead sheets based on its appearance and the way it is manufactured. It is hence important to understand the parameters that affect the formation of the mottled appearance and to understand how it is reproducible.

Lead being one of the most recycled materials, scrap used for manufacture of sheet lead primarily consists of lead from buildings and construction industries. This scrap often contains many impurities and often refining is required. Elemental analysis of different batches of scrap used for manufacture of sandcast lead sheet revealed it to be relatively clean with trace amounts of impurities. The overall impurity content in melt batches used in manufacture of sand cast lead sheet was found to be very low even after being mixed with scrap lead since scrap lead consists of mostly secondary lead. It was observed that these trace amounts of impurities had an effect on the appearance of the pattern on the surface of the sheet. Different mixtures of scrap and pure lead were experimented with, and it was observed that good reproducible results were obtained when a mixture of pure to scrap lead was used. The addition of scrap results in formation of the patterned surface due to concentration of oxides and carbonates which appear as white and dark (or dull and shiny) patches on the top surface. It was also observed that hardness values of sandcast lead were similar to that of continuously cast sheets hence proving that presence of small amounts of impurities do not substantially affect the mechanical properties of the sheet. However higher amounts of these impurities could result in drastic changes in properties of the cast sheet.

Just like any other casting process, sandcast lead sheet also suffers from the presence of defects. In this investigation the focus has been laid on a surface defect type, addressed as ‘grooves’, appearing on the sand side of cast lead sheets. These grooves are categorised as a quality defect in the industry and hence it is important to understand the formation of this defect and way to eliminate/minimise them. The

presence of groove-type defects in the final cast sheet was quantified by estimating the ratio of their total length to the sample unit area. There are several factors potentially affecting the formation of this type of defects. Based on process observation, literature review and foundry experience, all possible factors affecting quality of sheets were listed. The initial set of factors selected was narrowed down based on a set of screening experiments, literature review and the experience of foundry engineers. Analysis of Variance (ANOVA) was implemented in order to identify the process parameters or factors which had the most significant contribution to the formation of grooves while an optimal set of process parameters was proposed in order to minimise defects in the final product. The majority of the defects produced in lead sheet casting industry can be attributed to mould properties and moulding materials. The trials conducted with the green sand mixture showed an improved surface finish and substantial reduction in the grooves produced on the sand side. Addition of bentonite in the sand mixture resulted in substantial reduction of groove defects in sand cast lead sheet. The quality of the melt was also observed to have a noticeable effect on the formation of the grooves.

As mentioned previously, very little scientific research has been conducted in this area. As a result, there is very limited knowledge on the effect of different process parameters involved in the process. Most of the skillsets are transferred from experienced operators. To understand the effect of different parameters, a 2-dimensional CFD model was developed to simulate the melt flow and solidification of lead during the sandcasting process. The objective of the study was to investigate the effects of process parameters such as the pouring temperature, strickle velocity and clearance between the sandbed on the strickle on the quality of the lead sheet. Simulation results were observed to be in good agreement with experimental observations. From the results obtained, it was concluded that the clearance between the sandbed and

the strickle can be effectively used to control the sheet thickness for a specific range of pouring temperature values. The findings of these studies were very useful to the company and helped in formulating improved standard operating procedures for the casting of lead sheet and in quality control. The present study can also be used as a steppingstone for further numerical investigation of the sandcasting method for producing lead sheets. The investigation of the effects of additional process characteristics such as the inclination of the sandbed and the strickle geometry on the quality of the cast sheet should be further investigated. Moreover, the current model can be used as the basis of an optimisation case study aiming at selecting the optimum process parameters for superior lead sheet quality.

The Direct Method or the single drum continuous casting process is a very efficient and cost-effective method for manufacture of sheet lead since the process directly converts liquid lead to sheet form. As a part of this thesis, an investigation into the energy consumption of the process and its comparison with competing rolling process was conducted. The study investigated energy consumption and costs associated at various stages of the DM process. It was observed that the actual energy consumption of the DM process is substantially lower than the theoretically calculated figures for conventional rolling technique. The process is also very quick, allows manufacture in smaller batches and requires minimum human intervention. It can be reasonably concluded that the process can be used as a very good alternative to the conventional rolling method. Methods for further improving the energy efficiency of the DM process like melt pre-heating and improving Operational Material Efficiency were suggested to the company. Further study needs to be conducted in this area especially investigating the formation of lumps on cast spools potentially due to formation of residual stresses as this can result in further improvement of yield of the process.

Similar to the sandcasting process, due to the obsolete nature of the process, very limited research specific to the DM process has been conducted before. In order to understand the effect of different parameters another 2-dimensional numerical model was developed to simulate the DM process. Different process parameters like effect of heat transfer coefficient, volume flow rate, melt temperature, immersion of the casting drum into the melt and speed of rotation of the casting drum were investigated. It was observed that, controlling volume flow rate of liquid metal into the casting tray is vital in order to control the thickness of the cast sheet. The effect of volume flow rate becomes more prominent while trying to cast very thin codes (for example code 1 and 2) because even slight variations in immersion levels can affect the thickness of the cast sheet at such low thicknesses. Traditionally, volume flow rate is not controlled in the process and this was suggested to the company as an area for improvement. The heat transfer coefficient was also observed to affect the thickness of the cast sheet. Heat transfer coefficient also depends on surface roughness of the casting drum and utmost care needs to be taken to ensure that the roughness of the casting drum is uniform throughout in order to avoid variation in thickness across the width of the drum. This resulted in the company investing in developing a new drum with improved helical cooling system and uniform surface roughness. It was observed that the sheet cast using the new drum was substantially improved and the variation in thickness observed across the sheet was minimal. This helped the company to manufacture sheets close to the nominal value. As per the industry practise, the price per kilogram of lead sheet is calculated based on the nominal thickness of the cast sheets. A tolerance of +/- 5% is allowed on this normal value. Ability to cast sheet closer to the nominal value or in the negative region of the tolerance value results in huge economic benefits considering the huge volume of sheets manufactured annually. It was also observed that temperature of melt is

a prominent factor and needs to be controlled. Higher temperature could result in the drum being unable to solidify the melt over it. Hence it is important to keep the temperature at a suitable range by using improved heating elements to keep the melt temperature uniform across the casting tray. The study can be further developed, and optimum values of different process parameters could be identified to obtain good castings. Being able to further control the variation in thicknesses of cast sheet products can potentially result in huge savings for the industry. The DM process is a much better alternative to rolling process considering the low cost of investment required.

Appendix A

Defect Elimination in Sandcasting of lead sheet

Additional Experiments

A set of additional experiments were conducted to understand the root cause of the groove defects. Various parameters associated with the casting processes were altered to observe any trend in the formation of the grooves as a part of initial root cause analysis.

The formation of the defects was not affected by altering the temperature of pour of the molten metal. An increase in the moisture content resulted in formation of new defects like blow holes on the castings. The use of a coarser sand resulted in poor surface finish without any changes in the formation of the grooves.

The grooves are formed along the direction of flow which is same as the direction of motion of the screed rail which is used to level the sheets to wipe of excess metal and to obtain the desired thickness. To check the effect of the stress induced by

Experiment	**Observation**
Increase temperature of melt to 360°C	Presence of grooves more pronounced towards the bottom of the bed
Reduce temperature of melt to 340°C	Presence of grooves, melt solidified before mold filling
Increase moisture content by 100%	Presence of grooves with other gas defects
Change of sand mix to Mansil 45+ Red foundry sand (3:1 Ratio)	Presence of grooves, Rougher surface finish
Casting without the use of screed rail to wipe off the excess metal	Presence of grooves
Inclination of bed with horizontal made to 0 degrees	Presence of grooves
Increased angle of inclination of bed to -5 degrees with horizontal	Presence of grooves

Table A.1: Preliminary Experimentation

the screed rail on the metal during the process in formation of defects, trials were conducted by casting sheets without the use of the screed rail. Trials were also conducted by altering the inclination of the sand bed to confirm if the flow rate of the metal has any impact on the formation of defects as described in Table A.1.

The experiments were conducted using 5 different molding mixtures. The mixture was prepared at John Winter & Co and they were stored in sealed containers in order to preserve the moisture. Each trial was repeated 3 times to ensure repeatability. Table A.2 shows the details of the molding mixture used and the results obtained.

All the green sand mixtures supplied by John Winter & Co. provided improved results. Trials were carried out using green sand mixture with a sand conditioner. Even though there was substantial reduction in the grooves, it was difficult to prepare the bed after the first cast for subsequent runs since the sandbed became very hard. The sand had to be re-prepared using a muller and this was not favourable in a

Sand mixture	Experiment	Observation
S1	Silica Sand 60 AFM - 96% Clay - 2.5 % Water -1.5%	Improved sand surface. Results not satisfactory.
S2	Silica sand 80 AFM-93.5% Clay - 6% Water - 1.5 % SC#2 green sand conditioner-0.5%	Good results, the groves reduced in number substantially. Difficulty in reworking the sand after casting.
S3	Silica Sand 60 AFM-93.5% Clay 6% SC#2 green sand conditioner 0.5% Water 1.5 % of total weight of mixture	Good results, the groves reduced in number substantially Sand Surface of sheet rougher in appearance Difficulty in preparing the bed
S4	Silica sand 80 AFM-94% Clay 6% Water 1.5 %	Relatively easy to Prepare bed Relatively easy to rework Good surface on sand side
S5	Silica sand 70.05% Red Pulverised sand 23.45% foundry sand 3:1 mix Clay 6% Water 1.5% SC#2 green sand conditioner 0.5%	Poor Results Sand side finish very rough

Table A.2: Experiments with different green sand mixtures

production environment due to the time taken. Trials were conducted with sand S4 (without the conditioner). The cast produced was free of any grooves and the sandbed was relatively easier to prepare for the next casting. It was observed that the amount of binder affected the workability of the sand after a cast

Bibliography

[1] W. Hofmann, "Lead and lead alloys," in *Lead and Lead Alloys*, Springer, 1970, pp. 25–320.

[2] B.-Y. Erez, V. Yitzhak, C. van den Brink Edwin, and B. Ron, "A new ghassulian metallurgical assemblage from bet shemesh (israel) and the earliest leaded copper in the levant," *Journal of Archaeological Science: Reports*, vol. 9, pp. 493–504, 2016.

[3] E. Rocca, F. Mirambet, and J. Steinmetz, "Study of ancient lead materials: A gallo-roman sarcophagus—contribution of the electrolytic treatment to its restoration," *Journal of materials science*, vol. 39, no. 8, pp. 2767–2774, 2004.

[4] J. Smythe, "A lead etching effect," *Nature*, vol. 145, no. 3679, pp. 704–704, 1940.

[5] D. R. Blaskett and D. Boxall, *Lead and its alloys*. Ellis Horwood Ltd, 1990.

[6] "Roman baths museum," in *Bath, UK*.

[7] L. F. Salzman, *Building in England, Down to 1540: A Documentary History*. Clarendon Press, 1952.

[8] G. C. Allen, L. Black, P. D. Forshaw, and N. J. Seeley, "Raindrops keep falling on my lead," *Journal of Architectural Conservation*, vol. 9, no. 1, pp. 23–44, 2003.

[9] "Principal uses of lead and zinc," in *International Lead Zinc Study Group*, 2008.

[10] A. J. Davidson, S. P. Binks, and J. Gediga, "Lead industry life cycle studies: Environmental impact and life cycle assessment of lead battery and architectural sheet production," *The International Journal of Life Cycle Assessment*, vol. 21, no. 11, pp. 1624–1636, 2016.

[11] T. Brinkmann, G. G. Santonja, F. Schorcht, S. Roudier, and L. D. Sancho, "Best available techniques (bat) reference document for the production of chlor-alkali," *JRC Science and policy reports EUR*, vol. 26844, 2014.

[12] I. Thornton, R. Rautiu, and S. Brush, "Lead the facts," *IC Consultants Ltd, London, UK*, 2001.

[13] "International lead association," in. [Online]. Available: `https://www.ila-lead.org/lead-facts/lead-production--statistics`.

[14] W. M. Haynes, *CRC handbook of chemistry and physics*. CRC press, 2014.

[15] "Construction," in *European Lead Sheet Industry Association*. [Online]. Available: `http://elsia.org.uk/uses-benefits/construction`.

[16] D. J. Rowe, *Lead manufacturing in Britain: a history*. Routledge, 2017.

[17] A. Prabhakar, J. Mielnicka, M. Jolly, and K. Salonitis, "Improving energy efficiency in direct method for continuous casting of lead sheets," in *TMS Annual Meeting & Exhibition*, Springer, 2018, pp. 121–132.

[18] "European lead development committee," in *Lead 65*, Pergamon, 1967, p. i, ISBN: 978-0-08-011425-5. [Online]. Available: `http://www.sciencedirect.com/science/article/pii/B9780080114255500012`.

[19] E. Randich, W. Duerfeldt, W. McLendon, and W. Tobin, "A metallurgical review of the interpretation of bullet lead compositional analysis," *Forensic science international*, vol. 127, no. 3, pp. 174–191, 2002.

[20] A. Prabhakar, K. Salonitis, and M. Jolly, "Characterisation of lead sheet manufactured using traditional sand-casting technique," in *Shape Casting*, Springer, 2019, pp. 283–292.

[21] L. Teoh, "Technological developments in near-net-shape casting for mini-steelmills," *Journal of materials processing technology*, vol. 44, no. 3-4, pp. 249–256, 1994.

[22] J. F. Healy, *Mining and metallurgy in the Greek and Roman world*. Thames and Hudson London, 1978, vol. 191.

[23] S. Khambholja, A. Abhishek, D. Satikunvar, and B. Thakore, "Thermophysical properties of pb-li," in *AIP Conference Proceedings*, AIP Publishing LLC, vol. 1942, 2018, p. 030 021.

[24] S. Whillock, J. Charles, and G. Smith, "Microstructures and mechanical properties of milled and continuously cast lead sheet part 1 microstructures," *Materials science and technology*, vol. 5, no. 11, pp. 1074–1083, 1989.

[25] S. Whillock, J. Charles, and G. Smith, "Microstructures and mechanical properties of milled and continuously cast lead sheet," *Materials science and technology*, vol. 7, no. 12, pp. 1116–1127, 1991.

[26] S. Stuart, "Discussion.," in *Lead 65*, 1967, ISBN: 9780080114255.

[27] S. Whillock, J. Charles, and G. Smith, "Microstructures and mechanical properties of milled and continuously cast lead sheet part 1 microstructures," *Materials science and technology*, vol. 5, no. 11, pp. 1074–1083, 1989.

[28] B. E. 12588:2006, "Lead and lead alloys — rolled lead sheet for building purposes," *British Standards Institute*, 2007.

[29] O. Ikumapayi, E. Akinlabi, P. Onu, and O. Abolusoro, "Rolling operation in metal forming: Process and principles–a brief study," *Materials Today: Proceedings*, 2020.

[30] S. SHIDA, H. AWAZUHARA, K.-i. YASUDA, and S. TSUMURA, "Simulation of hot rolling of steel using lead," *Transactions of the Iron and Steel Institute of Japan*, vol. 19, no. 11, pp. 700–705, 1979.

[31] S. K. Singha and S. J. Singh, "Analysis and optimization of sand casting defects with the help of artificial neural network," *International*

Journal of Research in Engineering and Technology, vol. 4, no. 5, pp. 24–29, 2015.

[32] H. Khandelwal and B. Ravi, "Effect of molding parameters on chemically bonded sand mold properties," *Journal of Manufacturing Processes*, vol. 22, pp. 127–133, 2016.

[33] A. Kumari, R. Ohdar, and H. Banka, "Multi-objective parametric optimization of green sand moulding properties using genetic algorithm," in *2016 3rd International Conference on Recent Advances in Information Technology (RAIT)*, IEEE, 2016, pp. 279–283.

[34] D. A. Scott, "A note on the metallographic preparation of ancient lead," *Studies in conservation*, vol. 41, no. 1, pp. 60–62, 1996.

[35] M. Perzyk and A. Kochański, "Detection of causes of casting defects assisted by artificial neural networks," *Proceedings of the Institution of Mechanical Engineers, Part B: Journal of Engineering Manufacture*, vol. 217, no. 9, pp. 1279–1284, 2003.

[36] R. Rajkolhe and J. Khan, "Defects, causes and their remedies in casting process: A review," *International Journal of Research in Advent Technology*, vol. 2, no. 3, pp. 375–383, 2014.

[37] J. Campbell, *Complete casting handbook: metal casting processes, metallurgy, techniques and design*. Butterworth-Heinemann, 2015.

[38] M. Jolly, "Prof. john campbell's ten rules for making reliable castings," *JOM: the journal of the Minerals, Metals Materials Society*,

vol. 57, pp. 19–28, May 2005. DOI: 10.1007/s11837-005-0091-4.

[39] W. M. A. Jadayil, "Studying the effects of varying the pouring rate on the casting defects using nondestructive testing techniques," *Jordan Journal ofMechanical and Industrial Engineering*, vol. 5, pp. 521–526, 2011.

[40] S. Chaudhari and H. Thakkar, "Review on analysis of foundry defects for quality improvement of sand casting," *International Journal of Engineering Research and Applications*, vol. 4, no. 3, pp. 615–618, 2014.

[41] A. Reis, Z. Xu, R. Tol, and R. Neto, "Modelling feeding flow related shrinkage defects in aluminum castings," *Journal of manufacturing processes*, vol. 14, no. 1, pp. 1–7, 2012.

[42] I. Kay, M. Nagel, C. Metals, D. Plaines, and A. T. Spada, *Modern Casting*, 2002.

[43] C. Saikaew and S. Wiengwiset, "Optimization of molding sand composition for quality improvement of iron castings," *Applied Clay Science*, vol. 67, pp. 26–31, 2012.

[44] H. Pandit, A. Sata, V. Mane, and U. A. Dabade, "A novel web-based system for casting defect analysis," in *technical transactions of 60th Indian Foundry Congress*, vol. 2, 2012.

[45] V. Mane, A. Sata, and M. Khire, "New approach to casting defects classification and analysis supported by simulation," in *a technical*

paper for 59th Indian foundry congress, Chandigarh, 2010, pp. 87–104.

[46] U. A. Dabade and R. C. Bhedasgaonkar, "Casting defect analysis using design of experiments (doe) and computer aided casting simulation technique," *Procedia Cirp*, vol. 7, pp. 616–621, 2013.

[47] S. Guharaja, A. N. Haq, and K. Karuppannan, "Optimization of green sand casting process parameters by using taguchi's method," *The International Journal of Advanced Manufacturing Technology*, vol. 30, no. 11-12, pp. 1040–1048, 2006.

[48] S. Kumar, A. K. Gupta, and P. Chandna, "Optimization of process parameters of pressure die casting using taguchi methodology," *World Academy of Science, Engineering and Technology*, vol. 68, pp. 590–594, 2012.

[49] O. Chopra *et al.*, "Solidification of lead and lead alloys in continuous drum sheet casting," 1975.

[50] A. Prabhakar, M. Papanikolaou, K. Salonitis, and M. Jolly, "Sand casting of sheet lead: Numerical simulation of metal flow and solidification," *The International Journal of Advanced Manufacturing Technology*, vol. 106, no. 1-2, pp. 177–189, 2020.

[51] S. Hakimi, S. M. Zahraee, and J. M. Rohani, "Application of six sigma dmaic methodology in plain yogurt production process," *International Journal of Lean Six Sigma*, 2018.

[52] A. Kumaravadivel and U. Natarajan, "Optimization of sand-casting process variables—a process window approach," *The International Journal of Advanced Manufacturing Technology*, vol. 66, no. 5-8, pp. 695–709, 2013.

[53] S. S. Wulff, *A first course in design and analysis of experiments*, 2003.

[54] M. Hossain, N. Rahim, M. Aman, and J. Selvaraj, "Application of anova method to study solar energy for hydrogen production," *International Journal of Hydrogen Energy*, vol. 44, no. 29, pp. 14 571–14 579, 2019.

[55] B. H. Cohen, *Explaining psychological statistics*. John Wiley & Sons, 2008.

[56] P. Dhrymes, "The general linear model iii," in *Introductory Econometrics*, Springer, 2017, pp. 115–228.

[57] *Using the r-squared statistic in anova and glms*, Sep. 2012. [Online]. Available: `https://www.isixsigma.com/tools-templates/regression/using-the-r-squared-statistic-in-anova-and-general-linear-models/`.

[58] J. Miles, "R squared, adjusted r squared," *Wiley StatsRef: Statistics Reference Online*, 2014.

[59] M. Ferry, *Direct strip casting of metals and alloys*. Woodhead Publishing, 2006.

[60] T. Robic and B. Filipic, "In search for an efficient parameter tuning method for steel casting," *BIOINSPIRED OPTIMIZATION METHODS AND THEIR APPLICATIONS*, 2004.

[61] C. Hendricks, "Strip casting technology-a revolution in the steel industry?" *Metall Plant Technol. Int.*, vol. 18, pp. 42–49, 1995.

[62] A. Gerber and A. Sousa, "A parametric study of the hazelett thin-slab casting process," *Journal of materials processing technology*, vol. 49, no. 1-2, pp. 41–56, 1995.

[63] P. Manohar, A. Hunter, and M. Ferry, "Direct strip casting of steel-historical perspective and future direction," in *Materials Forum*, vol. 24, 2000, pp. 19–36.

[64] (). Twin belt casting, [Online]. Available: `https://www.totalmateria.com/page.aspx?ID=CheckArticle&site=ktn&NM=346`.

[65] M. Yun, S. Lokyer, and J. Hunt, "Twin roll casting of aluminium alloys," *Materials Science and Engineering: A*, vol. 280, no. 1, pp. 116–123, 2000.

[66] P. Bradbury, "A mathematical for the twin roll casting process," PhD thesis, D. Phil. Thesis, Oxford University, Oxford, 1995.

[67] G. Laurie and D. Lauriente, "Continously cast lead sheet—production and uses," *Canadian Metallurgical Quarterly*, vol. 7, no. 3, pp. 159–166, 1968.

[68] G. Li and B. G. Thomas, "Transient thermal model of the continuous single-wheel thin-strip casting process," *Metallurgical and Materials transactions B*, vol. 27, no. 3, pp. 509–525, 1996.

[69] P. Bradbury and J. Hunt, "A coupled fluid flow, deformation and heat transfer model for a twin roll caster," Minerals, Metals and Materials Society, Warrendale, PA (United States), Tech. Rep., 1995.

[70] Y. Zhang, "Modelling of vertical twin-roll casting of magnesium alloy," 2012.

[71] T. Haga and S. Suzuki, "A twin-roll caster to cast clad strip," *Journal of materials processing technology*, vol. 138, no. 1-3, pp. 366–371, 2003.

[72] J. Birat, M. Larrecq, J. Lamant, and J. Petegnief, "Mold operation for quality and productivity," in *Iron and Steel Society, Warrendale, PA*, vol. 15086, 1991, pp. 3–14.

[73] J. Sengupta, B. Thomas, and M. Wells, "The use of water cooling during the continuous casting of steel and aluminum alloys," *Metallurgical and Materials Transactions A*, vol. 36, no. 1, pp. 187–204, 2005.

[74] S. Zhang, H. Myo, K. Lim, K. Tong, M. Yong, S. Pook, and M. Fu, "Processing of thin metal strip by casting-cum-rolling," *Journal of materials processing technology*, vol. 192, pp. 101–107, 2007.

[75] O. Chopra *et al.*, "Solidification of lead and lead alloys in continuous drum sheet casting," 1975.

[76] M. Shamsi and S. Mehrotra, "A two-dimensional heat and fluid-flow model of single-roll continuous-sheet casting process," *Metallurgical and Materials Transactions B*, vol. 24, no. 3, pp. 521–535, 1993.

[77] D. Bouchard, F. G. Hamel, J.-P. Nadeau, D. Simard, S. Bellemare, F. Dreneau, and D.-A. Tremblay, "Effects of substrate surface conditions on heat transfer and shell morphology in the solidification of a copper alloy," *Metallurgical and Materials Transactions B*, vol. 32, no. 1, pp. 111–118, 2001.

[78] D. C. Zipperian, "Metallographic specimen preparation basics," *Pace technology*, 2001.

[79] S. Wong, P. D. Hodgson, and P. F. Thomson, "Room temperature deformation and recrystallisation behaviour of lead and lead–tin alloys in torsion and plane strain compression," *Materials science and technology*, vol. 15, no. 6, pp. 689–696, 1999.

[80] K. Ednie, "Metallographic preparation of soft materials: Lead alloys," *Materials Characterization*, vol. 36, no. 4-5, pp. 243–255, 1996.

[81] A. Reikher and K. M. Pillai, "A fast simulation of transient metal flow and solidification in a narrow channel. part i: Model development using lubrication approximation," *International Journal of Heat and Mass Transfer*, vol. 60, pp. 797–805, 2013.

[82] C. Reilly, N. Green, and M. R. Jolly, "The present state of modeling entrainment defects in the shape casting process," *Applied Mathematical Modelling*, vol. 37, no. 3, pp. 611–628, 2013.

[83] S. Sulaiman and A. Hamouda, "Modelling and experimental investigation of solidification process in sand casting," *Journal of Materials Processing Technology*, vol. 155, pp. 1723–1726, 2004.

[84] A. Kermanpur, S. Mahmoudi, and A. Hajipour, "Numerical simulation of metal flow and solidification in the multi-cavity casting moulds of automotive components," *Journal of materials processing technology*, vol. 206, no. 1-3, pp. 62–68, 2008.

[85] M. Papanikolaou, E. Pagone, K. Georgarakis, K. Rogers, M. Jolly, and K. Salonitis, "Design optimisation of the feeding system of a novel counter-gravity casting process," *Metals*, vol. 8, no. 10, p. 817, 2018.

[86] M. Papanikolaou, E. Pagone, K. Salonitis, M. Jolly, and C. Makatsoris, "A computational framework towards energy efficient casting processes," in *International Conference on Sustainable Design and Manufacturing*, Springer, 2018, pp. 263–276.

[87] A. Krimpenis, P. Benardos, G.-C. Vosniakos, and A. Koukouvitaki, "Simulation-based selection of optimum pressure die-casting process parameters using neural nets and genetic algorithms," *The International Journal of Advanced Manufacturing Technology*, vol. 27, no. 5-6, pp. 509–517, 2006.

[88] I. Flow Science, *Flow-3d, version 12.0*, Santa Fe, NM, 2019. [Online]. Available: `https://www.flow3d.com/`.

[89] M. Barkhudarov and C. Hirt, "Casting simulation: Mold filling and solidification–benchmark calculations using flow-3d {reg_sign}," Minerals, Metals and Materials Society, Warrendale, PA (United States), Tech. Rep., 1995.

[90] C. W. Hirt and B. D. Nichols, "Volume of fluid (vof) method for the dynamics of free boundaries," *Journal of computational physics*, vol. 39, no. 1, pp. 201–225, 1981.

[91] C. Hirt and J. Sicilian, "A porosity technique for the definition of obstacles in rectangular cell meshes," in *International Conference on Numerical Ship Hydrodynamics, 4th*, 1985.

[92] M. Barkhudarov, "Advanced simulation of the flow and heat transfer processes in simultaneous engineering," *Flow Sci. Inc.*, vol. 1257, 1998.

[93] T. E. Weyand, "The oxidation kinetics of liquid lead and lead alloys," 1970.

[94] K. Ednie, "Metallographic preparation of soft materials: Lead alloys," *Materials Characterization*, vol. 4, no. 36, pp. 243–255, 1996.

[95] E.-R. Bagherian, Y. Fan, M. Cooper, B. Frame, and A. Abdolvand, "Effect of antimony addition relative to microstructure and mechanical properties of continuous cast lead alloy," in *25th International Conference on Metallurgy and Materials METAL 2016*, TANGER Ltd., 2016, pp. 1294–1300.

[96] S. R. D. GOFF L I, "Lead products by continuous casting.," in *Lead 65*, Pergamon, 1967, p. i, ISBN: 978-0-08-011425-5.

[97] R. E. Smallman, *Modern physical metallurgy*. Elsevier, 2016.

[98] J. Campbell, "An overview of the effects of bifilms on the structure and properties of cast alloys," *Metallurgical and Materials Transactions B*, vol. 37, no. 6, pp. 857–863, 2006.

[99] C. Tian, J. Law, J. Van Der Touw, M. Murray, J.-Y. Yao, D. Graham, and D. S. John, "Effect of melt cleanliness on the formation of porosity defects in automotive aluminium high pressure die castings," *Journal of materials processing technology*, vol. 122, no. 1, pp. 82–93, 2002.

[100] J. Thiel, M. Ziegler, P. Dziekonski, and S. Joyce, "Investigation into the technical limitations of silica sand due to thermal expansion," *Transactions of the American Foundry Society, Vol. 115*, vol. 115, pp. 383–400, 2007.

[101] L. Á. Oliveira, J. C. Santos, T. H. Panzera, R. T. Freire, L. M. Vieira, and F. Scarpa, "Evaluation of hybrid-short-coir-fibre-reinforced composites via full factorial design," *Composite Structures*, vol. 202, pp. 313–323, 2018.

[102] I. D. Sredović Ignjatović, A. E. Onjia, L. M. Ignjatović, Ž. N. Todorović, and L. V. Rajaković, "Experimental design optimization of the determination of total halogens in coal by combustion–ion chromatography," *Analytical Letters*, vol. 48, no. 16, pp. 2597–2612, 2015.

[103] D. Montgomery, "Guidelines for designing experiments," *Design and Analysis of Experiments*, 2008.

[104] M. Jolly, "Castings," 2003.

[105] J. Brown, *Foseco Foundryman's Handbook: Facts, Figures and Formulae*. Butterworth-Heinemann, 1994.

[106] O. M. I. Resource. (). Matweb, [Online]. Available: `http://www.matweb.com`.

[107] K. Ho and R. D. Pehlke, "Metal-mold interfacial heat transfer," *Metallurgical Transactions B*, vol. 16, no. 3, pp. 585–594, 1985.

[108] Lead, "Pb," [Online]. Available: `http://www.matweb.com/search/DataSheet.aspx?MatGUID=ebd6d2cdfdca4fc285885cc4749c36-%20b1&ckck=1`.

[109] M. Barkhudarov, "Enhancement to heat transfer and solidification shrinkage models in flow-3d," *Flow Science, Inc., Rep FSI-95-TN43*, 1995.

[110] P. V. Tota, "Turbulent flow over a backward-facing step using the rng k-ε model," *Flow Sci*, vol. 1, pp. 1–15, 2009.

[111] N. Stathopoulos, M. El Mankibi, and M. Santamouris, "Numerical calibration and experimental validation of a pcm-air heat exchanger model," *Applied Thermal Engineering*, vol. 114, pp. 1064–1072, 2017.

[112] J. Banaszek, S. McFadden, D. J. Browne, L. Sturz, and G. Zimmermann, "Natural convection and columnar-to-equiaxed transition prediction in a front-tracking model of alloy solidification," *Metallur-*

gical and Materials Transactions A, vol. 38, no. 7, pp. 1476–1484, 2007.

[113] A. Paquier, F. Moisy, and M. Rabaud, "Viscosity effects in wind wave generation," *Physical Review Fluids*, vol. 1, no. 8, p. 083 901, 2016.

[114] K. van Gastel, P. A. Janssen, and G. J. Komen, "On phase velocity and growth rate of wind-induced gravity-capillary waves," *Journal of Fluid Mechanics*, vol. 161, pp. 199–216, 1985.

[115] *Department of energy and climate change*,

[116] K. Salonitis, M. R. Jolly, B. Zeng, and H. Mehrabi, "Improvements in energy consumption and environmental impact by novel single shot melting process for casting," *Journal of Cleaner Production*, vol. 137, pp. 1532–1542, 2016.

[117] M. R. Jolly and K. Salonitis, "Primary manufacturing, engine production and on-the-road co2: How can the automotive industry best contribute to environmental sustainability," 2017.

[118] S. Kalpakjian, *Manufacturing engineering and technology*. Pearson Education India, 2001.

[119] B. Zeng, M. Jolly, and K. Salonitis, "Manufacturing cost modeling of castings produced with crimson process," in *Shape Casting: 5th International Symposium 2014*, Springer, 2014, pp. 201–208.

[120] K. Salonitis, B. Zeng, H. A. Mehrabi, and M. R. Jolly, "The challenges for energy efficient casting processes," 2016.

[121] S. Ja, V. Varun, and V. V. Vignesha, "Waste heat recovery from metal casting and scrap preheating using recovered heat," *Procedia Engineering*, vol. 97, pp. 267–276, 2014.

[122] A. E. Schwaneke and W. L. Falke, "Surface tension and density of liquid lead," *Journal of Chemical and Engineering Data*, vol. 17, no. 3, pp. 291–293, 1972.